

T-4470

***THE EFFECT OF RADICAL INITIATORS
UPON FUEL INSTABILITY***

BY

Abdullah S. Aldhuwaihi

ARTHUR LAKES LIBRARY
COLORADO SCHOOL OF MINES
GOLDEN, CO 80401

ProQuest Number: 10783949

All rights reserved

INFORMATION TO ALL USERS

The quality of this reproduction is dependent upon the quality of the copy submitted.

In the unlikely event that the author did not send a complete manuscript and there are missing pages, these will be noted. Also, if material had to be removed, a note will indicate the deletion.



ProQuest 10783949

Published by ProQuest LLC (2018). Copyright of the Dissertation is held by the Author.

All rights reserved.

This work is protected against unauthorized copying under Title 17, United States Code
Microform Edition © ProQuest LLC.

ProQuest LLC.
789 East Eisenhower Parkway
P.O. Box 1346
Ann Arbor, MI 48106 – 1346

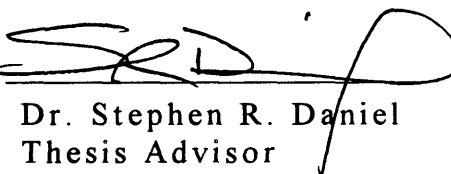
Submittal Sheet

A thesis submitted to the Faculty and the Board of Trustees of the Colorado School of Mines in Partial fulfillment of the requirements for the degree of Master of Science (Chemistry).

Golden, Colorado

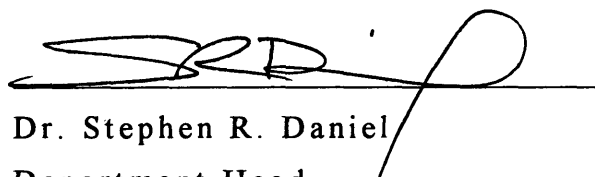
Date August 6, 1993

Signed: 
Abdullah S. Al-Dhuwaihi

Approved: 
Dr. Stephen R. Daniel
Thesis Advisor

Golden, Colorado

Date August 6, 1993


Dr. Stephen R. Daniel
Department Head
Chemistry and Geochemistry

ABSTRACT

This study examined the effect of radical initiators on fuel instability. A solution of tetralin in dodecane (1/10, V/V) was used as model fuel for this study. The behavior of this model was compared to a conventional Jet A fuel. This study included 1) liquid phase kinetic studies for the autoxidation of tetralin, and formation of tetralone, tetralol, and insoluble deposit, and 2) structural examination of the model fuel deposit.

The model fuel was developed to permit study of a system much less complex than real fuels. However, this simple model fuel produces a very complex mixture of products which makes analysis very difficult.

The model fuel was stressed for 8 days at $127 \pm 2^\circ \text{C}$ in a sealed vial to provide a limited amount of oxygen. Addition of benzoyl peroxide or azobisisobutyronitrile was studied to test the hypothesis that with limited oxygen the rate of autoxidation of tetralin and the rate of formation of the intermediate products (tetralone and tetralol) could be increased and the rate of forming deposits decreased. However, deposition was also found to accelerate. It was found that deposit produced early in the process has high peroxide content. Later in the process, the deposit has no peroxide content. Initial and final Jet A deposits

were found to contain no peroxides. Initial deposit that forms upon stressing the model fuel system was found to consist of a mixture of aromatic compounds that contain hydroxyl, carbonyl and peroxide functional groups. Final deposit consists of a mixture of aromatic compounds that contain hydroxyl, carbonyl and ether functional groups, but no peroxide. Both initiators increase the amount of deposit formed in both model and Jet A fuels.

ACKNOWLEDGMENTS

The author would like to express gratitude to Dr. Stephen Daniel for giving me the opportunity to work and learn from him about this project.

I also want to thank Dr. Stephen Daniel for his help, assistance, guidance and encouragement in every aspect of this study.

I want to thank Drs. Voorhees and Cowley for serving as my committee and providing valuable suggestions and analysis.

I want to thank Department of Chemistry and Geochemistry and Saudi Aramco Company for their financial support and analysis.

I want to thank Mr. Al-Houtan and Mr. Al-Turki (Saudi Aramco Company) for their support and encouragement they have given me.

I also would like to thank Drs. Al-Suhaibani, Al-Uasil (King Saud University), and Abo Abdon (King Fahad University of Petroleum and Minerals) for their help.

TABLE OF CONTENTS

	Page
ABSTRACT.....	iii
ACKNOWLEDGMENTS.....	v
TABLE OF CONTENTS.....	vi
LIST OF FIGURES.....	viii
LIST OF TABLES.....	xiv
1. INTRODUCTION.....	1
1.1. DEPOSIT FORMATION IN THE MODEL FUEL.....	12
1.1.1. FORMATION OF HYDROPEROXIDE.....	12
1.1.2. HYDROPEROXIDE DECOMPOSITION.....	15
1.1.3. REACTION OF THE OXIDATION PRODUCTS.....	16
1.1.4. FORMATION OF THE DEPOSIT.....	20
2. EXPERIMENTAL SECTION.....	35
2.1. PREPARATION OF CHEMICALS AND REAGENTS.....	35
2.2. INSTRUMENTATION.....	36

2.3. AUTOXIDATION OF TETRALIN IN MODEL FUEL	41
2.4. EFFECT OF RADICAL INITIATORS ON MODEL AND JET FUEL INSTABILITY.....	42
3. RESULTS AND DISCUSSION.....	44
3.1. AUTOXIDATION OF MODEL FUEL	44
3.2. EFFECT OF RADICAL INITIATORS UPON MODEL FUEL STABILITY	50
3.3. CHARACTERIZATION OF MODEL FUEL DEPOSIT.....	68
4. CONCLUSIONS.....	93
5. REFERENCES	95
APPENDIX A.....	A-101
APPENDIX B	B-122
APPENDIX C	C-124

LIST OF FIGURES

	Page
Figure 1: Diesel fuel decomposition during ambient storage (Beaver, 1991).....	5
Figure 2: Oxidation products of 1-tetralone (Zarrabi, 1987)	18
Figure: 3: Postulated mechanism for deposit formation. (A) disproportionation reaction of tetralin hydroperoxide and (B) condensation reaction between tetralone and tetralin hydroperoxide (Worstell, 1980).....	23
Figure 4. Possible scheme of deposit formation (Zarrabi, 1987).	25
Figure 5: Possible mechanism for sequential autoxidations and condensations to produce polymeric products	27
Figure 6: Possible mechanism for condensation reactions between hydroperoxide and diketone groups.	28

Figure 7: Possible mechanism of condensation reactions of ring-opening oxidation products.	29
Figure 8: Possible mechanism for final deposit formation by condensation reaction of tetralone oxidation products.	30
Figure 9: Calibration curve for ferric chloride standards (peroxide determination).	40
Figure 10: Rate of tetralin autoxidation. Error bars define range of duplicate determinations.	45
Figure 11: Kinetics of the autoxidation of tetralin and of formation of tetralone, tetralol, and deposits.	48
Figure 12: Rates of tetralin autoxidation with additive (benzoyl peroxide) and without additive. A is tetralin concentration and A_i is initial tetralin concentration. Error bars define range of duplicate determinations.	51
Figure 13: Rates of tetralin autoxidation with additive (AIBN) and without additive. A is tetralin concentration and A_i is initial tetralin concentration. Error bars define range of duplicate determinations.	52

Figure 14: Kinetics of tetralone formation with and without additive (benzoyl peroxide). Error bars define range of duplicate determinations.	55
Figure 15: Kinetics of tetralone formation with and without additive (AIBN). Error bars define range of duplicate determinations.	56
Figure 16: Kinetics of tetralol formation with and without additive (benzoyl peroxide). Error bars define range of duplicate determinations.	57
Figure 17: Kinetics of tetralol formation with and without additive (AIBN). Error bars define range of duplicate determinations.	58
Figure 18: Kinetics of deposit formation with and without additive (benzoyl peroxide). Error bars define range of duplicate determinations.	59
Figure 19: Kinetics of the deposit formation with and without additive (AIBN). Error bars define range of duplicate determinations.	60
Figure 20: A and B are possible mechanisms of the formation of tetralone in the intermediate stage.	61

Figure 21: Kinetics of the autoxidation of tetralin and of tetralone, tetralol, and deposit formation 100 ppm AIBN added.	62
Figure 22: Kinetics of the autoxidation of tetralin and of tetralone, tetralol, and deposit formation 1000 ppm AIBN added.	63
Figure 23: Kinetics of the autoxidation of tetralin and of tetralone, tetralol, and deposit formation 2000 ppm AIBN added.	64
Figure 24: Kinetics of the autoxidation of tetralin and of tetralone, tetralol, and deposit formation 100 ppm benzoyl peroxide added.	65
Figure 25: Kinetics of the autoxidation of tetralin and of tetralone, tetralol, and deposit formation 1000 ppm benzoyl peroxide added.	66
Figure 26: Kinetics of the autoxidation of tetralin and of tetralone, tetralol, and deposit formation 2000 ppm benzoyl peroxide added.	67
Figure 27: GC-MS chromatograms of A) initial deposit from model fuel. B) initial deposit from model fuel containing 1000 ppm benzoyl peroxide. C) initial deposit from model fuel containing 1000 ppm AIBN.	69

Figure 28: GC-MS chromatograms of A) final deposit from model fuel. B) final deposit from model fuel containing 1000 ppm benzoyl peroxide. C) final deposit from model fuel containing 1000 ppm AIBN..... 70

Figure 29: Compounds that have been identified by GC/MS analysis of the initial deposit from model fuel without additives..... 71

Figure 30: Compounds that have been identified by GC/MS analysis of final deposit from model fuel without additives..... 72

Figure 31: FT-IR spectrum of the initial deposit from model fuel without additives..... 76

Figure 32: FT-IR spectrum of the final deposit from model fuel without additives..... 77

Figure 33: FT-IR spectrum of the initial deposit from model fuel containing 1000 ppm benzoyl peroxide. 79

Figure 34: FT-IR spectrum of the initial deposit from model fuel containing 1000 ppm AIBN..... 80

Figure 35: FT-IR spectrum of the final deposit from model fuel containing 1000 ppm benzoyl peroxide.	81
Figure 36: FT-IR spectrum of the final deposit from model fuel containing 1000 ppm AIBN.	82
Figure 37: Py-MS spectrum of initial deposit from model fuel.	86
Figure 38: Possible fragmentation reactions for the proposed molecular ions in the initial deposit.	87
Figure 39: Py-MS spectrum of final deposit from model fuel.	88
Figure 40: Possible structures for final deposit components.	89

LIST OF TABLES

	Page
Table 1: Detailed specifications of aviation turbine fuels (ASTM D 1655).....	7
Table 2: Elemental analysis of the model deposit and Jet A deposit (Worstell, 1980).	20
Table 3: Rate constants for the autoxidation of tetralin (Worstell, 1980).....	22
Table 4: Effect of additives upon Jet A fuel instability. Quinoline at 5 ppm, azobisisobutylnitrile at concentration of 8.9×10^{-3} mole/L and benzoyl peroxide at a concentration of 1.56×10^{-2} mole/L (Worstell, 1980).....	32
Table 5: Rate constants of tetralin autoxidation with and without initiators (from slopes in Figures 12 and 13).	53
Table 6: Effects of radical initiators upon the formation of final deposit for model and Jet A fuels.....	91

1. INTRODUCTION

The energy stored in petroleum is put to use by combining petroleum products with oxygen. This energy can be used for industrial or domestic purposes in forms such as gasoline, diesel fuel and heating oils (Nixon, 1962).

It is true that oxygen is essential to combust petroleum products, but on the other hand, oxygen can produce undesired reactions when it is present in petroleum products during short-term high-temperature stress or during long-term storage. Oxygen can act as an enemy because it can react with petroleum components and eventually form, after a sequence of reactions, nonvolatile materials called gums. The portion which is soluble in fuel is called dissolved or potential gum and the insoluble material is called deposited gum (Brinkman, 1979).

Fuel stability can be divided into two major types: storage stability and thermal stability. Storage instability is a term used to describe the tendency for chemical degradation of a given fuel while it is in storage facilities. Thermal instability is a term used to describe the tendency for chemical degradation of fuel at high temperature in an aircraft's fuel system prior to combustion. Fuels which have poor stability can produce deposited gum by a series of reactions that lead to the formation of insoluble materials.

Significant maintenance costs arise when these deposits plug injectors and decrease efficiency of heat exchangers in the engine. The term fuel stability is used for gasoline, jet fuels, diesel fuels and heating oils.

Gasoline is a complex mixture of hydrocarbons with a boiling range from 100 to 400 F° (ASTM D-4814-92). When gasoline is stored a deposit (or gum) is formed on the tank walls. In storage facilities, pipes and valves can be plugged by deposit formation. In carbureted engines, only 0.01 % gum in gasoline can plug the carburetor causing valve malfunction and producing piston and crankcase fouling. In fuel injection systems, deposits can clog injection nozzles (Nixon, 1962).

Many studies of the storage stability of gasoline were conducted in the early 1920's. These studies indicated that gum is present in gasoline as intermediate soluble products. These intermediate products are converted to deposits by evaporation of the gasoline (Mardles et al., 1929; Norris et al., 1929; Wagner et al., 1929). Brooks (1926) concluded that these intermediate products are organic peroxides. This conclusion has been confirmed by many investigators (Martin et al., 1933; Morrell et al., 1934a,b; Dryer et al., 1934).

Morrell (1934 a,b) reported that as the concentration of peroxides increases, the amount of gum formation increases. Later, many investigators identified the important organic

peroxides as hydroperoxides (e.g. Farmer et al., 1942). Flood (1933) concluded that decreases in octane number during storage may be attributed to the formation of oxygenated compounds during gum formation.

Morrell (1934 a,b) and Dryer (1934) concluded that change in the color of gasoline is caused by the presence of peroxides and as the concentration of peroxides is increased, the color of the gasoline becomes darker, gum formation increases and antiknock value decreases. Also, they identified peroxides, aldehydes, and acids as possible products of gasoline decomposition, but they did not determine alcohols and ketones. They concluded that the rate of deposit formation is proportional to the peroxide content and independent of the aldehyde and acid concentrations. Any effect of alcohols or ketones was not mentioned. They also suggested that these organic peroxides are only intermediates which decompose and polymerize during evaporation to form deposited gum by unknown reactions.

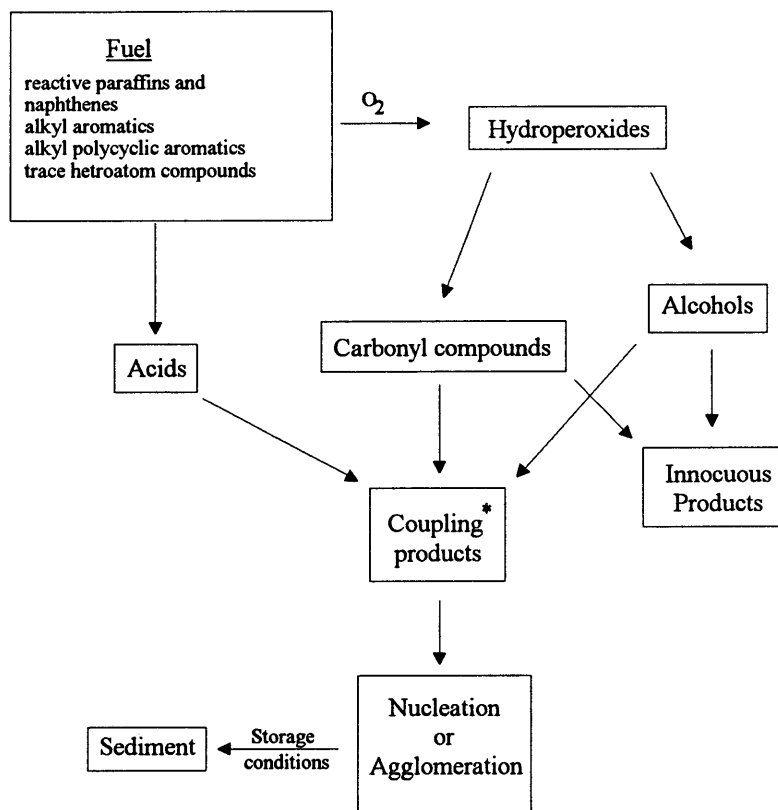
Flood (1933) concluded that aliphatic diolefins, cyclic diolefins, and mono-or diolefins attached to a benzene ring are responsible for gum formation and form the greatest amount of deposit. Yule (1931) suggested that the rate of gum formation is proportional to the organic peroxide concentration and concluded that organic peroxides are intermediates that form deposited gum by

unknown reactions. This conclusion has been confirmed by Morrell (1934 a,b).

Schwartz et al. (1964, 1972) concluded that nitrogen and sulfur compounds increase the rate of deposit formation. In addition, they determined that the concentration of nitrogen in the deposits is greater than that present in the original fuel.

Jet and Diesel fuels fall within the distillation range called middle distillate. Diesel fuel is used in high speed engines in trucks and buses. It has a boiling range of 360 to 600 °F (ASTM D-579-92). Jet fuel is used in aircraft engines. It has a boiling range of 350 F° to 550 F° (ASTM D-1655-92).

The mechanism of storage deposit formation in Diesel fuel is not well understood, but many investigators have pointed out that deposit formation can be attributed to the autoxidation of the hydrocarbons present in the fuel (Robertson et al., 1948; Mushrush et al., 1985). Generally, the deposit formation mechanism is believed to involve a series of reactions leading to soluble oxidation products and eventually to deposits. One such mechanism is presented in Figure 1 (Beaver, 1991).



*Molecules whose molecular weight has increased due to chemical reactions such as esterification or electrophilic aromatic substitution

Figure 1: Diesel fuel decomposition during ambient storage (Beaver, 1991).

Clinkenbeard (1959) suggested that deposit formation in Diesel fuel is due to the autoxidation of hydrocarbons present in the fuel and then reaction with oxygen, sulfur, and nitrogen compounds. Elmquist (1959) suggested that deposited gum formation in Diesel fuel is due to the presence of readily oxidizable aromatic thiols, hydrocarbons, and oxygen.

Offenhauer (1957) reported that storage stability of catalytically cracked distillate is increased by removing aromatic thiols, 1-naphthol or pyrrole type compounds from the fuel and is decreased when returning them to the fuel. Also, aliphatic thiols and diaryldisulfides do not increase deposit formation. Thompson (1949) found that pyrroles cause the largest rate of deposit formation and pyridines are also harmful to fuel stability, but to a lesser extent, and that both degrade color. He also found that indoles increase the insoluble gum and color becomes darker. Commercial jet fuel specifications are given in Table 1:

Table 1: Detailed specifications of aviation turbine fuels (ASTM D 1655).



D 1655

TABLE 1 Detailed Requirements of Aviation Turbine Fuels^A

Property	Jet A or Jet A-1	Jet B	ASTM Test Method ^B
Acidity, total max, mg KOH/g	0.1	...	D 974 or D 3242
Aromatics, max, vol %	20 ^C	20 ^C	D 1319
Sulfur, mercaptan, ^D max, weight %	0.003	0.003	D 3227
Sulfur, total max, weight %	0.3	0.3	D 1266 or D 1552 or D 2622 or D 4294
Distillation temperature, °C:			
10 % recovered, max, temp	205	...	D 86
20 % recovered, max, temp	...	145	
50 % recovered, max, temp	report	190	
90 % recovered, max, temp	report	245	
Final boiling point, max, temp	300	...	
Distillation residue, max, %	1.5	1.5	
Distillation loss, max, %	1.5	1.5	
Flash point, min, °C	38	...	D 56 or D 3828 ^J
Density at 15°C, kg/m ³	775 to 840	751 to 802	D 1298 or D 4052
Vapor pressure, 38°C, max, kPa	...	21	D 323
Freezing point, max, °C	-40 Jet A ^E -47 Jet A-1 ^E	-50 ^E	D 2386
Viscosity -20°C, max, mm ² /s ^L	8.0		D 445
Net heat of combustion, min, MJ/kg	42.8 ^G	42.8 ^G	D 4529, D 2382, D 3338, or D 4809
Combustion properties: one of the following requirements shall be met:			
(1) Luminometer number, min, or	45	45	D 1740
(2) Smoke point, min, mm, or	25	25	D 1322
(3) Smoke point, min, mm, and	20 ^F	20 ^F	D 1322
Naphthalenes, max, vol, %	3	3	D 1840
Corrosion, copper strip, 2 h at 100°C, max	No. 1	No. 1	D 130
Thermal stability:			
Filter pressure drop, max, mm Hg	25 ^K	25 ^K	D 3241 ^M
Tube deposit less than	Code 3	Code 3	
Existent gum, max, mg/100 mL	7	7	D 381
Water reaction:			
Interface rating, max	1b	1b	D 1094
Additives	See 5.2	See 5.2	
Electrical conductivity, pS/m	1	1	D 2624 or D 4308

^A The requirements herein are absolute and are not subject to correction for tolerance of the test methods. If multiple determinations are made, average results shall be used.

^B The test methods indicated in this table are referred to in Section 10.

^C Fuels with an aromatic content over 20 volume % but not exceeding 25 volume % are permitted provided the supplier (seller) notifies the purchaser of the volume, distribution and aromatic content within 90 days of date of shipment unless other reporting conditions are agreed to by both parties.

^D The mercaptan sulfur determination may be waived if the fuel is considered sweet by the doctor test described in 4.2 of Specification D 235.

^E Other freezing points may be agreed upon between supplier and purchaser.

^F Fuels having a smoke point less than 20 but not less than 18 and a maximum of 3 volume % of naphthalenes are permitted provided the supplier (seller) notifies the purchaser of the volume, distribution and smoke point and naphthalenes content within 90 days of date of shipment unless other reporting conditions are agreed to by both parties.

^G For all grades use either Eq 1 or Table 1 in Test Method D 4529 or Eq 2 in Test Method D 3338. Test Methods D 2382 or D 4809 may be used as alternatives. In case of dispute, Test Method D 2382 shall be used.

^H Thermal stability test (JFTOT) shall be conducted for 2.5 h at a control temperature of 260°C, but if the requirements of Table 1 are not met, the test may be conducted at 245°C. Results at both temperatures shall be reported in this case. Tube deposits shall always be reported by the Visual Method: a rating by the Tube Deposit Rating (TDR) optical density method is desirable but not mandatory. If the deposit includes peacock (rainbow) colors, rate these as code P ("P" for peacock). If some part of the deposit does match the Color Standards, it shall also be rated. Record and report the rating of the maximum color which matches the Color Standards plus "P", or "P" only if the tube contains peacock deposits only. Fuels that give Test Method D 3241 tubes with peacock colors fail to meet thermal stability requirements.

^I A limit of 50 to 450 conductivity units (pS/m) applies only when an electrical conductivity additive is used and under the condition at point of use.

$$1 \text{ pS/m} = 1 \times 10^{-12} \Omega^{-1} \text{ m}^{-1}$$

^J Results obtained by Test Methods D 3828 may be up to 2°C lower than those obtained by Test Method D 56 which is the preferred method. In case of dispute, Test Method D 56 will apply.

^K Preferred SI units are 3.3 kPa, max.

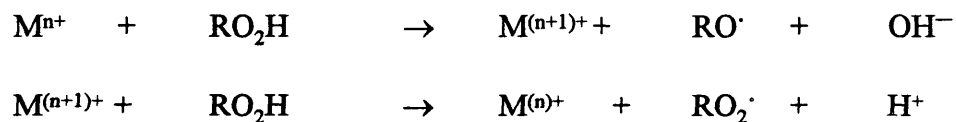
^L 1 mm²/s = 1 cSt.

Recent studies have shown that the high cost of domestic crude oil has resulted in the use of lower quality crude oils and shale oils which contain relatively higher concentrations of heteroatoms, aromatics, metals, and asphaltenes (Cernansky, 1984). Oil refiners were forced to increase the use of catalytic cracking to convert the branched hydrocarbons to middle distillate fuel and to blend it with straight run middle distillate to meet the increase in demand for middle distillate after World War II (Beaver, 1991). The stability of middle distillate depends on the refining process. Straight-run middle distillate is more stable than catalytic middle distillate, and the least stable is thermal middle distillate (Johnson, 1954). Lower quality crude oil produces lower quality middle distillate. Therefore cracked components in distillates produce both lower storage and thermal stability (Beaver, 1991; Cernansky, 1984).

Contact of copper surfaces with jet fuel increases the rate of deposit formation but steel does not (Walters et al., 1949). Dahlin et al., (1981) studied the effects of various nitrogen compounds (pyridines, quinolines, indoles and pyrroles) on Jet-A stability and concluded that their effect on deposition rates is related to the basicity of these nitrogen compounds. The relative order of effect of these compounds on rates of deposition is generally pyridines > quinolines >> indoles > pyrroles. The rate of deposit formation can be increased by addition of polysulfides, aliphatic mercaptans,

and thiophenols to JP-3 fuel (Johnson, 1954). Also he concluded that there are no large effects of nitrogen-containing compounds on the storage stability of jet fuel.

Deposit formation can be increased by adding metal ion complexes to fuel. When metal ions such as those of cobalt, manganese, copper and iron are added to fuel, the hydroperoxide decomposition is catalyzed as shown in the following reaction (Rahhal et. al., 1988; Walters et al., 1949):



In jet aircraft, fuel is used to cool turbine lubricants in its path to the combustion chamber. Heating fuel in the presence of oxygen can accelerate the rate of deposited gum formation which indeed can decrease the efficiency of heat exchangers and plug the fuel manifolds, combustor spray nozzles and filters which lead to engine operating difficulties. Deposit formation (or thermal instability of jet fuel) in aircraft engines can lead to high maintenance expenses for manufacturers and users of fuel (Nixon, 1962).

Thermal stability is a very important subject and many studies have been applied to improve jet fuel stability. Taylor (1969) studied the deposit formation of a series of paraffins and found that deposit formation at a given temperature is increased as the molecular weight of the paraffin is decreased. Also, branched paraffins form deposits more rapidly.

Bushueva (1971) concluded that sediment formation in jet fuels is mainly due to the oxidation of aromatic hydrocarbons and aromatics with branched side chains produce the maximum amount of deposit. Deposit formation is increased as the length of side-chains of naphthenic hydrocarbons increases. Also he concluded that thermal stability can be increased by removing polycyclic naphthenic or aromatic hydrocarbons.

Taylor (1969) investigated the effect of pure sulfur compounds such as sulfides, disulfides, thiols, and condensed thiophenes on deposit formation from hydrocarbons. He concluded that diphenylsulfide and benzothiophene have only small effects and the other sulfur compounds increase the rate of deposit formation.

Fuels are very complex and contain a large number of potential reactants for oxidation reactions. Therefore, a large number of reactions may occur producing a tremendous number of products. This makes mechanistic studies of jet fuel instability very challenging (Reddy et al., 1992).

As a result, one basic approach is to study one or two fuel components to simplify interpretation of deposit formation mechanisms. A model fuel has been developed by Daniel and his group (Worstell, 1980) which mimics stability behavior of jet fuels but contains only two components. Since aliphatic hydrocarbons are the major constituents in jet fuel, dodecane, which has a boiling point in the jet fuel distillate range, was selected as one component of the model fuel .

Tetralin was selected as the second component of the model fuel for the following reason:

1. Jet fuel specifications require that aromatic components amount to less than 20 volume per cent (ASTM D-1655-81).
2. Schwartz (1972) has shown that deposits are enriched in aromatics.
3. Tetralin is a naphthene which readily oxidizes to the hydroperoxide.

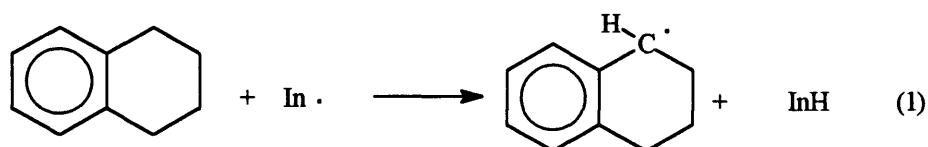
1.1. DEPOSIT FORMATION IN THE MODEL FUEL

Autoxidation of tetralin has been studied by many workers and they conclude that tetralin autoxidation is a first order reaction (George, 1946 a; George, 1946 b; George, 1946 c; Bolland and Gee , 1946a; Bolland and Gee , 1946b; Bolland and Gee , 1946c; Nixon, 1962; Nixon, 1962; Woodward, 1953; Robertson, 1948 a; Robertson, 1948 b; Robertson, 1948 c). Worstell 1980 studied the autoxidation of tetralin in dodecane and he found it to be first order in tetralin concentration. He proposed that deposit formation in the model fuel can be divided into four parts (1) formation of tetralin hydroperoxide (2) decomposition of tetralin hydroperoxide (3) further oxidation of the decomposition products (4) condensation of oxidation products.

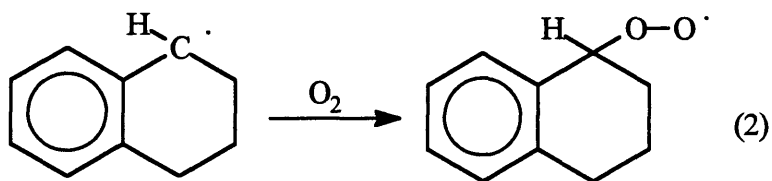
1.1.1. FORMATION OF HYDROPEROXIDE

The formation of the hydroperoxide in autoxidation of pure tetralin has been studied by several workers and is well understood (George, 1946 a; George, 1946 b; George, 1946 c; Bolland and

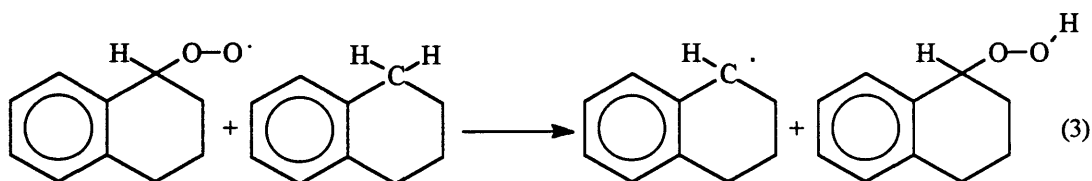
Gee , 1946; Bolland and Gee , 1946 b; Bolland and Gee , 1946 c; Nixon, 1962; Nixon, 1962; Woodward, 1953; Robertson, 1948 a; Robertson, 1948 b; Robertson, 1948 c). Autoxidation of tetralin is a typical free radical process involving: initiation, propagation and termination steps. Tetralin reacts with an initiator (In) to generate a tetralin free radical as in reaction (1) which initiates the autoxidation chain:



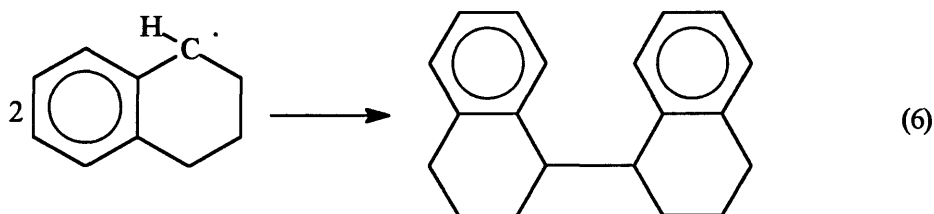
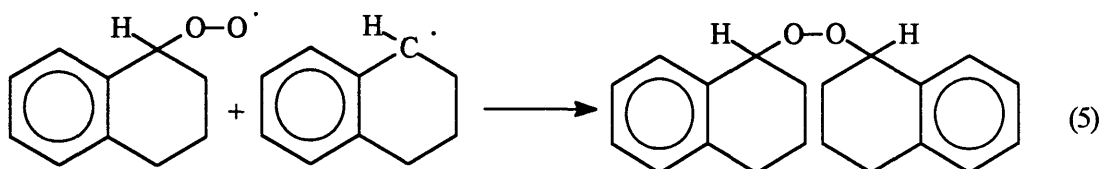
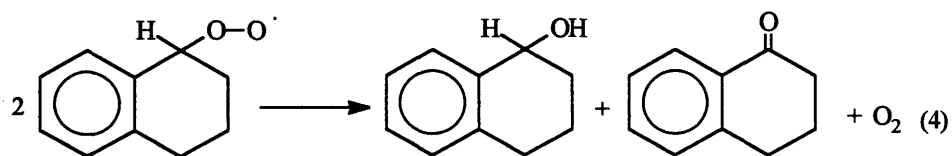
Propagation can be represented by reactions (2) and (3). Tetralin radical reacts with oxygen to produce tetralin hydroperoxide radical .



At sufficiently high oxygen concentrations reaction (3) is usually the rate controlling step (Beaver, 1991). Tetralin hydroperoxide radical reacts with another tetralin to produce tetralin hydroperoxide and another tetralin radical:

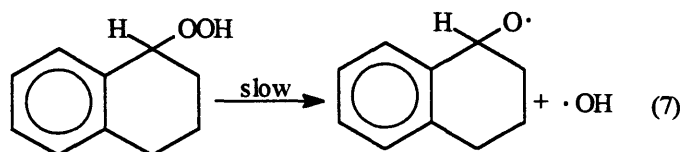


Reaction (4), (5), and (6) are possible termination reactions:

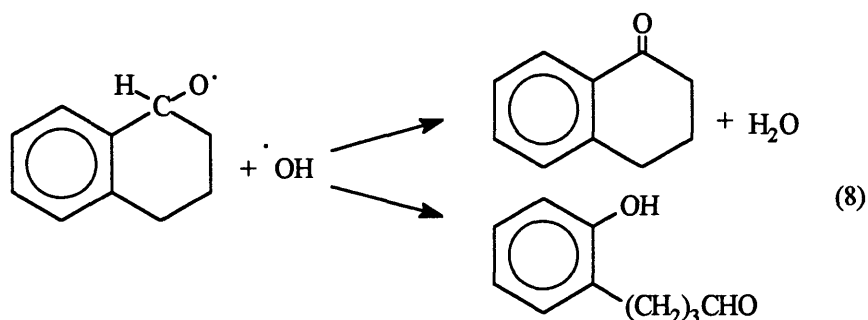


1.1.2. HYDROPEROXIDE DECOMPOSITION

Decomposition of tetralin hydroperoxide has been investigated by Robertson (1948). He suggested the following as possible reactions. Tetralin hydroperoxide can undergo a slow unimolecular homolysis reaction (7) and then rapid reactions of the free radical thus produced (8) (Robertson, 1948).

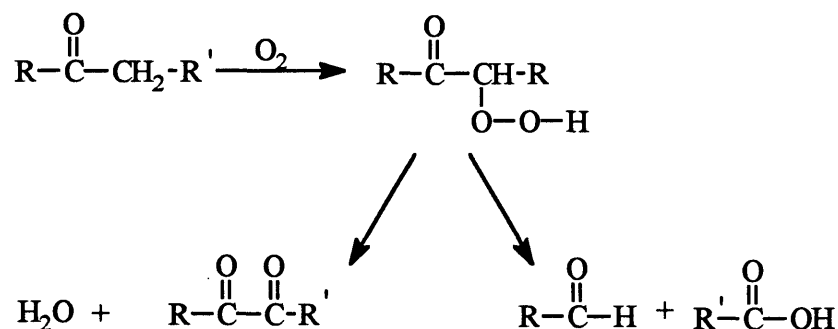


The more rapid second step mainly produces tetralone and γ -o-hydroxyphenylbutaldehyde as in reaction (8) (Robertson, 1948):

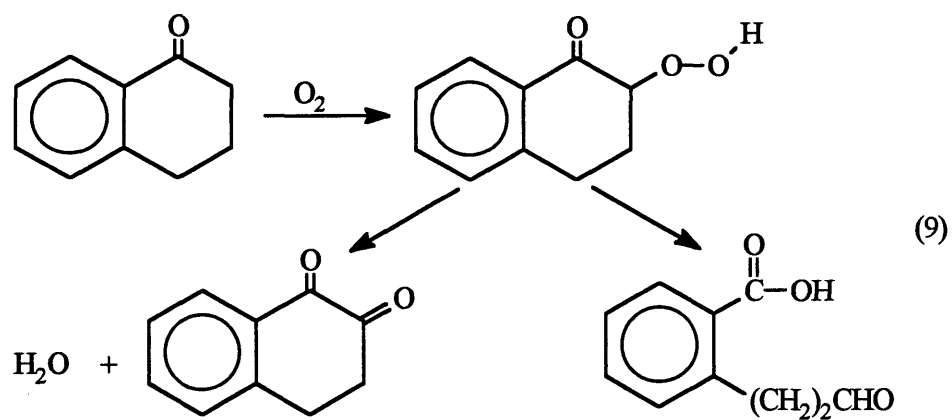


1.1.3. REACTION OF THE OXIDATION PRODUCTS

Farmer (1942) suggested that, in autoxidation of ketones, adjacent methylene groups are activated by the carbonyl toward hydroperoxide formation at the α position:



Therefore, tetralone which is a product of the autoxidation of tetralin, can be further autoxidized to give two products: tetrahydronaphthalene-1:2-dione and γ -o-hydroxyphenyl-butyric acid as in reaction 9 (Robertson, 1948):



Zarrabi (1987) identified the following components as oxidation products of 1-tetralone (Figure 2).

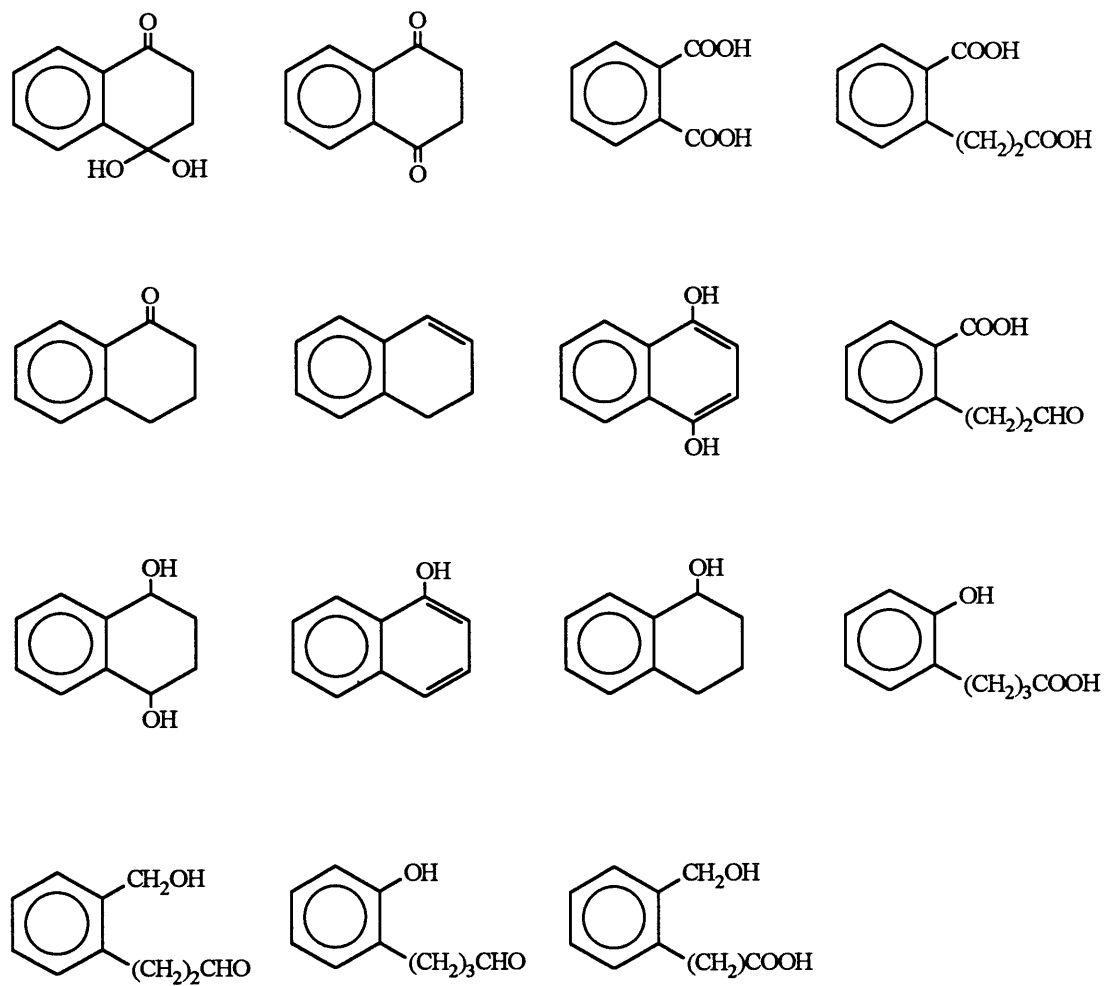
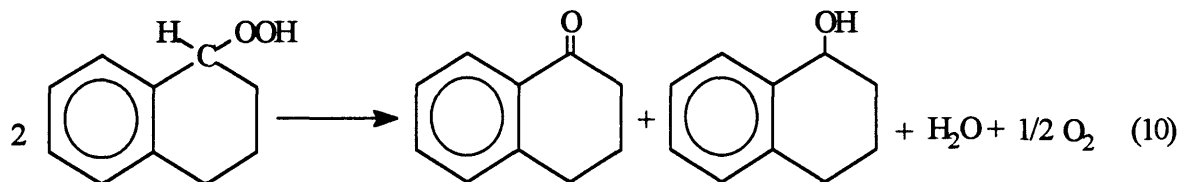
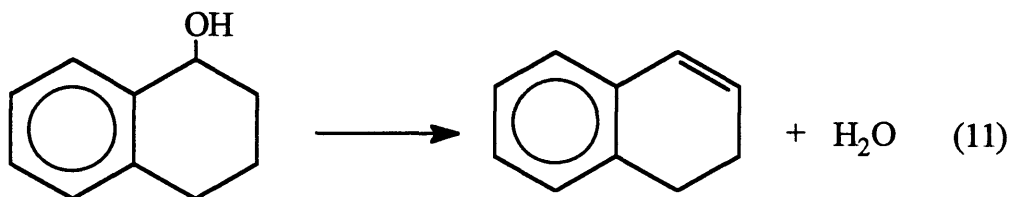


Figure 2: Oxidation products of 1-tetralone
(Zarrabi, 1987)

The hydroperoxide can disproportionate to tetralone and tetralol as in reaction (10) (Taylor, 1970):



1,2-dihydronaphthalene can be produced from the dehydration of the tetralol as in reaction (11) (Taylor, 1970):



1.1.4. FORMATION OF THE DEPOSIT

The oxidation products in the previous section do not represent actual deposit components. These monomeric oxidation products are generally more soluble in the model fuel and of lower molecular weight (average molecular weight of model deposit was found to be 600 (Zarrabi, 1987)) than the deposits.

Worstell (1980) prepared model deposit and Jet A fuel deposit by stressing model and Jet A fuel at 121° C for more than a week. Elemental analysis results showed that the model and Jet A deposits are similar (Table 2).

Table 2: Elemental analysis of the model deposit and Jet A deposit (Worstell, 1980).

Fuel sample	% C	% H	% N	%O (by difference)
Jet A	69.3	5.3	0.25	25.15
Model Fuel	70.2	6.1	0.29	23.41

Jet A deposit is a brown to black solid which is partially soluble in THF and CH_2Cl_2 . Model deposits are more soluble in these solvents. Both model and Jet A deposits have low volatility.

It is difficult to interpret the structure of model fuel deposits because of the large number of possible oxidation products of tetralin which may be involved in the process of the deposit formation. Also the low solubility and low volatility of the deposits make analysis difficult.

The autoxidation of tetralin is pseudo first order in tetralin concentration, i.e.

$$-\frac{d[T]}{dt} = k[T]$$

where $[T]$ represents the tetralin concentration and k is the rate constant when O_2 concentration is held constant (Bolland and Gee, 1946a,b,c).

Worstell (1980) studied the model fuel (dodecane/tetralin 10/1) system and obtained the first order rate constants in Table 3 at temperatures of 118, 121, and 129°C.

Table 3: Rate constants for the autoxidation of tetralin (Worstell, 1980)

Rate [Tetralin] /sec x10 ⁶	[Tetralin] mole/L	1000/T °k	k sec ⁻¹ x 10 ⁶
1.16	1.18	2.49	2.26
0.69	1.15	2.54	1.38
0.64	1.08	2.56	1.03

Worstell (1980) concluded that 1) in the model fuel, tetralin hydroperoxide and its oxidation products are involved in the process of deposit formation, 2) bases catalyze the decomposition of the hydroperoxide, and 3) the deposit which is formed from autoxidation of a solution containing 1-tetralone (0.5%) and tetralin hydroperoxide (0.5%) in dodecane in the presence of air is very similar to that from the model fuel. He suggested that the mechanism of deposit formation involves a disproportionation of the tetralin hydroperoxide and then condensation between tetralone and tetralin hydroperoxide. This mechanism is summarized in Figure 3.

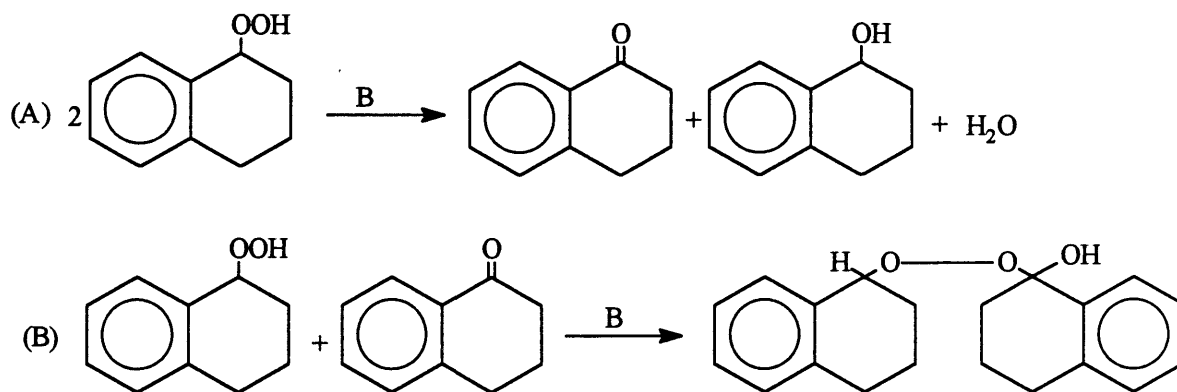


Figure: 3: Postulated mechanism for deposit formation. (A) disproportionation reaction of tetralin hydroperoxide and (B) condensation reaction between tetralone and tetralin hydroperoxide (Worstell, 1980).

Worstell studied the effect of tetralin hydroperoxide and its decomposition products on the rate of deposit formation and concluded that the addition of tetralone to the model fuel increases the rate of deposit formation. On the other hand, the addition of tetralol decreases the rate of deposit formation. He suggested that this decrease in deposit formation rate was because of the antioxidant capability of tetralol or because tetralol increases the solvating ability of the fuel. Zarrabi (1987) found that while tetralin hydroperoxide and tetralone react in the presence of air to produce deposits which are very similar in appearance (both visually and by IR spectroscopy) to model fuel deposit, no deposit formed when oxygen was excluded. Also, the oxygen content of Worstell's proposed deposit structure (15.68 %) is lower than the elemental analysis results for the model deposit (Table 2). Therefore, tetralone and tetralin hydroperoxide are not directly involved in a condensation reaction to form deposit. Further oxidation is required.

Zarrabi (1987) suggested the following as a possible scheme of deposit formation (Figure 4):

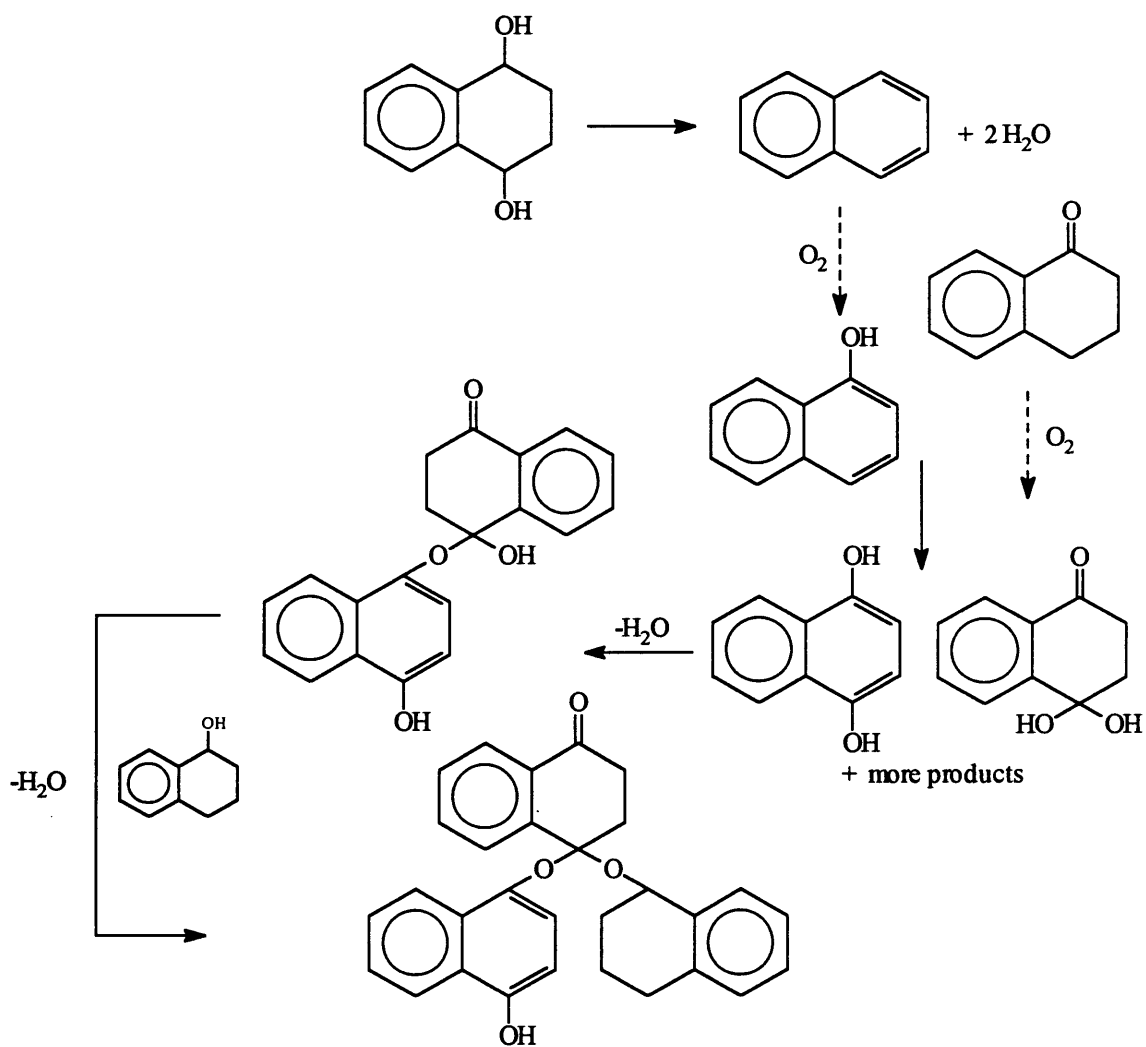


Figure 4. Possible scheme of deposit formation (Zarrabi, 1987).

Several possible mechanisms responsible for deposit formation can be postulated. For example,

1. Sequential autoxidation and condensations of hydroperoxide and ketone groups can, for example, produce such polymeric products as are shown in Figure 5. The other possibility is additional oxidation of tetralone to a diketone and then condensations of hydroperoxides and diketone groups can take place as in Figure 6 to produce oligomers.

2. Condensation of ring-opening oxidation products as in Figure 7 can occur.

3. Formation of ether linkages between tetralone oxidation products as in Figure 8 may be important.

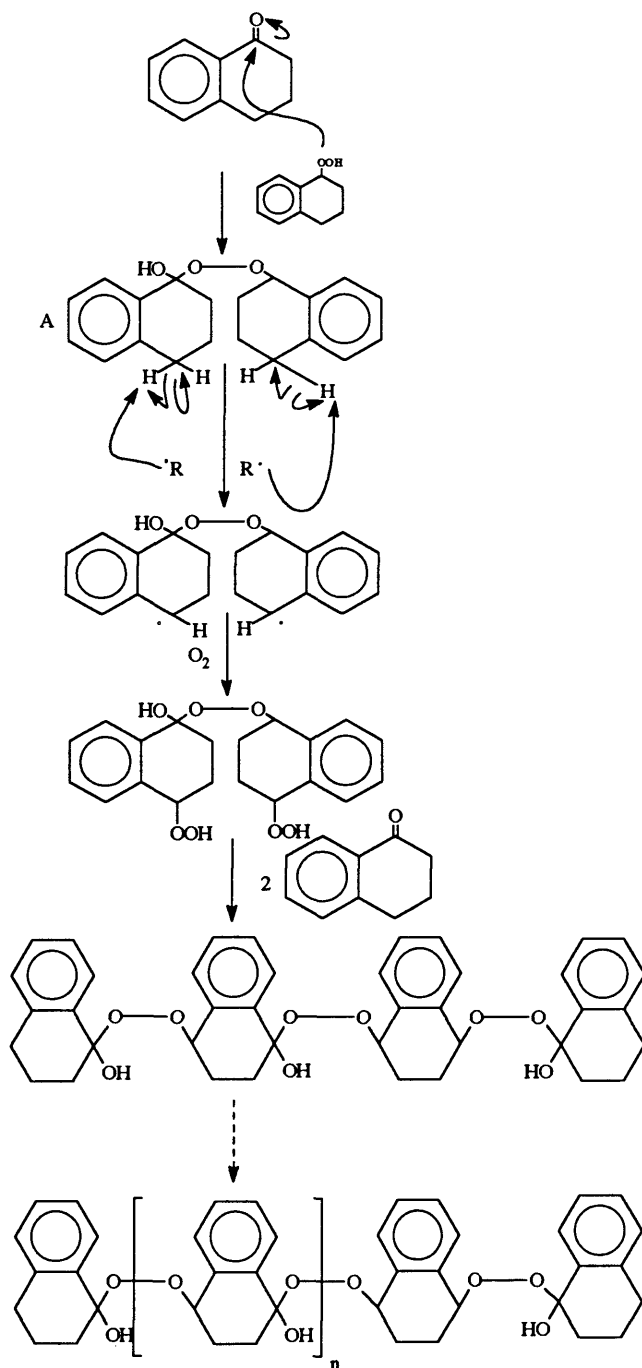


Figure 5: Possible mechanism for sequential autoxidations and condensations to produce polymeric products

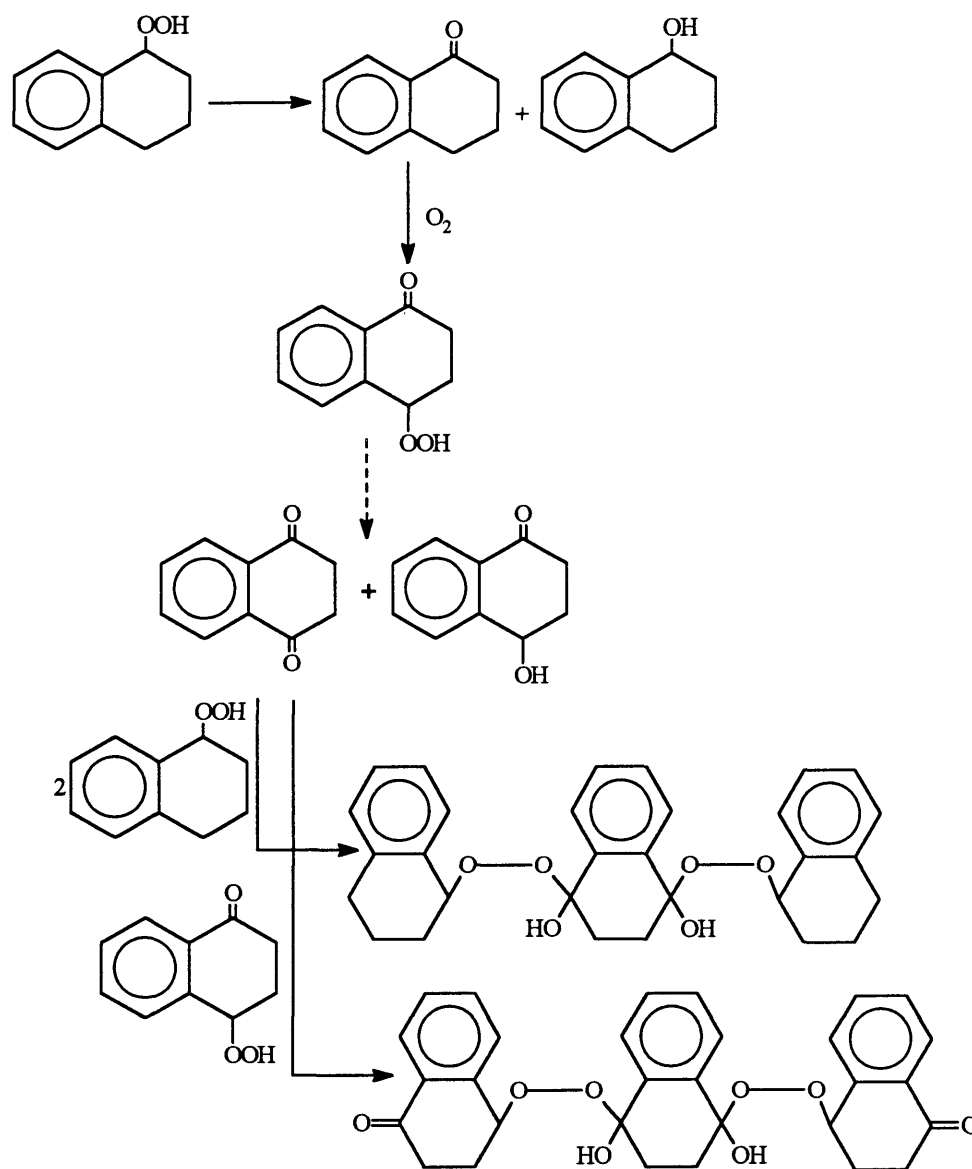


Figure 6: Possible mechanism for condensation reactions between hydroperoxide and diketone groups.

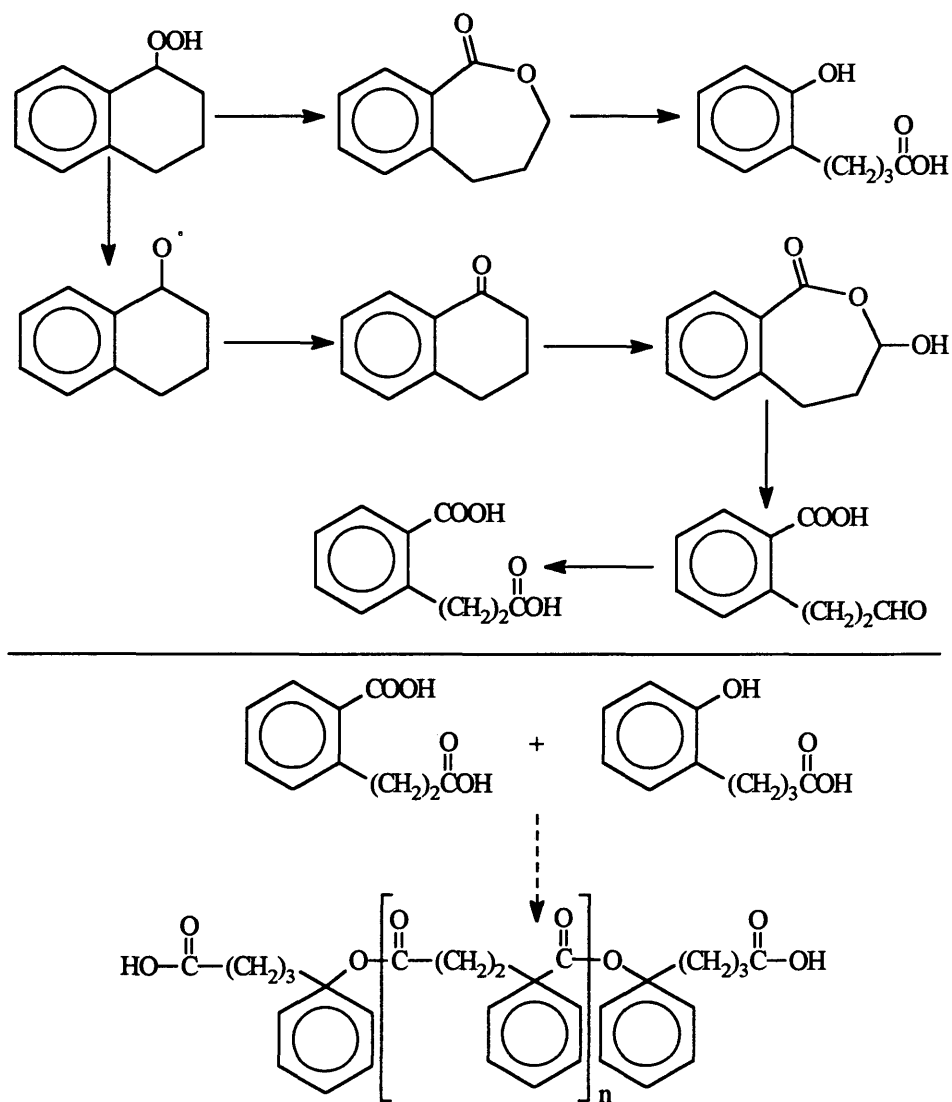


Figure 7: Possible mechanism of condensation reactions of ring-opening oxidation products.

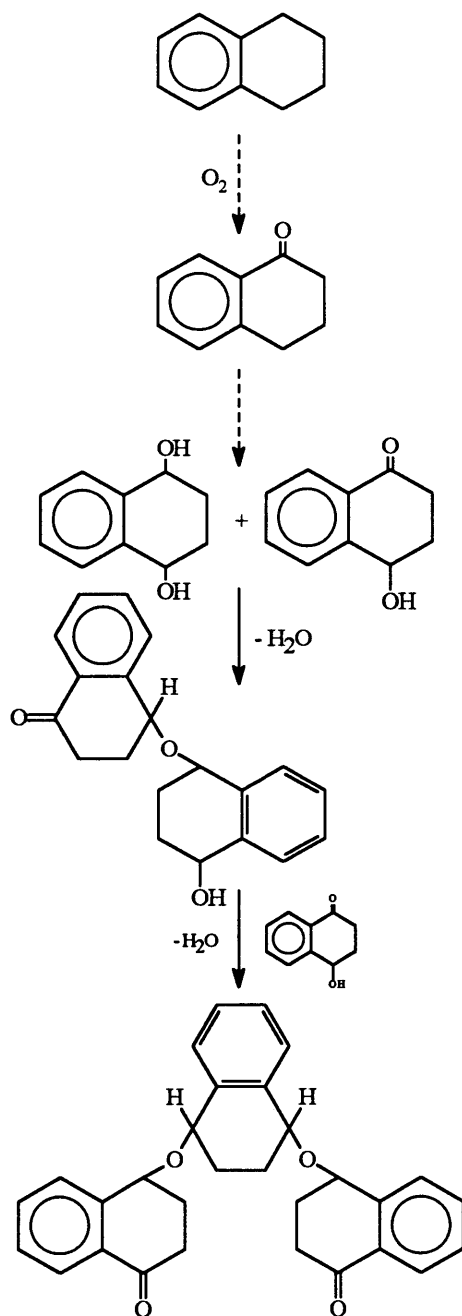


Figure 8: Possible mechanism for final deposit formation by condensation reaction of tetralone oxidation products.

The autoxidation of tetralin (in chlorobenzene) in the presence of radical initiators has been shown to obey the following rate law:

$$-\frac{dO_2}{dt} = k_3 \left(e_i \frac{k_7}{k_6} \right)^{\frac{1}{2}} [RH][\text{Initiator}]^{\frac{1}{2}}$$

Where e_i is the efficiency of initiation (Woodward, 1953).

Worstell (1980) investigated the effect of radical initiators (benzoyl peroxide and azobisisobutyronitrile) and bases (quinoline) on the rate of the deposit formation in Jet A fuel. He concluded that the initiators do cause an increase in the amount of deposit in the earlier stage of the reaction, but not at the end of the experiment period (7 days). Jet A fuel that was spiked with benzoyl peroxide formed less deposit after 7 days than did neat Jet A (Table 4) while Jet A spiked with quinoline formed more deposit.

Table 4: Effect of additives upon Jet A fuel instability. Quinoline at 5 ppm, azobisisobutyronitrile at concentration of 8.9×10^{-3} mole/L and benzoyl peroxide at a concentration of 1.56×10^{-2} mole/L (Worstell, 1980).

Time (Hours)	Control	Jet A + quinoline	Jet A + AIBN	Jet A + BP
	(g/mm ²) x 10 ⁷			
24	0.00	0.21	1.44	1.34
48	0.00	4.94	2.37	1.03
72	0.31	6.50	2.57	1.03
96	0.52	6.18	3.50	1.75
120	2.00	6.68	3.48	1.23
144	3.40	6.50	3.69	1.54
168	3.40	7.71	3.50	1.54

Worstell (1980) concluded that the transition state complex for the rate determining step probably involves acid-base reactions rather than free radical species. Zarrabi (1987) studied the effect of benzoyl peroxide and azobisisobutyronitrile (AIBN) on the model fuel (tetralin/dodecane 1/10) and he observed the same effects for benzoyl peroxide and AIBN in model fuel as reported by Worstell (1980) for Jet A.

These results of the benzoyl peroxide experiments raise a very interesting question. "How does benzoyl peroxide decrease the absolute amount of deposit?". One possible explanation is that acceleration of tetralin autoxidation to produce soluble intermediate products consumes oxygen leaving none available for the additional oxidation required to form deposits.

The objective of this study was, therefore, to determine if acceleration of the initial oxidation steps can be exploited to prevent or retard deposit formation.

To that end, the following were investigated:

1. The kinetics of tetralin autoxidation, and of tetralone and tetralol formation both with and without added initiators.
2. The effect of radical initiators on the amounts of deposit formed in model fuel and Jet A fuel.
4. The nature of the resulting deposits.

2. EXPERIMENTAL SECTION

2.1. PREPARATION OF CHEMICALS AND REAGENTS

Dodecane (Fluka AG, Buchs SG) was washed with concentrated H_2SO_4 until the acid layer was colorless to remove unsaturated compounds and other reactive species. The dodecane was then washed sequentially with 50 mL portions of distilled water, (10 %) aqueous sodium bicarbonate solution, and water; dried over potassium carbonate; filtered; and then distilled.

1,2,3,4-Tetrahydronaphthalene (tetralin) (Fluka AG, Buchs SG) was kept in a bottle containing activated ($380^\circ C$ for 24 hours) silica gel, then filtered, and distilled. The distilled tetralin was stored in a bottle containing activated silica gel to remove peroxides.

Benzoyl peroxide (Fluke GA, Chemische Fabrik CH-9470 Buchs), azobisisobutyronitrile (Riedel-deHaën), ferrous ammonium sulfate (J. T. Baker Chemical Co), ammonium thiocyanate (J. T. Baker Chemical Co), ferric chloride (anhydrous, purified grade, Fisher Scientific Company) were used as received.

All solvents used as the mobile phases for liquid chromatographic experiments were purchased as high performance liquid

chromatography (HPLC) grade reagents. Chloroform (Mallinckrodt), isooctane (Mallinckrodt, Nanograde), and acetonitrile (Fisher ChemAlert) were used as received.

Jet A fuel, originally obtained from the National Aeronautics and Space Administration (NASA) Lewis Research Laboratory Center, had been stored in a refrigerator for several years.

2.2. INSTRUMENTATION

An Incos 50 gas chromatograph mass spectrometer equipped with DB5 (30m x 0.25 mm i.d, 0.25 μ film thick) column and a CTC-A 2005 auto sampler was used to determine and monitor the tetralin, tetralone, and tetralol concentrations during autoxidation of model fuel. Injector temperature was 250° C, split ratio was 1:400, and 0.1 μ l of the sample was injected. The gas chromatograph was programmed to run from 70° C to 310° C at 8° C/min. These analyses were performed in Saudi Aramco Laboratory Department (Dhahran, Saudi Arabia).

A HP-5840 A gas chromatograph interfaced to an HP-5985 mass detector (quadrupole), equipped with a 15-m x 0.25 mm fused silica DB5-bonded-phase column (J & W Scientific) was used for

the deposit analysis. The operational conditions for the gas chromatograph were: injector temperature 230° C, initial temperature of the oven 70° C programmed to 250° C at 8° C/min., transfer line temperature 280° C. The ionization energy was 70 eV and the mass scanning range was from 35 to 350 amu. The deposits were dissolved in methanol/toluene (50/50, v/v) for analysis.

A Perkin-Elmer Series 4 liquid chromatograph with microprocessor-controlled solvent delivery system, HP 79925SI-5S4 Lichrospher SI-60 5 μ m, 125-4 NP HPLC column, and Perkin-Elmer LC-85B Spectrophotometric UV detector was used for the determination of compound purity and for monitoring the autoxidation of the tetralin and the formation of tetralin hydroperoxide, tetralone, and tetralol. The wavelength of the detector was set at 254 nm. The mobile phase consisted of 75% isooctane, 24.5% chloroform and 0.5% acetonitrile. 200 μ l of the model fuel liquid phase was diluted with 4 mL of 100 ppm o-nitroaniline (as internal standard) in mobile phase.

Pyrolysis mass spectral (Py-MS) analysis of deposits was obtained using an Extrel Model EL-400 triple quadrupole mass spectrometer, fitted with a Curie-point pyrolysis inlet. A Fischer Model 0310 (1 kW) rf generator was used to supply power to the Curie-point coil. The solids were loaded onto ferromagnetic wires (Curie point 310°C) in methanol/toluene solution. Solvent was evaporated prior to analysis.

A Digilab FTS-20/80 FT-IR was used for infrared spectral analyses. FT-IR analysis of deposit was performed by spreading the deposit solution (model deposit dissolved in methanol/toluene 50/50) onto a CaF_2 window and evaporating the solvent in a stream of air.

Organic peroxide content of initial and final deposits formed without initiators (to avoid interferences from the additives) was determined using a ferrous thiocyanate colorimetric method. Organic peroxides can be reduced in an acidified solution of ferrous thiocyanate in methanol. Spectrophotometric measurement of the resulting ferric thiocyanate then can be used to analyze peroxide content. (Siggia) The ferrous thiocyanate reagent was prepared by dissolving 1 g of ammonium thiocyanate and 1 ml of 25% by weight sulfuric acid in 200 ml of methanol. Finely pulverized ferrous ammonium sulfate (0.2 gram) was dissolved in the solution. The reagent was purged with nitrogen, and kept in a brown glass-stoppered bottle. This solution was prepared daily. Figure 9 shows a linear calibration curve for various standard concentrations of ferric chloride. Solutions of 0.00407 g of the initial deposit and 0.00573 g of the final deposit in 25 mL methanol were prepared. One ml of each solution was introduced into a 25 mL volumetric flask and diluted to the mark with ferrous thiocyanate reagent. The colorimeter cell was filled with the mixture and after 10 min. its absorbance was measured using a DU-2 spectrophotometer at

422 nm. Zero absorbance was set by using a blank of the ferrous thiocyanate reagent. Jet A deposit samples that had been stressed for 2, 4, 6, 8, 10, 12, 14, and 17 days were dissolved in 0.5 ml of a mixture of tetrachloroethylene/ methanol (50/50, v/v). 0.5 ml of the Jet A deposit solution was diluted with 2 ml of ferrous thiocyanate reagent. 0.5 of the Jet A liquid phase was diluted with ferrous thiocyanate reagent.

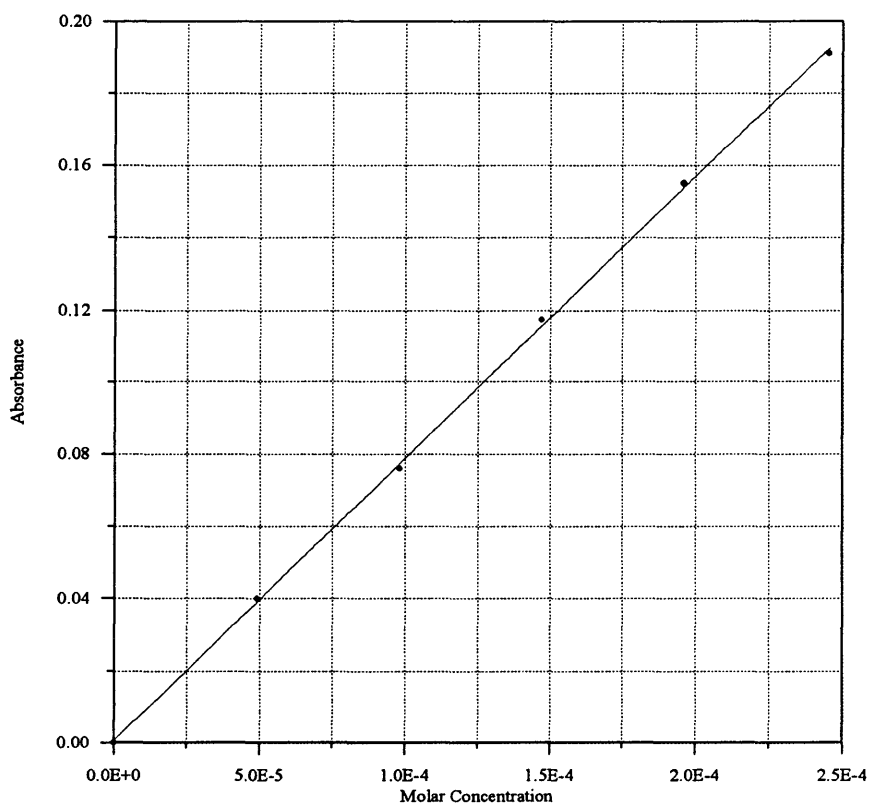


Figure 9: Calibration curve for ferric chloride standards (peroxide determination).

2.3. AUTOXIDATION OF TETRALIN IN MODEL FUEL

A. Two sets of model fuel and jet fuel samples were prepared. One half (0.5) mL of model fuel (dodecane/tetralin, 10/1) or Jet A was introduced into a 10 mL ampule (Wheaton) resulting in a fuel to air ratio of 1/19. Each set consisted of 18 samples. Each 10 mL ampule was cooled to -55°C using a dry ice/acetone bath to minimize vapor pressure of the solution and sealed using an O_2 /natural gas torch. The two sets of samples were placed in an oven at $127^{\circ}\text{C} \pm 2$. At 4, 12, 24, 48, 72, 96, 120, 144, and 168 hours, two samples of each set were removed from the oven. The exterior of each ampule was cleaned with methanol and dried. The tip of the ampule was broken off, the solution was removed using a Pasteur pipette, and transferred to a screw cap vial for later analysis by HPLC. Three ml hexane was introduced into the ampule which was then placed in an ultrasonic bath for 5 min. This process was repeated three times with three mL portions of hexane to remove model fuel liquid phase. The ampule was then dried using a stream of air and weighed. Deposit adhering to the ampule was then dissolved in three 3-ml portions of methanol/toluene (50/50). The ampule was then air dried and weighed again.

B. In a second set of experiments, one-half mL of model fuel (dodecane/tetralin, 10/1, V/V) or Jet A was introduced into a three dram vial (Baxter Healthcare Corporation) and covered with Teflon sheet and sealed with a screw cap. The above procedure was used for collecting the reaction mixture and weighing the vials.

C. In a third set of experiments, one-half-mL portions of model fuel were introduced into 40 mL vials and then sealed with a Teflon-coated silicone septum (Supelco). The above procedure was used for collecting the reaction mixture and weighing the vial. This method was adopted to stress all model fuel samples.

2.4. EFFECT OF RADICAL INITIATORS ON MODEL AND JET FUEL INSTABILITY.

Stock solutions in model fuel of 2000 ppm benzoyl peroxide and 2000 ppm azobisisobutyronitrile (AIBN) were prepared. The stock solutions were diluted with model fuel to prepare the following concentrations: 100 and 1000 ppm of benzoyl peroxide or

AIBN. One half (0.5) mL of each solution was introduced into a vial or ampule and the above procedure was used to collect and weigh the deposit

All deposits used for characterization were prepared as follows: One half mL of model fuel (with or without 1000 ppm of benzoyl peroxide or AIBN) was introduced into a 40 mL vial and then sealed with a Teflon-coated silicone septum. The samples were then held at 127 °C for up to eight days. Deposits were collected after one day (initial deposit) and after eight days (final deposit). Initial and final deposits were dissolved in 25 mL of 50/50 methanol/toluene (deposit solution). The deposit weight was determined by difference. The deposit solution was analyzed by GC-MS, Py-MS, FT-IR, and for peroxide content as described above.

3. RESULTS AND DISCUSSION

3.1. AUTOXIDATION OF MODEL FUEL

It is very challenging to do mechanistic studies of jet fuel instability because of the large number of components and large number of possible reactions producing a tremendous number of products. As a result it is desirable to use a model fuel (dodecane/tetralin 10/1 V/V) which contains only two components and which mimics the stability behavior of jet fuels. In this model fuel, dodecane acts as a solvent for the tetralin autoxidation reactions; no significant oxidation of dodecane occurs under the experimental conditions used. (Zarrabi, 1987).

In this study, the rate of tetralin autoxidation at $127^{\circ}\text{C} \pm 2$ was measured and found to be first order in tetralin concentration with a rate constant of 9.05×10^{-6} (Figure 10), which is greater than that (2.26×10^{-6}) measured by Worstell. This difference may perhaps be attributed to the differences in the type of glass containers used. Christian (1958) concluded that the type of glass can affect the degradation rate of many fuels. He reported that soft glass has an inhibitory effect on the degradation of fuels, but borosilicate glass is essentially inert.

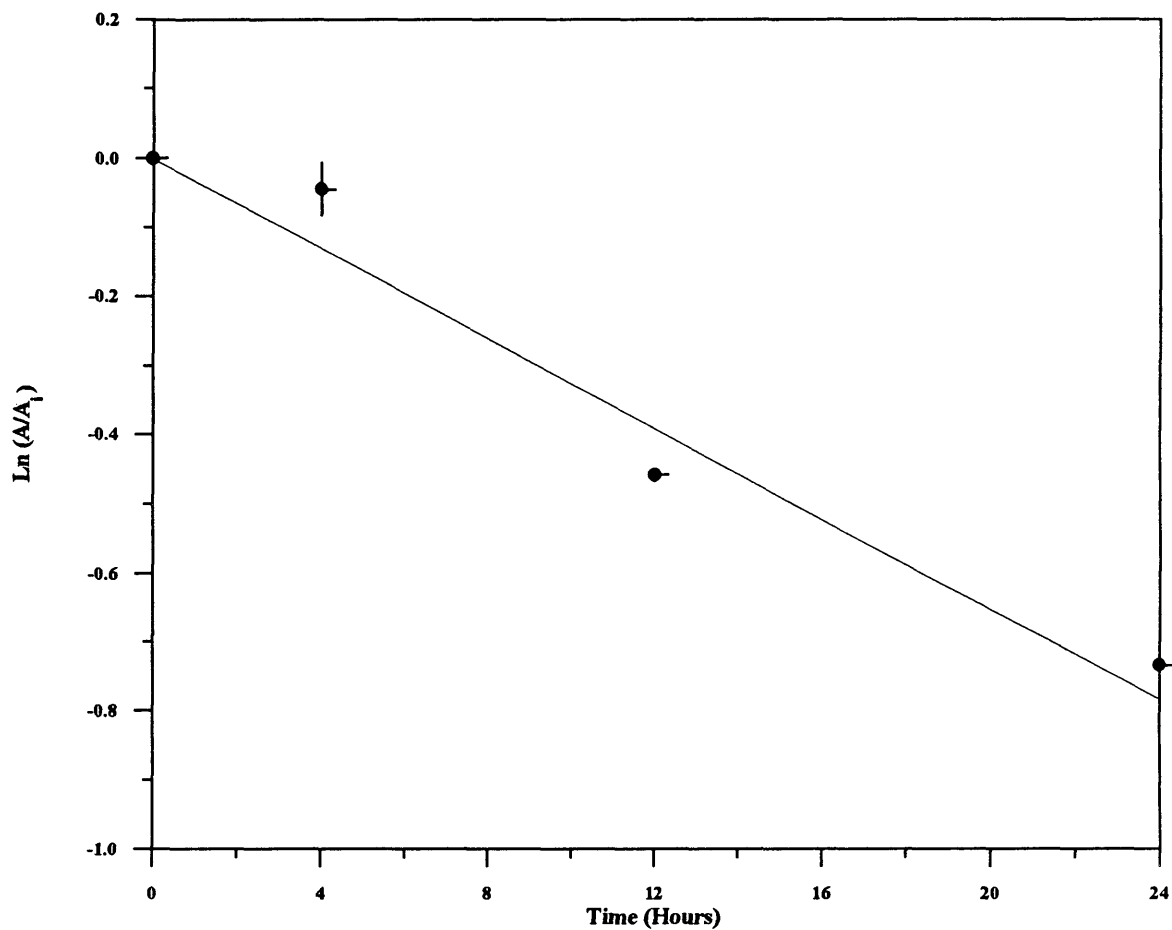


Figure 10: Rate of tetralin autoxidation. Error bars define range of duplicate determinations.

Note: A = tetralin concentration.
 A_i = tetralin Initial concentration.

In this study, model fuel was thermally stressed in various containers. The first experiment, which was described in section (2.3.1.A), was not reproducible. This was exhibited in differences in color, weight, and concentration of intermediate products in duplicates. Imperfect sealing of the ampules may have contributed to the variations.

Therefore, 3 dram vials were used to have more control in sealing the vial. Teflon was used between the lid and the vial to avoid contamination. The reducibility of this experiment was acceptable, but the amount of deposit produced was not detectable. An HPLC method used to monitor the reactions provided good data for concentrations of tetralin hydroperoxide, tetralone, and tetralol, but not for tetralin. Tetralin concentration decreased during the initial stage of the process but appeared to increase during the intermediate and final stages. This error arose from lack of resolution of tetralin from oxidation products in the HPLC method.

As a result, we decided to carry out the reaction in a larger volume of air (40 mL vial) to produce more deposit and to use a GC-MS technique to monitor the process.

Figure 11 shows fast autoxidation of tetralin in the early stage of the process (up to 1 day). No further autoxidation occurs to the end of the process. This might be attributed to the fact that oxygen concentration was too low to permit further autoxidation

of tetralin or that other components are autoxidized more easily than tetralin. After four hours, tetralone starts to form and then at 72 hours its concentration starts to decrease. Tetralol is also observed at about 4 hours and disappears after 48 hours. Deposit forms rapidly in the early stages of the reaction; the deposit formation rate falls between 48 and 72 hours, and then increases again.

This study shows that at 127°C there are at least three stages of deposit formation: early stage (first day), intermediate stage (2-3 days), and final stage (4-8 days) as shown in Figure 11.

In the early stage, as the tetralin concentration decreases, tetralone and tetralol concentrations increase, and the amount of deposit increases.

In the intermediate stage, the rate of deposit formation decreases. One possible explanation is that a second mechanism for deposit formation takes place at the same time that initial deposit is changing. If these changes involve weight loss then the net deposit weight may become essentially constant.

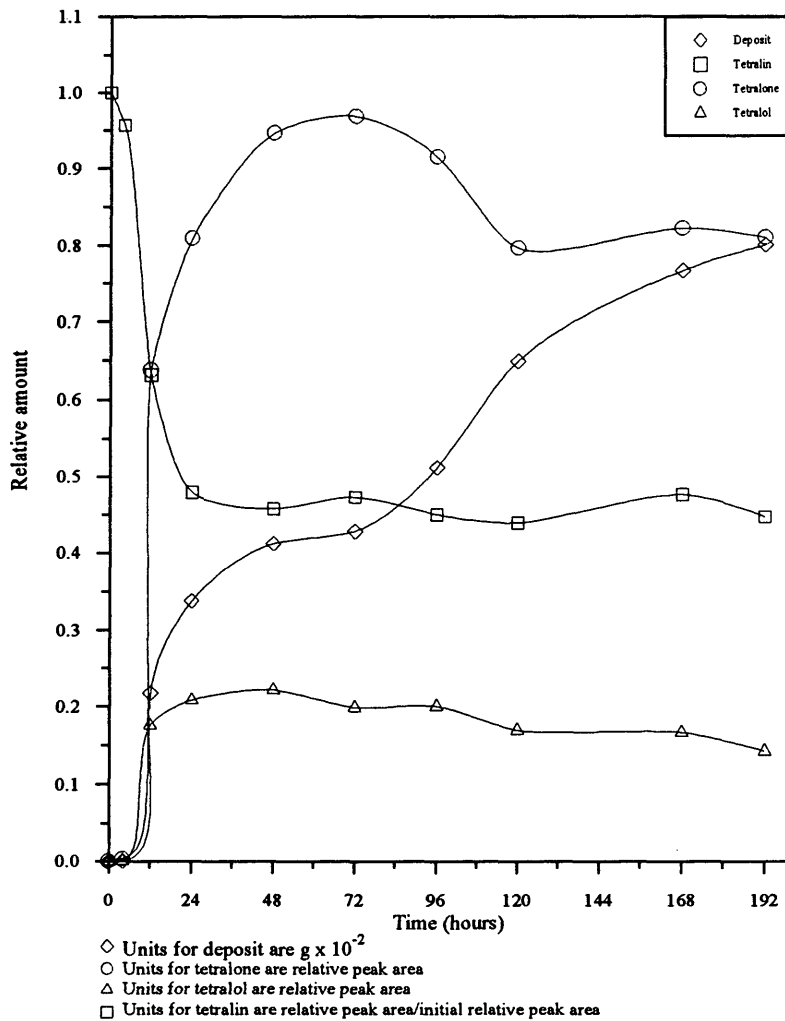


Figure 11: Kinetics of the autoxidation of tetralin and of formation of tetralone, tetralol, and deposits.

In the final stage, the concentration of tetralone and tetralol decrease and then stay constant to the end of the process while the amount of deposit continues to increase. This means that tetralone and tetralol are not directly involved in the final deposit formation process but their further oxidation products participate in deposit formation.

3.2. EFFECT OF RADICAL INITIATORS UPON MODEL FUEL STABILITY

The rate of the tetralin autoxidation in dodecane solution was found to be increased by the addition of both benzoyl peroxide and AIBN as shown in Figures 12 and 13. However, the rate changes do not follow the rate law reported by Woodward (1953). When the observed rate constant was divided by the square root of the initiator concentration, a constant was not obtained. Table 5 shows the observed rate constants for tetralin autoxidation in dodecane solution in the presence of these initiators.

The effects of the initiators on tetralone and tetralol concentrations and on the amount of the deposit formed during the reaction are shown in Figures 14, 15, 16, 17, 18 and 19. In general, the addition of either benzoyl peroxide or AIBN increases the rates of tetralone, tetralol, and deposit formation, compared to those without initiators in the early stages of the process. The addition of initiators decreases the tetralol concentration during the intermediate and final stages, compared to those without initiators (Figures 16 and 17).

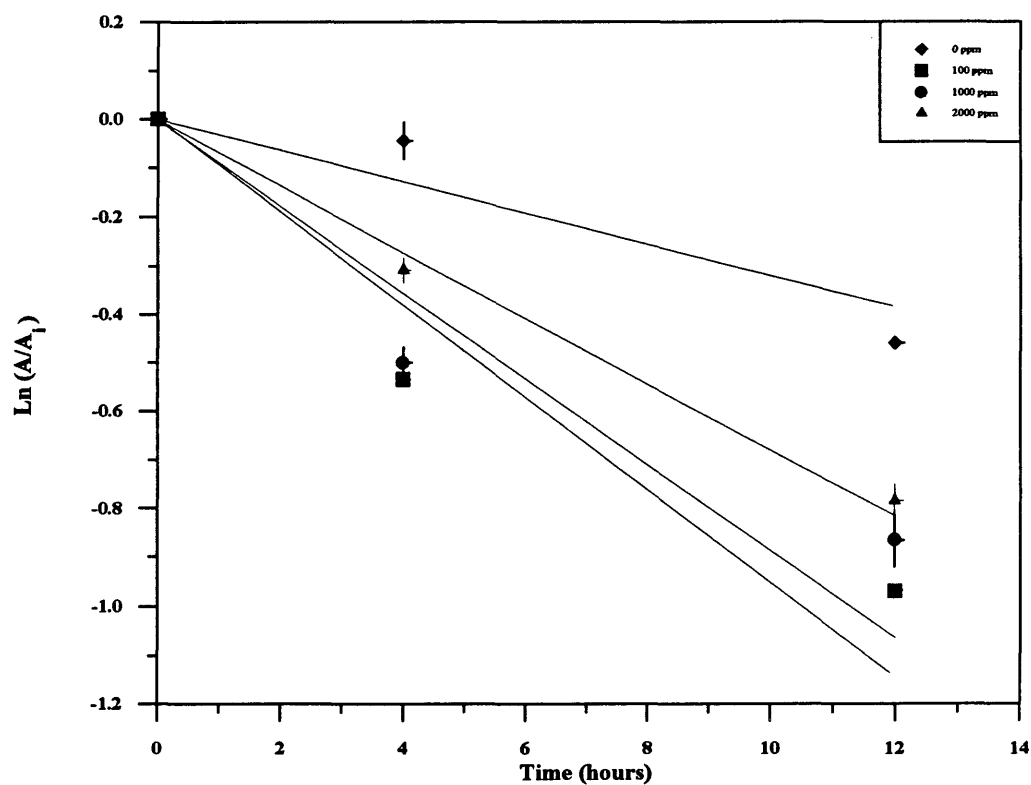


Figure 12: Rates of tetralin autoxidation with additive (benzoyl peroxide) and without additive. A is tetralin concentration and A_i is initial tetralin concentration. Error bars define range of duplicate determinations.

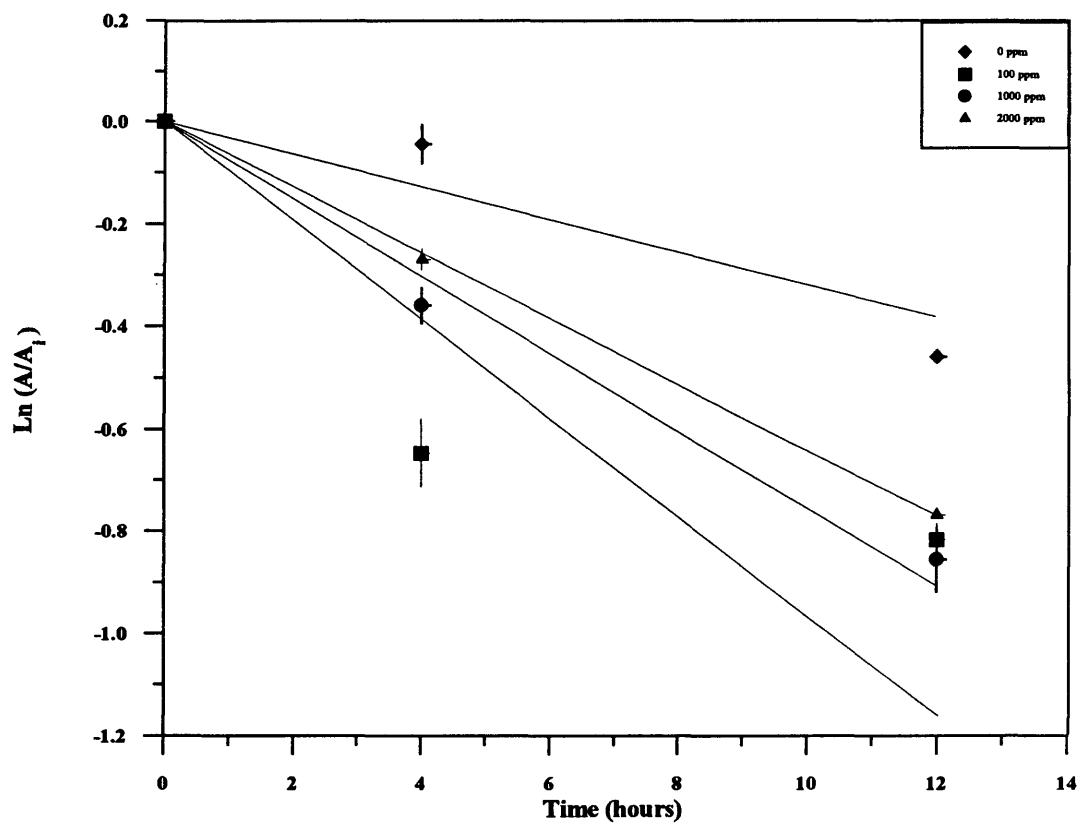


Figure 13: Rates of tetralin autoxidation with additive (AIBN) and without additive. A is tetralin concentration and A_i is initial tetralin concentration. Error bars define range of duplicate determinations.

Table 5: Rate constants of tetralin autoxidation with and without initiators (from slopes in Figures 12 and 13).

Tetralin/Dodecane (1/10, v/v)	k $s^{-1} \times 10^{-5}$	$k/[init.]^{1/2}$ $\times 10^{-6}$
No additive	0.905	
BP 100 PPM	2.64	2.64
AIBN 100 PPM	2.66	1.66
BP 1000 PPM	2.47	0.78
AIBN 1000 PPM	2.08	0.66
BP 2000 PPM	1.89	0.42
AIBN 2000 PPM	1.79	0.40

Samples with initiators show (Figures 14 and 15) that tetralone concentrations start to decrease at the beginning of the intermediate stage and then increase again. The formation of tetralone at this stage (intermediate stage) may not arise from the decomposition of tetralin hydroperoxide because the autoxidation of tetralin was stopped in the early stage and HPLC determination of the of the ampule samples show that tetralin hydroperoxide forms and decomposes very quickly during the stressing of the model fuel (Appendix C). One possible explanation for the second increase in tetralone concentration is further oxidation of tetralol in solution by peroxide linkages in the initial deposit or elimination reactions of intermediate oxidation products to produce tetralone (see Figure 20 for an example).

Figures 21, 22, 23, 24, 25 and 26 show concentrations of tetralin , tetralone, tetralol, and weights of deposit formed for model fuel without additives and with various concentrations (100, 1000, and 2000) of both benzoyl peroxide (BP) and azobisisobutyronitrile (AIBN).

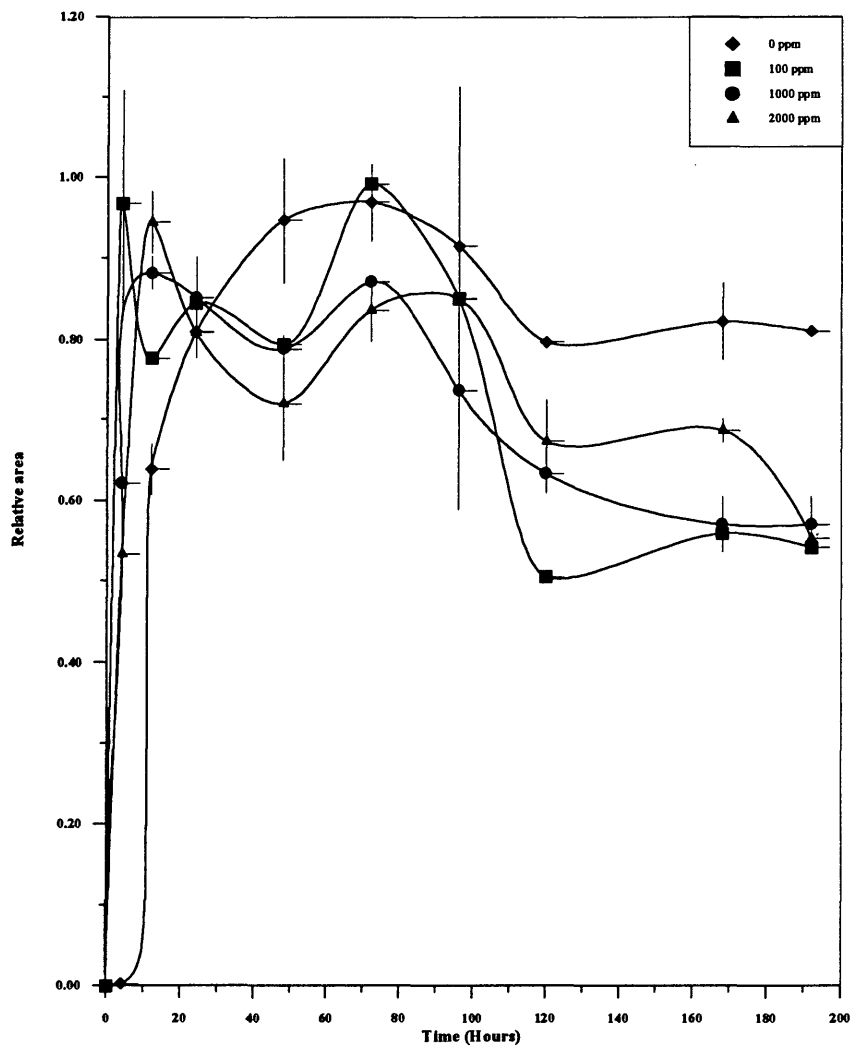


Figure 14: Kinetics of tetralone formation with and without additive (benzoyl peroxide). Error bars define range of duplicate determinations.

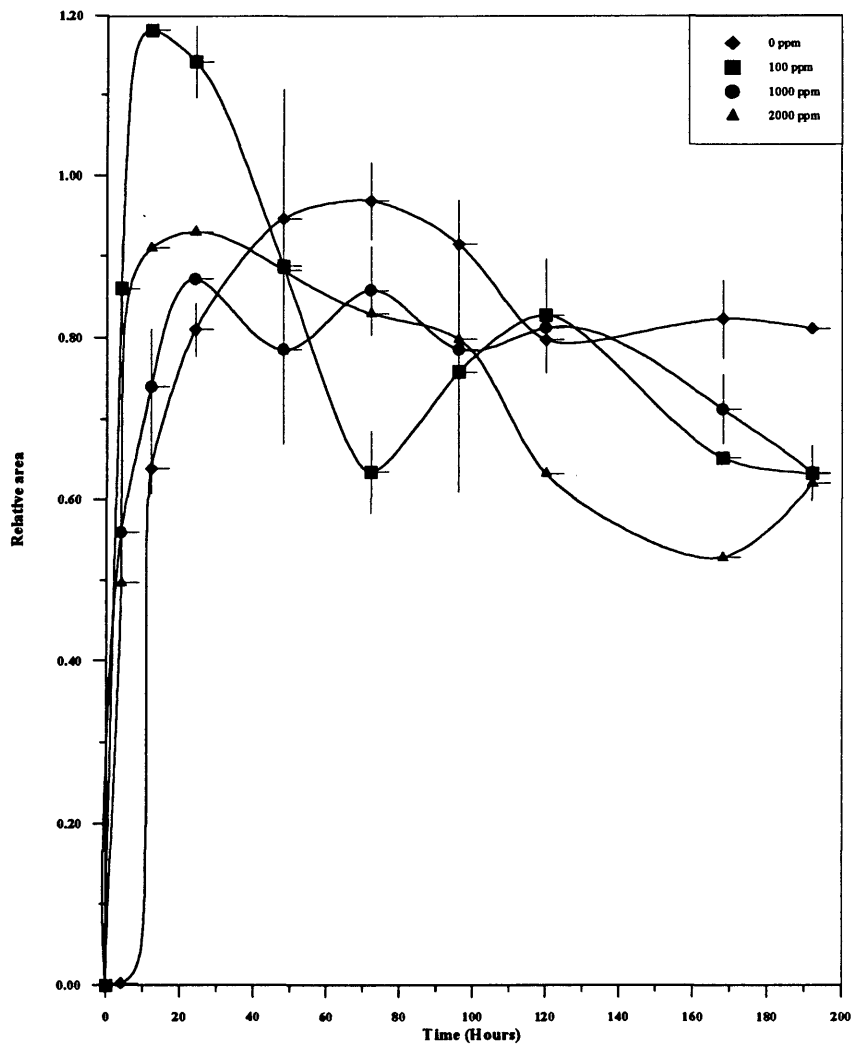


Figure 15: Kinetics of tetralone formation with and without additive (AIBN). Error bars define range of duplicate determinations.

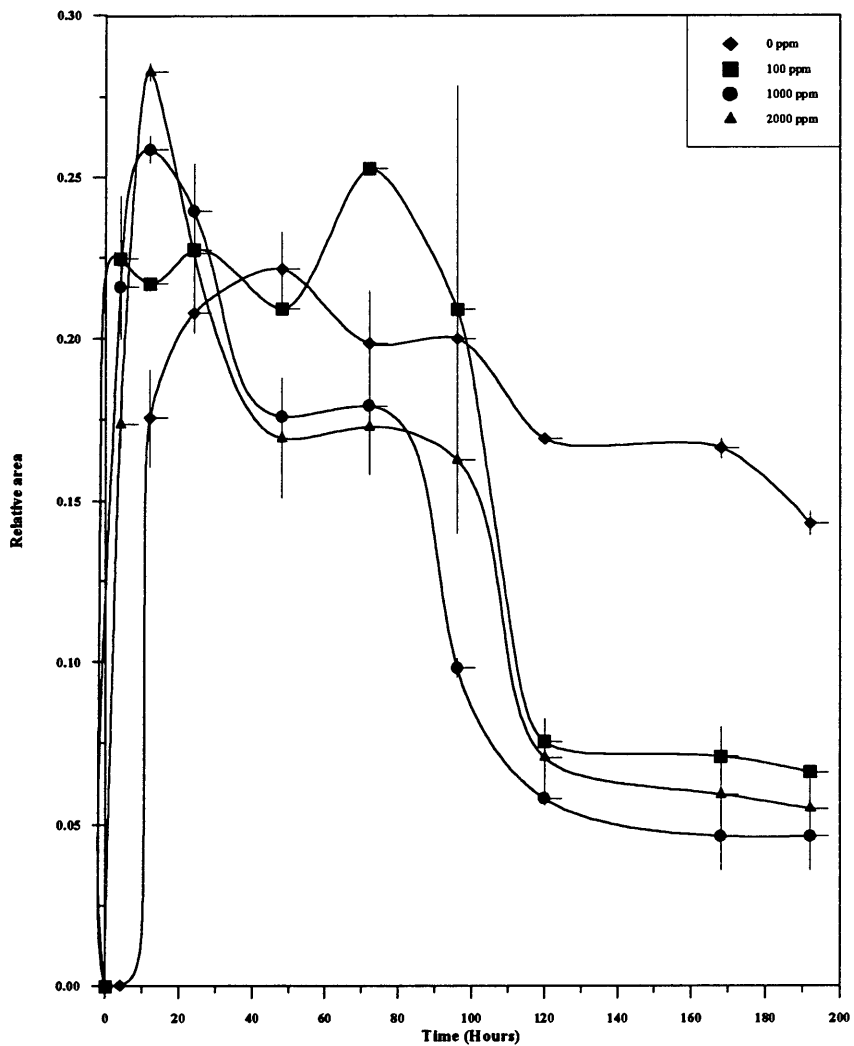


Figure 16: Kinetics of tetralol formation with and without additive (benzoyl peroxide). Error bars define range of duplicate determinations.

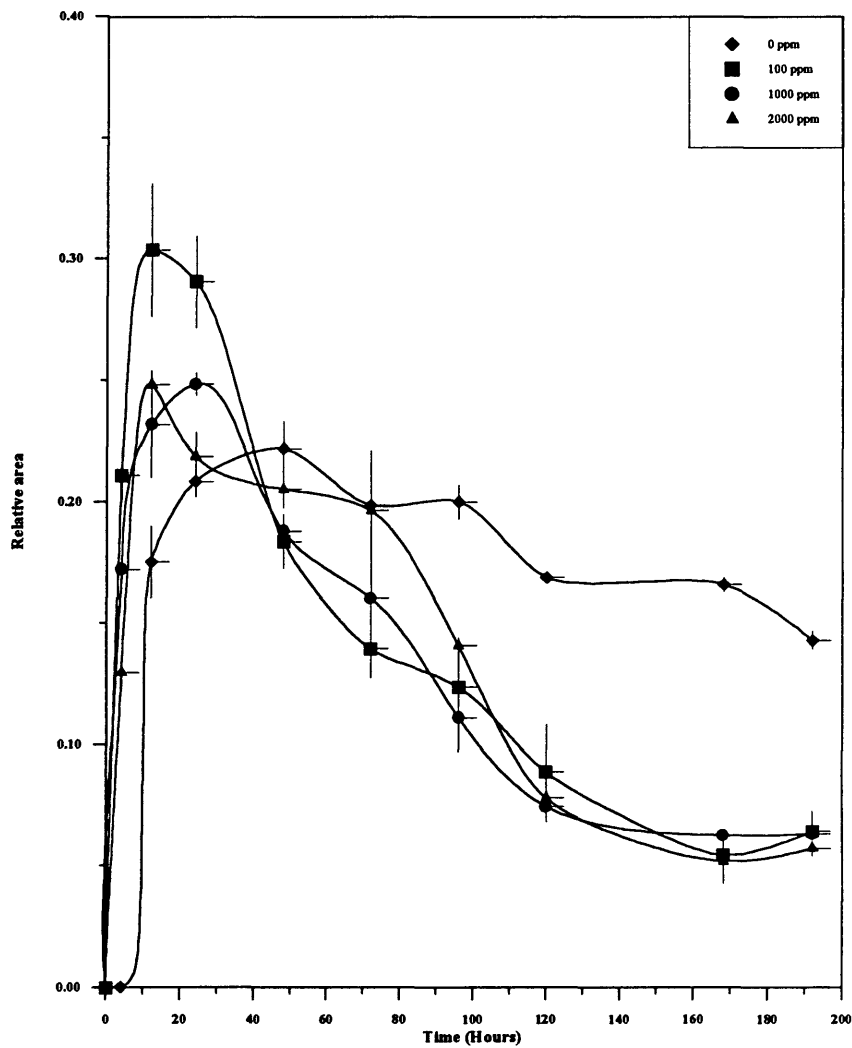


Figure 17: Kinetics of tetralol formation with and without additive (AIBN). Error bars define range of duplicate determinations.

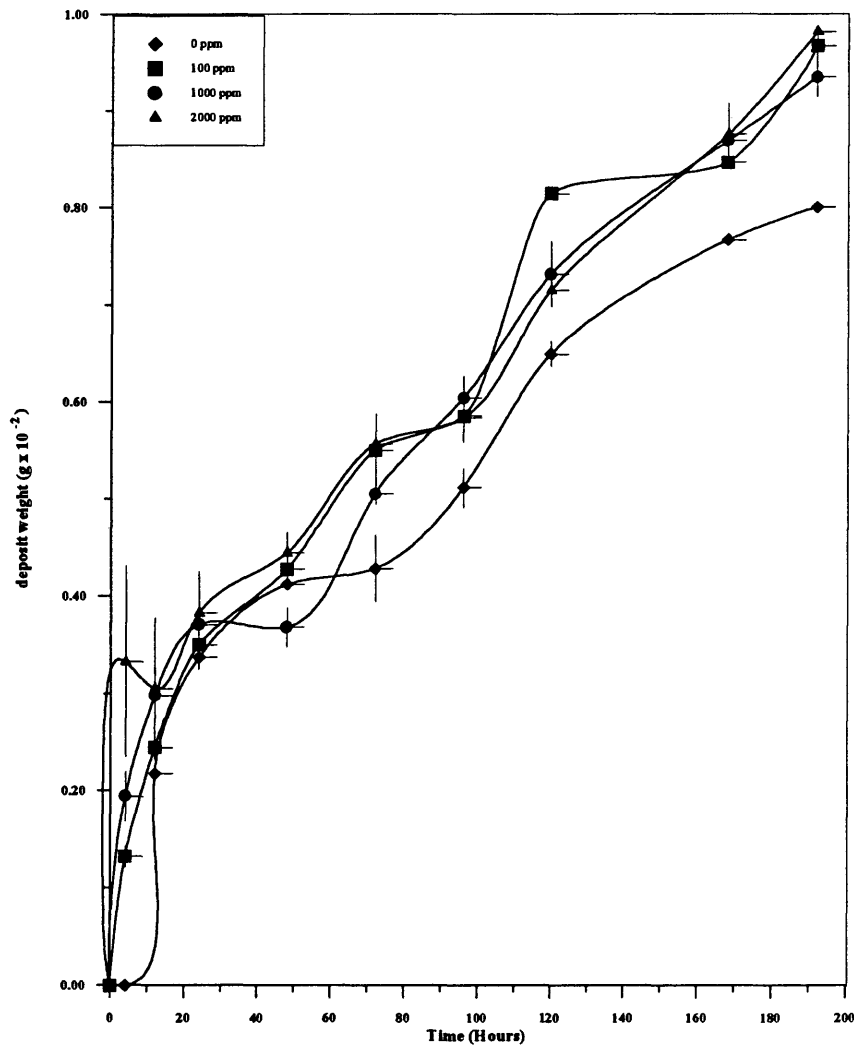


Figure 18: Kinetics of deposit formation with and without additive (benzoyl peroxide). Error bars define range of duplicate determinations.

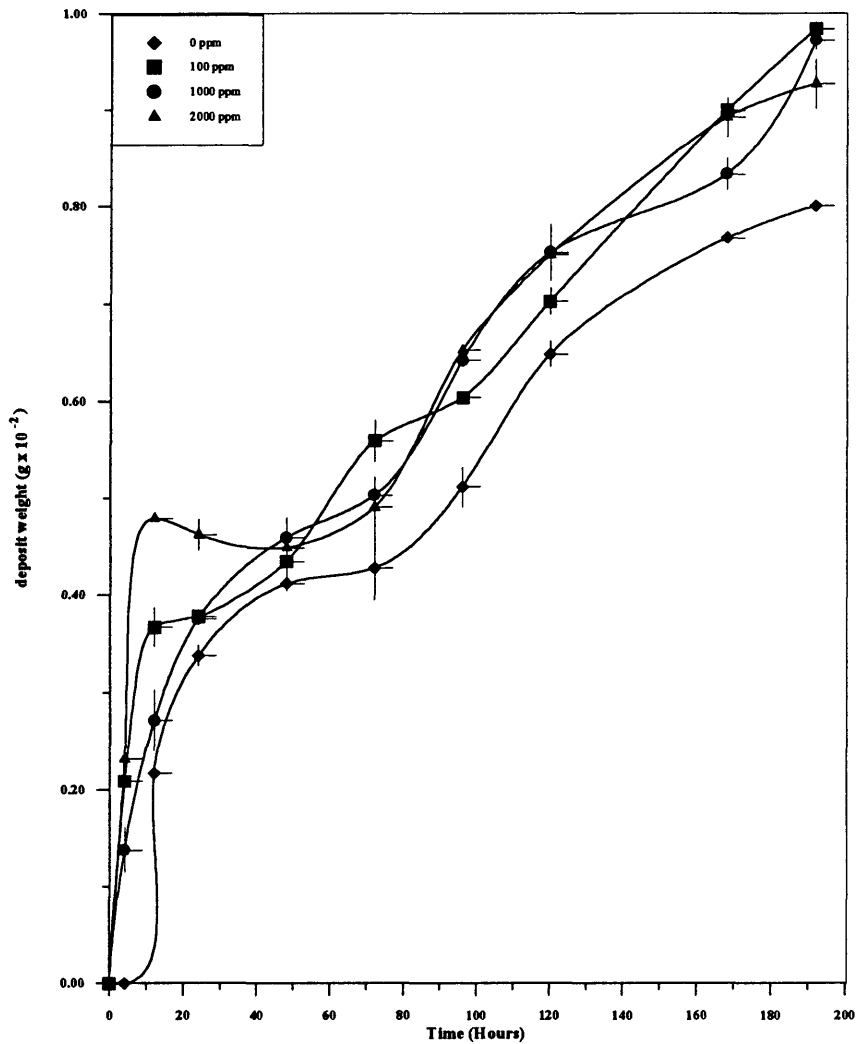


Figure 19: Kinetics of the deposit formation with and without additive (AIBN). Error bars define range of duplicate determinations.

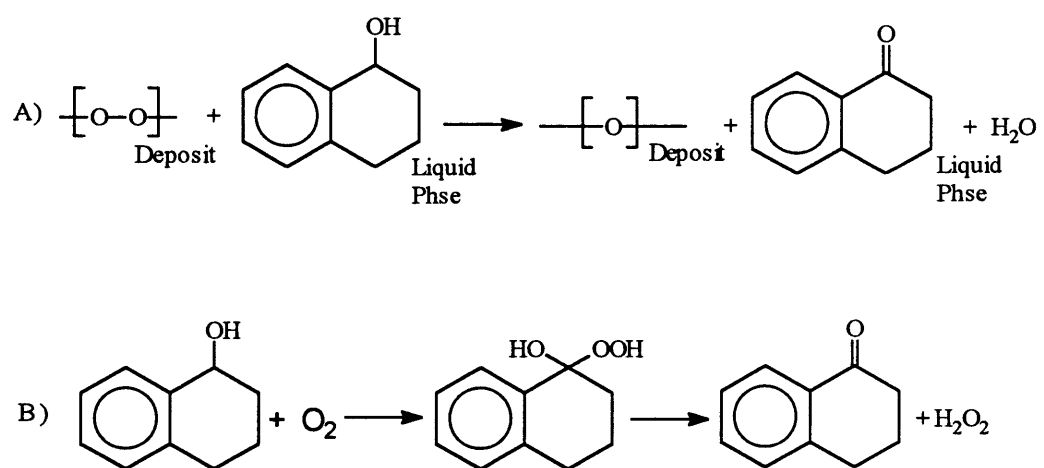


Figure 20: A and B are possible mechanisms of the formation of tetralone in the intermediate stage.

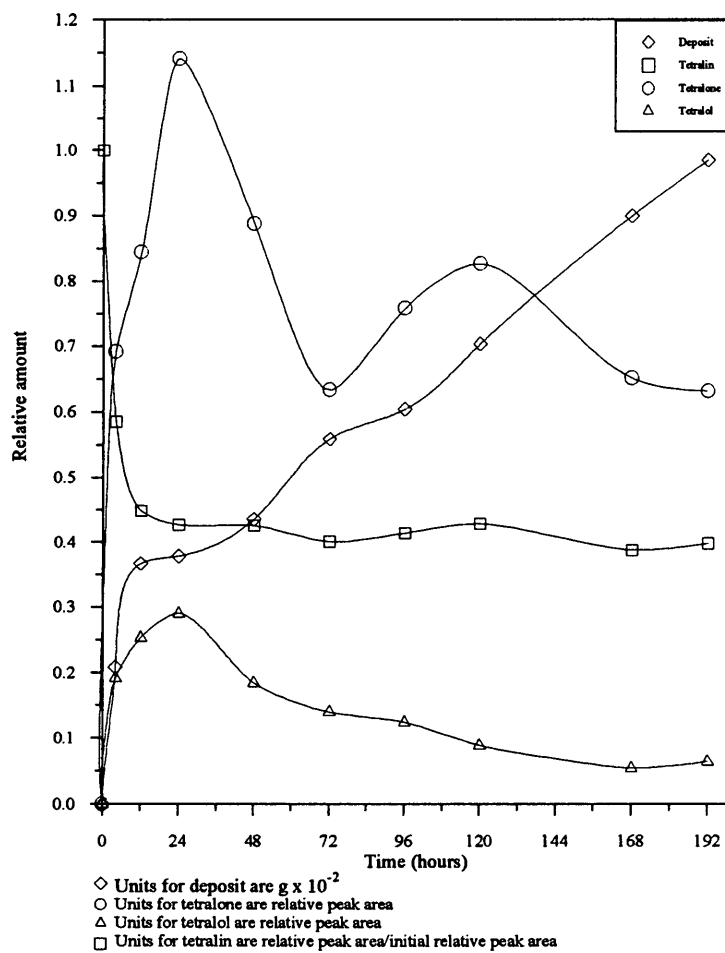


Figure 21: Kinetics of the autoxidation of tetralin and of tetralone, tetralol, and deposit formation 100 ppm AIBN added.

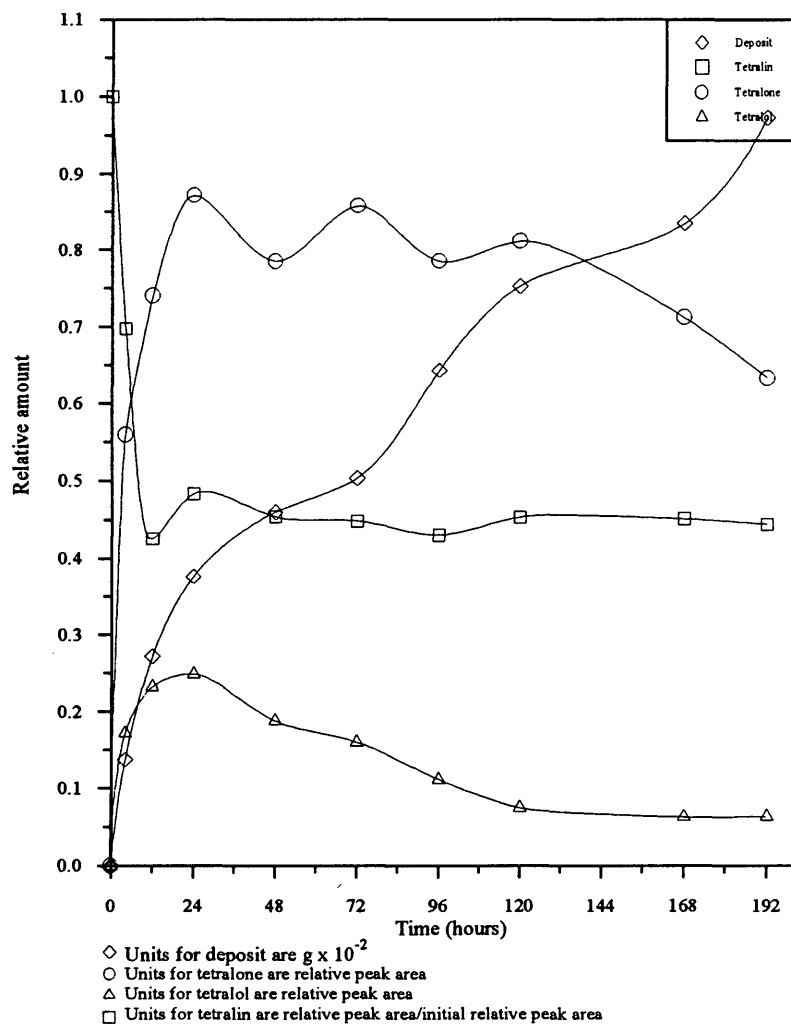


Figure 22: Kinetics of the autoxidation of tetralin and of tetralone, tetralol, and deposit formation 1000 ppm AIBN added.

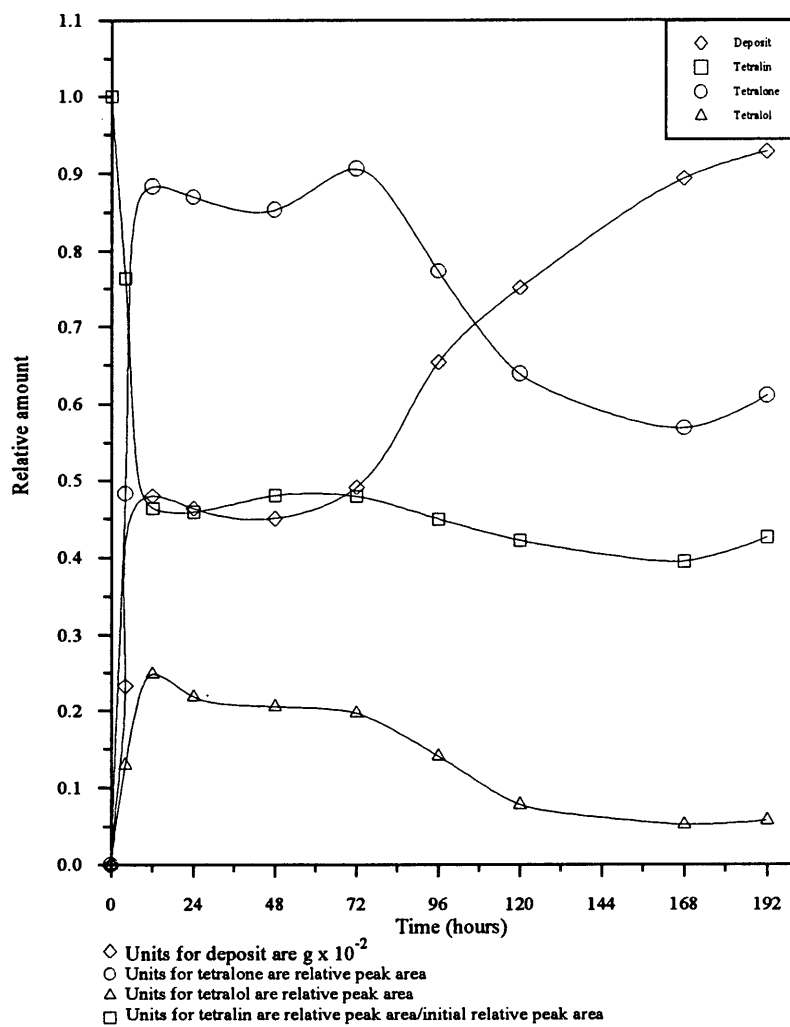


Figure 23: Kinetics of the autoxidation of tetralin and of tetralone, tetralol, and deposit formation 2000 ppm AIBN added.

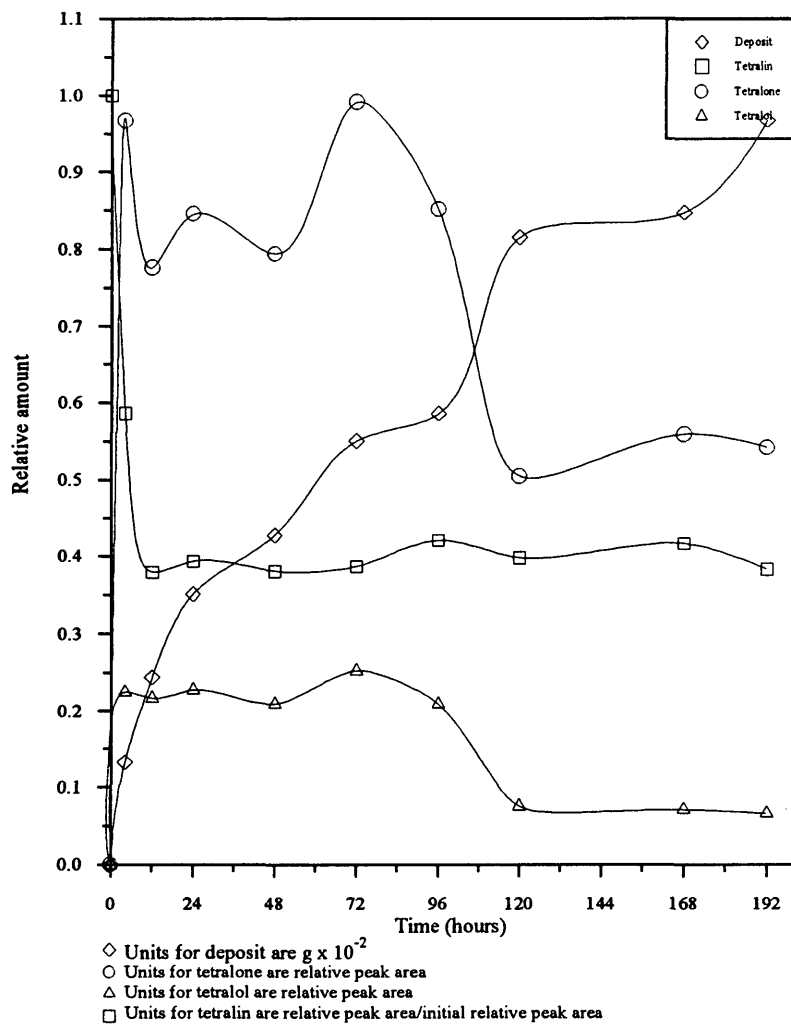


Figure 24: Kinetics of the autoxidation of tetralin and of tetralone, tetralol, and deposit formation 100 ppm benzoyl peroxide added.

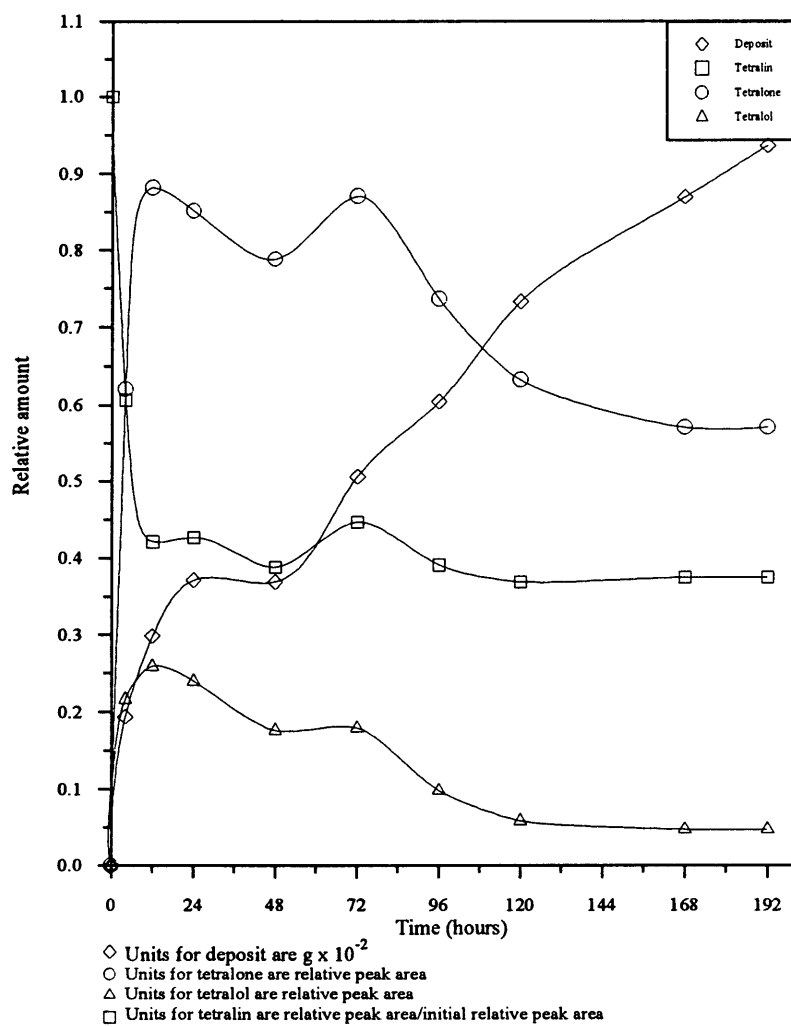


Figure 25: Kinetics of the autoxidation of tetralin and of tetralone, tetralol, and deposit formation 1000 ppm benzoyl peroxide added.

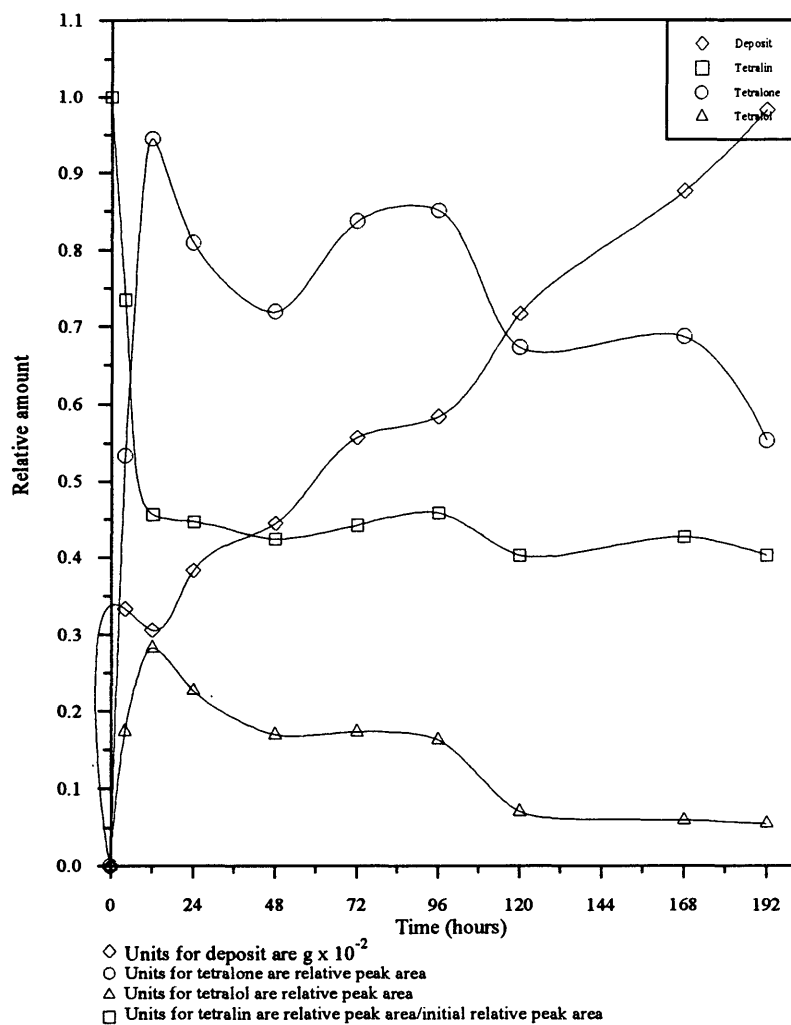


Figure 26: Kinetics of the autoxidation of tetralin and of tetralone, tetralol, and deposit formation 2000 ppm benzoyl peroxide added.

3.3. CHARACTERIZATION OF MODEL FUEL DEPOSIT

Although many oxidation products of tetralin have been identified (Zarrabi, 1987), which are involved in forming deposit is not clear. Therefore, the composition of model fuel deposits was examined.

The methanol/toluene solutions of the initial (formed after 24 hours at $127 \pm 2^\circ\text{C}$) and the final (formed after 8 days) deposit from model fuel with and without added radical initiators (1000 ppm of benzoyl peroxide or AIBN) were analyzed by GC-MS. The TIC chromatogram shows more components in the initial deposit than in the final deposit (Figure 27 and 28). By analyzing the mass spectra for components of the initial and the final deposits (Appendix A), only monomeric species were identified. These are presumably produced by decomposition of the actual deposit in the injection port. The other alternative is that these monomers were mainly adsorbed on the surface of the deposits. However, the excessive washing of deposits with hexane prior to analysis and the differences between results for the initial and final deposits argue against that explanation. Species that have been identified in the initial deposit without additives also have been identified in the initial deposit with additives (1000 ppm benzoyl peroxide or AIBN) but relative peak areas differ. Figure 29 lists compounds

that have been identified in the initial deposit (with and without additives).

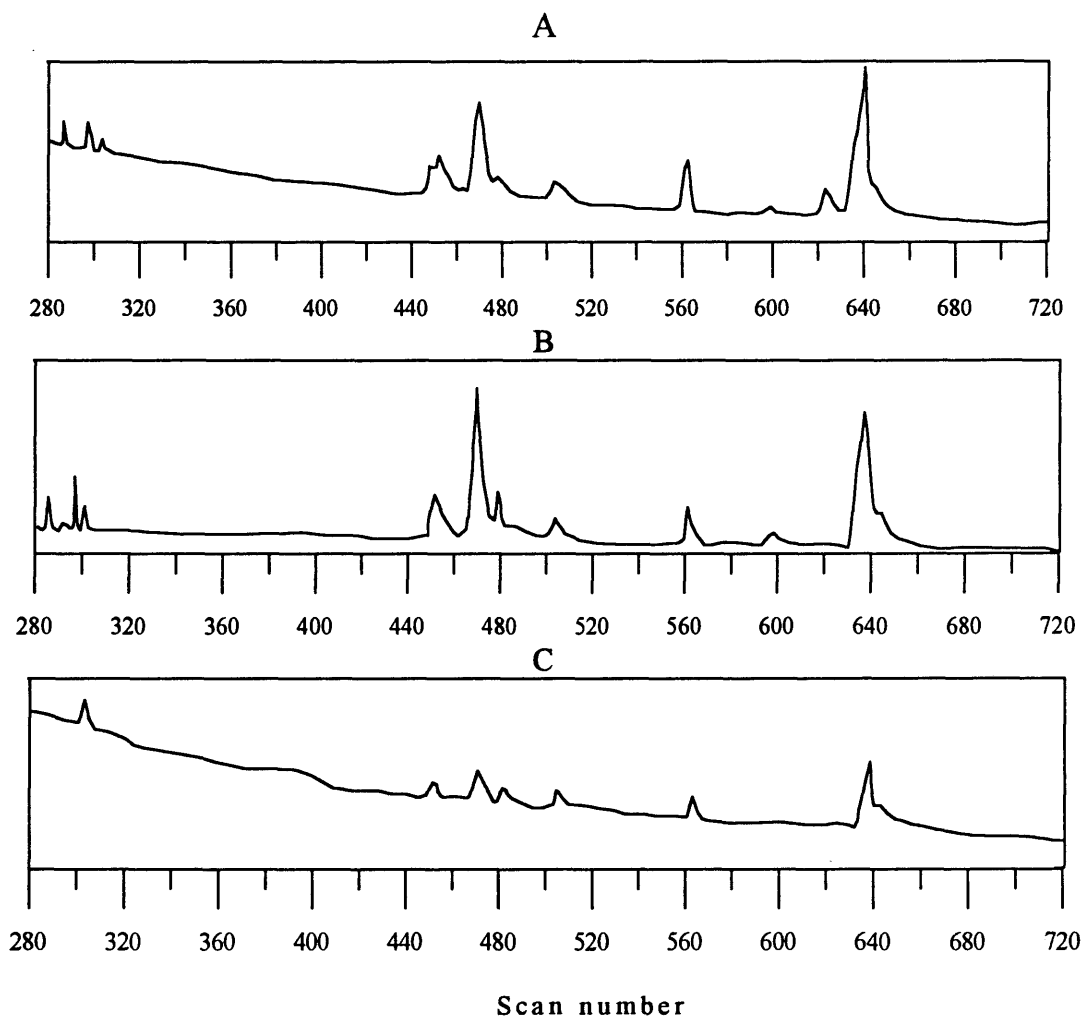


Figure 27: GC-MS chromatograms of A) initial deposit from model fuel. B) initial deposit from model fuel containing 1000 ppm benzoyl peroxide. C) initial deposit from model fuel containing 1000 ppm AIBN.

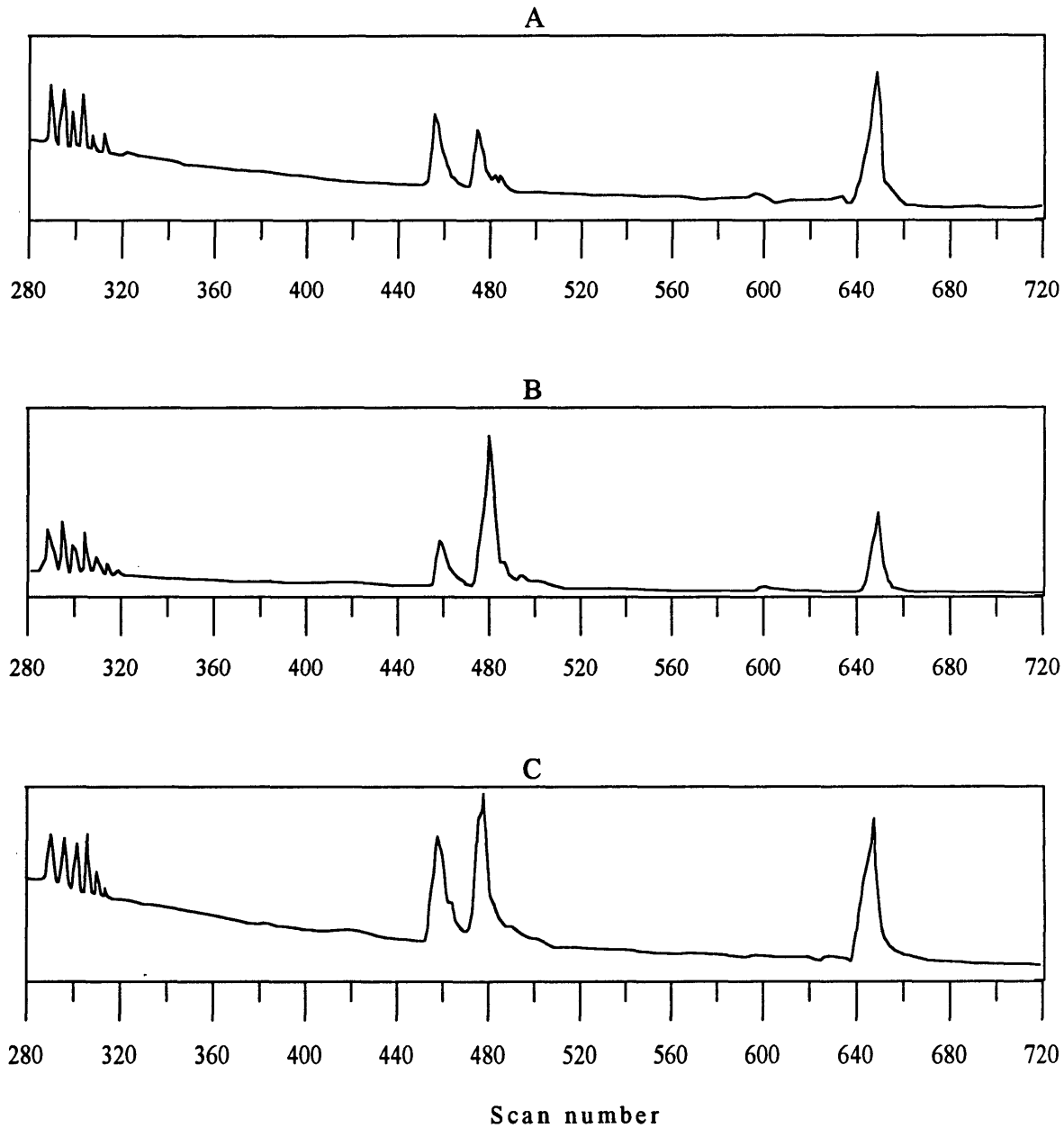
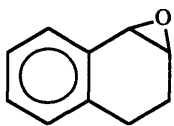
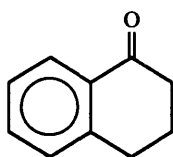


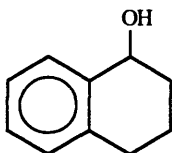
Figure 28: GC-MS chromatograms of A) final deposit from model fuel. B) final deposit from model fuel containing 1000 ppm benzoyl peroxide. C) final deposit from model fuel containing 1000 ppm AIBN.



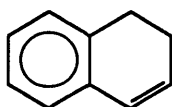
Scan = 467
Major Mass Units: 146, 131, 118, 177, 104, 115, 91.



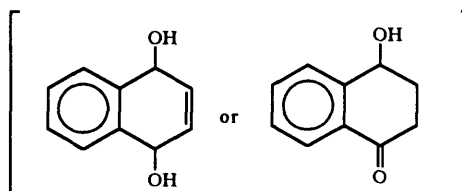
Scan = 478
Major Mass Units: 146, 118, 90.



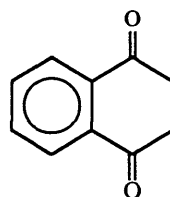
Scan = 450
Major Mass Units: 148, 147, 130, 120, 119, 105, 91.



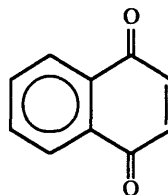
Scan = 285
Major Mass Units: 130, 129, 128, 115, 91, 65, 51, 50.



Scan = 638
Major Mass Units: 162, 147, 134, 120, 115, 105, 91, 77.



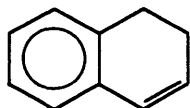
Scan = 561
Major Mass Units: 160, 131, 104, 91, 76, 51, 50.



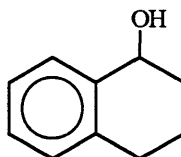
Scan = 503
Major Mass Units: 158, 130, 118, 104, 102, 91, 76.

Figure 29: Compounds that have been identified by GC/MS analysis of the initial deposit from model fuel without additives.

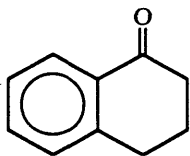
The final deposits from model fuel with and without additives have been analyzed and only the following compounds have been identified (Figure 30):



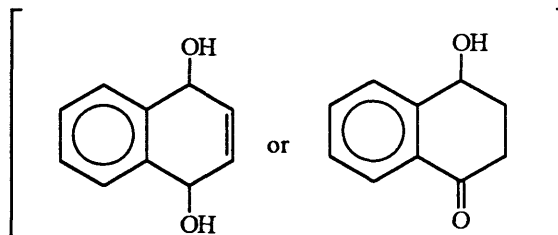
Scan = 289.
Major Mass Units: 130, 129, 128, 115, 91, 77.



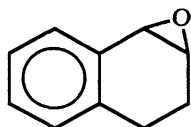
Scan = 450.
Major Mass Units: 148, 130, 120, 119, 115, 105, 91.



Scan = 476.
Major Mass Units: 146, 118, 91.



Scan = 648
Major Mass Units: 162, 147, 134, 120, 115, 105, 91, 77, 51, 50.



Scan = 476.
Major Mass Units: 146, 131, 118, 115, 91.

Figure 30: Compounds that have been identified by GC/MS analysis of final deposit from model fuel without additives.

These small molecules which have been identified can not themselves represent the deposit. They are much more soluble in the model fuel than is the deposit. However, the model deposit might decompose in the injector port to produce small volatile species that can elute through the GC column plus non-volatile species that stay in the injection port.

The GC-MS analysis result for the initial and the final deposits lead to the following hypotheses:

1. Structures of initial and the final deposit are different.
2. The initial deposit may contain a mixture of at least two components. The first one is the initial deposit which might decompose in the injection port of the GC-MS and produce components that are not produced from the final deposit. The second structure is that of the final deposit. Alternatively, the initial deposit structure may simply change during the stressing to form the final deposit.

Analysis for peroxides by the ferrous thiocyanate colorimetric method gives a positive result with the initial deposit and a negative result with the final deposit. The amount of the peroxide in the initial deposit was 1.88 mole peroxide/ mole of $C_{10}H_{10}O_2$ unit (assumed as empirical formula of deposit see

Appendix B). This result confirms that the initial deposit structure is different from that of the final deposit. Peroxide qualitative analysis for initial and final model fuel liquid phase was also performed. Initial model fuel contains a large quantity of peroxides and final model fuel contains a no peroxides. The initial deposit is not simply tetralin hydroperoxide because 1) tetralin hydroperoxide is more soluble in the model fuel than is the deposit, and 2) GC-MS of the initial deposit shows products that can not be produced from the decomposition of pure tetralin hydroperoxide. Peroxide qualitative analysis was performed for Jet A liquid phase and deposit. All liquid phase samples (after 2, 4, 6, 8, 10, 12, 14, and 17 days at 127° C) contain peroxide but much less than model fuel samples. All Jet A deposit samples contain no peroxide.

In the initial stage, there is a large possibility to form peroxide linkages between two species because of the large concentrations of tetralin hydroperoxide, tetralin radicals, tetralone, tetralol, oxygen and other species present. One possible explanation for the presence of peroxide linkages in the initial deposit and not in the final deposit is that, in the early stage, free radical reactions may take place to form peroxide linkages between radicals. In the intermediate stage, the autoxidation of tetralin is stopped because most of the oxygen was consumed in the early stage of the reaction. Therefore, tetralin hydroperoxide produc-

tion stops. As a result, the possibility of producing peroxide linkages is decreased. The final deposit contains no peroxide linkages which indicates that initial deposit changes with time. Alteration of the initial deposit is possible because peroxide linkages are, in general, weak and can dissociate at the reaction temperature ($127 \pm 2 \text{ C}^\circ$).

The initial and the final deposit from model fuel with no additive and with 1000 ppm of benzoyl peroxide or AIBN were analyzed by FT-IR to identify the functional groups present.

Significant differences are shown between the initial and the final deposits in Figures 31 and 32. The spectrum for the initial deposit without additives show a broad and strong absorption band at 3356 cm^{-1} corresponding to O-H bonds, and two weak absorption peaks at 3068 and 3030 cm^{-1} corresponding to aromatic C-H. Two absorption peaks at 2933 and 2868 cm^{-1} correspond to aliphatic C-H stretches in methyl and/ or methylene groups. The strong absorption at 1711 cm^{-1} corresponds to a C=O stretching vibration, and the medium intensity band at 1601 cm^{-1} is assigned to aromatic C=C absorption. The band at 930 cm^{-1} may be due to peroxide bonds. The strong absorption at 802 cm^{-1} corresponds to out-of-plane C-H aromatic bending.

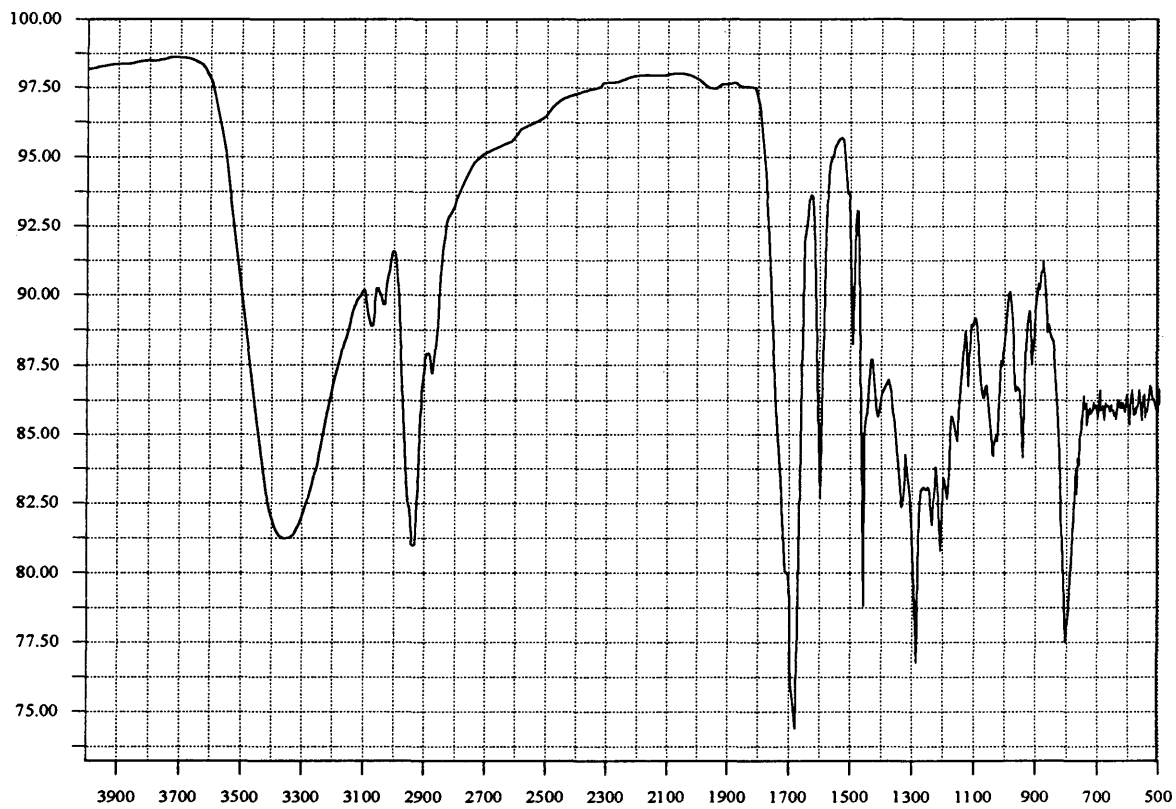


Figure 31: FT-IR spectrum of the initial deposit from model fuel without additives.



Figure 32: FT-IR spectrum of the final deposit from model fuel without additives.

The spectrum of the final deposit without additives is similar to that obtained for the initial deposit, except that the broad O-H stretch is much weaker than that for the initial deposit, suggesting that the initial deposit contains more O-H bonds. A new peak appears at 1231 cm^{-1} corresponding to C-O ether bonds. The strong absorption at 802 cm^{-1} , corresponding to out-of-plane C-H aromatic bending, is weaker than that for the initial deposit.

All initial deposits with or without additives (benzoyl peroxide or AIBN) exhibited similar spectra except for the out-of-plane C-H aromatic bending peak (Figure 33 and 34). Initial deposit with both additives has larger out-of-plane C-H aromatic bending peaks than for the deposit without additives. All final deposits with and without additives are also similar except for the out-of-plane C-H aromatic bending peak (Figure 35 and 36). The out-of-plane C-H aromatic peaks disappear in the final deposit with additives. The FT-IR result for the out-of-plane C-H aromatic bending peak suggests that the addition of initiators has changed the nature of the deposit. The increase in the out-of-plane band in initial deposit with additives compared to that without additives might occur because benzoyl peroxide is present in the initial deposit and therefore adds to intensity of the band due to its aromatic C-H content.

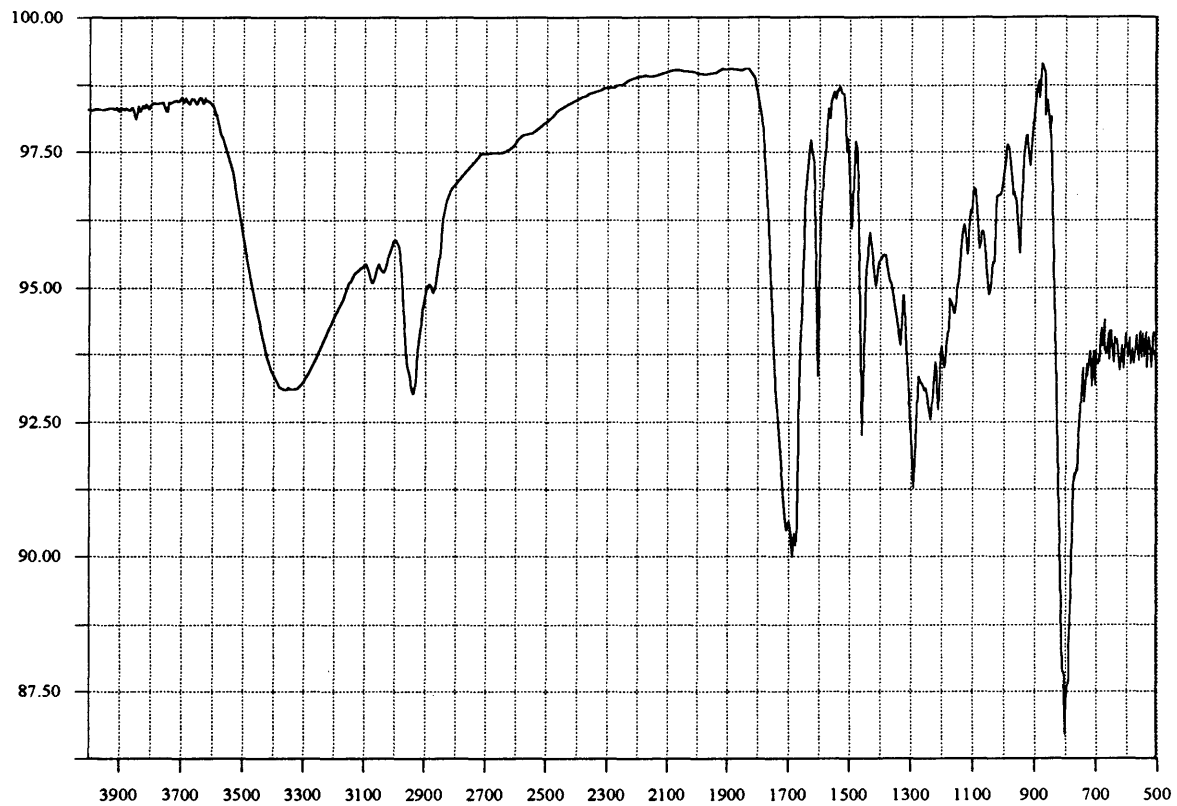


Figure 33: FT-IR spectrum of the initial deposit from model fuel containing 1000 ppm benzoyl peroxide.

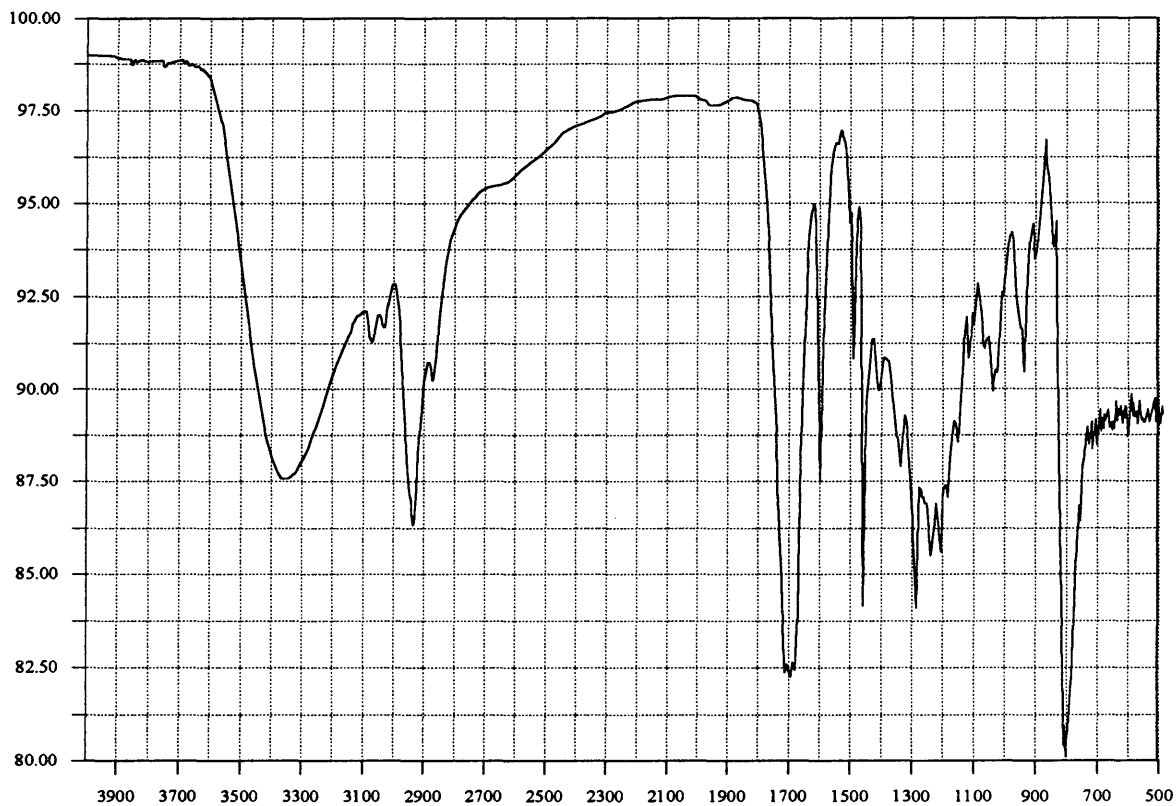


Figure 34: FT-IR spectrum of the initial deposit from model fuel containing 1000 ppm AIBN.

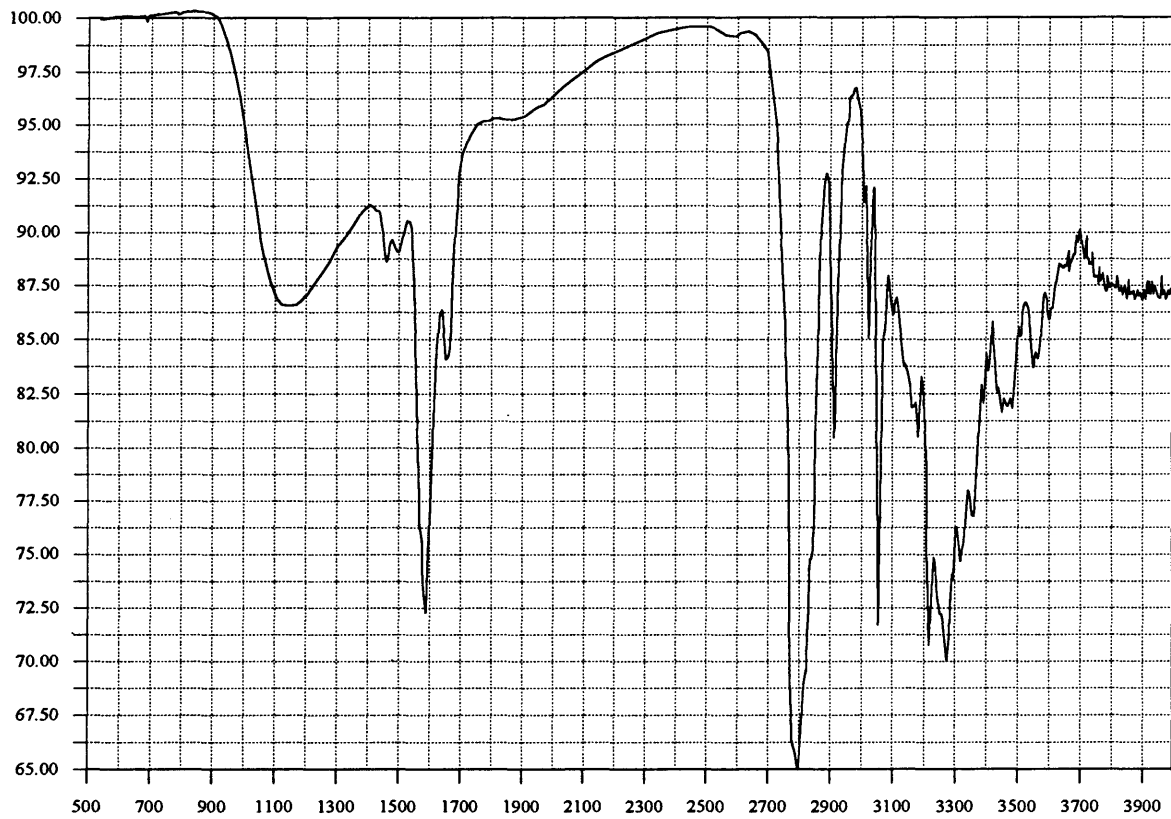


Figure 35: FT-IR spectrum of the final deposit from model fuel containing 1000 ppm benzoyl peroxide.

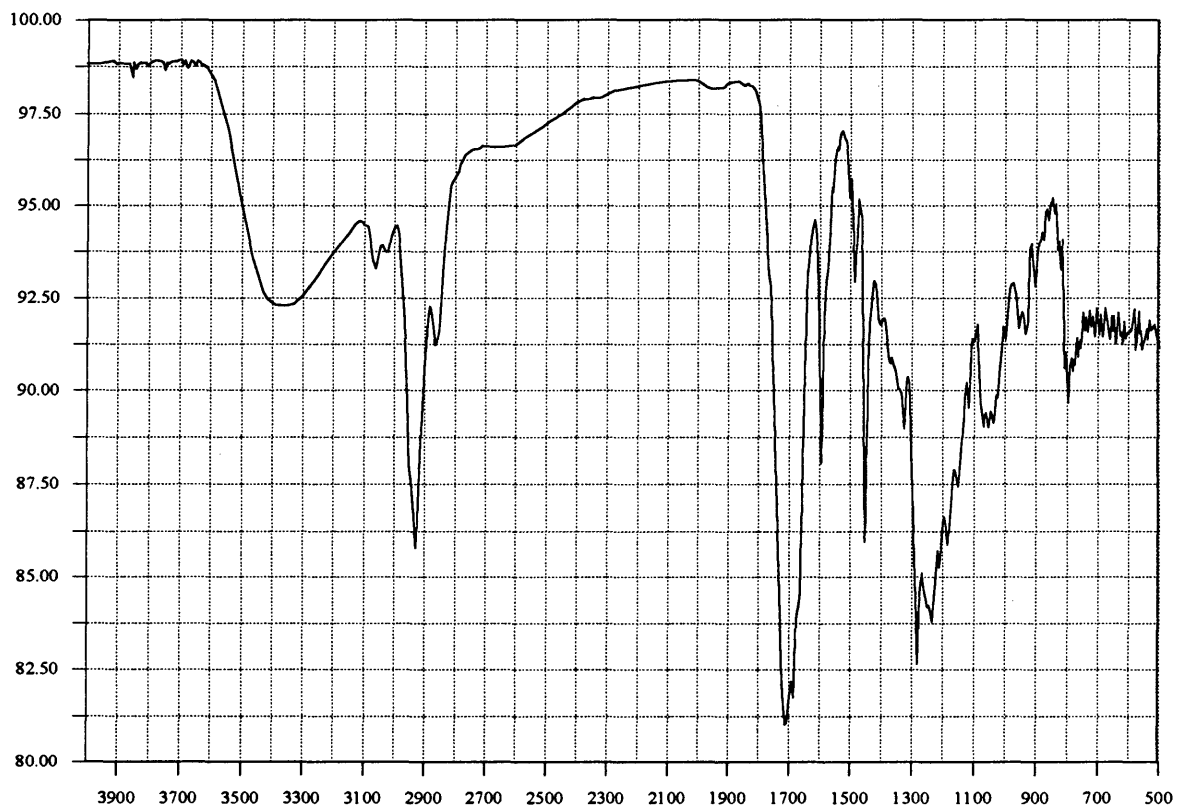


Figure 36: FT-IR spectrum of the final deposit from model fuel containing 1000 ppm AIBN.

If this hypothesis is true, the out-of-plane band in initial deposit from model fuel with AIBN additive will not increase because AIBN does not contain out-of-plane aromatic hydrogens. However, the out-of-plane band does increase in the initial deposit from model fuel with AIBN. In the final deposit with additives, either the concentration of out-of-plane aromatic hydrogen is decreased or vibration is made less favorable as the deposit structure becomes more rigid via cross-linking, or both.

Py-MS was used to analyze initial and final deposits from model fuel without additives. Identification of components from the Py-MS will concentrate on fragments rather than molecular ions because of the strong fragmentation tendency of the pyrolysis process. Each peak in a mass spectrum may result from contributions from several sources in the deposit mixture. The mass units 130, 129, 128, and 115 may, for example, correspond to a 1,2-dihydronaphthalene fragment. Peaks at 132, 104, and 91 may correspond to 1,2,3,4-tetrahydronaphthalene (tetralin). Peaks at 146, 118, 116, 117, 115, and 131 may correspond to 1 or 2-tetralone or 1a,2,3,7b-tetrahydronaphth[1,2-b]oxirene. Peaks at 144, 115, and 116 are 1-naphthalenol fragments. The mass units at 158, 130, 104, and 102 correspond to 1,4-naphthalenedione or 1,2-naphthalendione. Peaks at 126, 115, 116, 149, and 118 corresponds to 1,4-dihydroxynaphthalene. The previous compounds have been identified because they are known oxidation products of tetralin. Figure 37 shows fragments of mass higher than 162 which do not appear in the GC-MS analysis. Peaks of mass such as 386, 368, 302, 307, 336, and 180 (Figure 37) could be molecular ions or the sources of other fragments. Structures A, B, and C are reasonable candidates for a 386 molecular ion. Figure 38 suggests possible fragmentation consistent with the observed spectra.

All small molecules such as 1,2-dihydronaphthalene, 1,2,3,4-tetrahydronaphthalene, 1-tetralone or 1a,2,3,7b-tetrahydronaphth

[1,2-b]oxirene, 1-naphthalenol, 1,4-naphthalenedione, and 1,4-dihydroxynaphthalene that were identified in the initial deposit were also identified in the final deposit. Many peaks having mass above 170 were observed (Figure 39). These could be molecular ions or the sources of other fragments. Figure 40 suggests compounds which may represent final deposit.

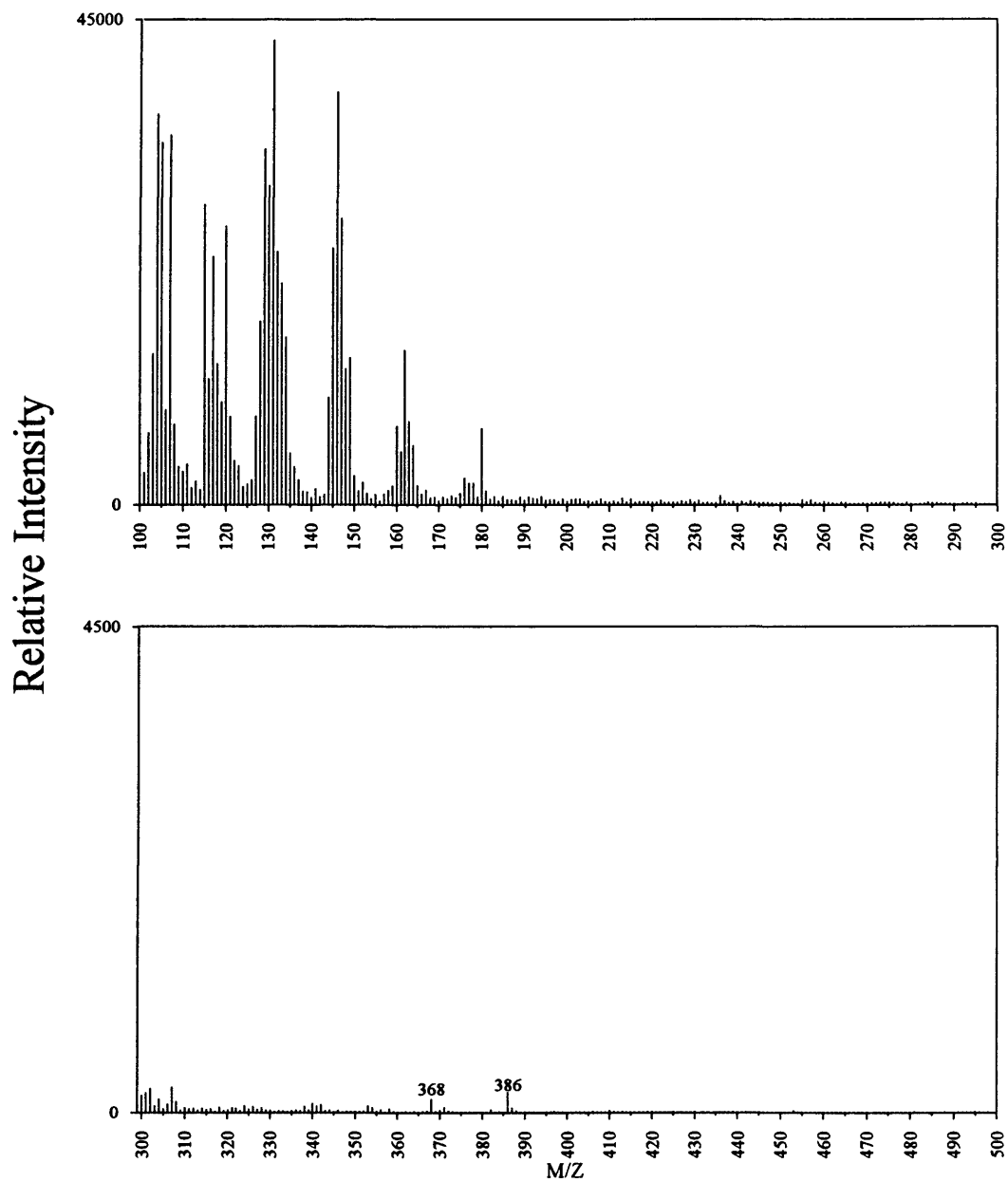


Figure 37: Py-MS spectrum of initial deposit from model fuel.

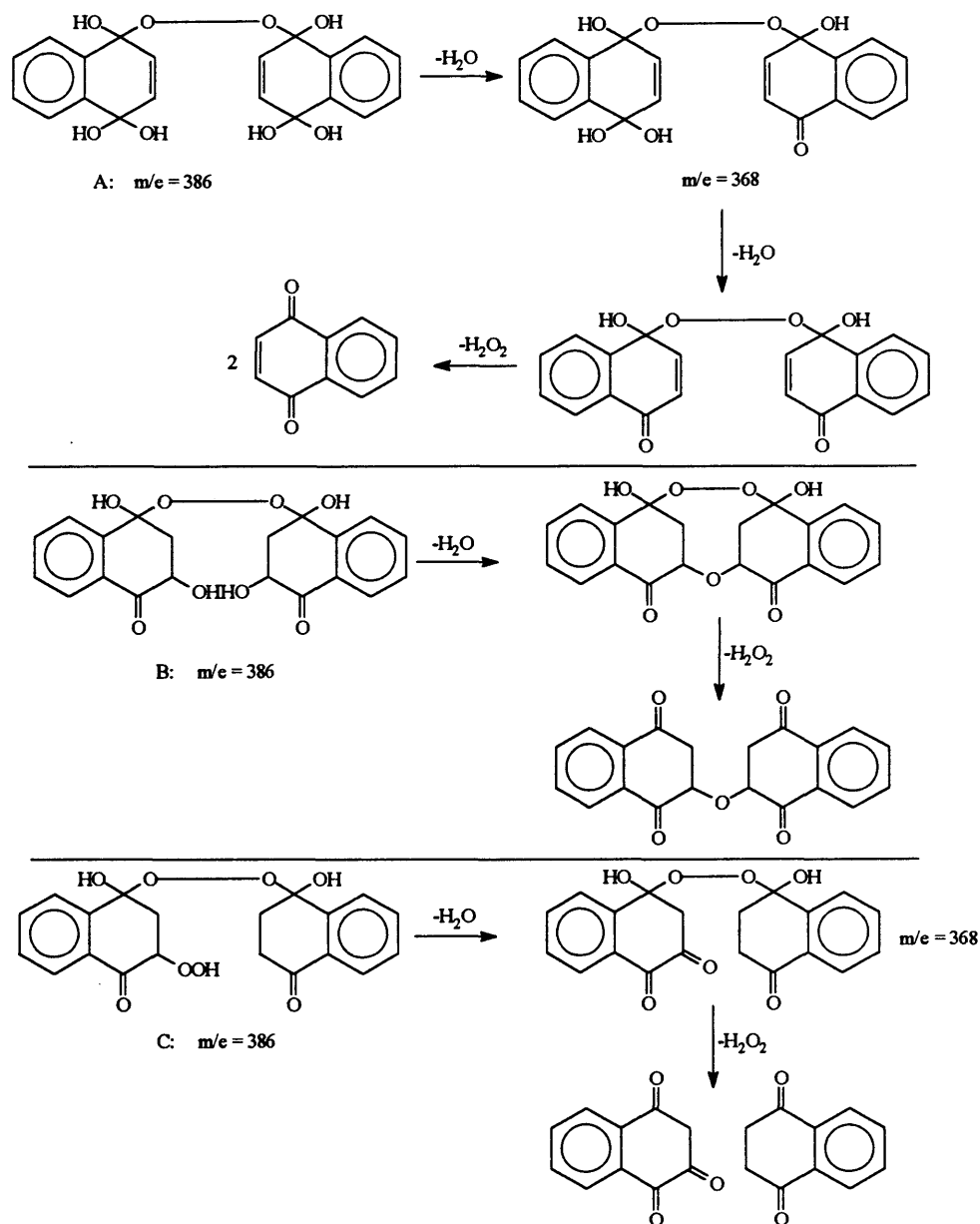


Figure 38: Possible fragmentation reactions for the proposed molecular ions in the initial deposit.

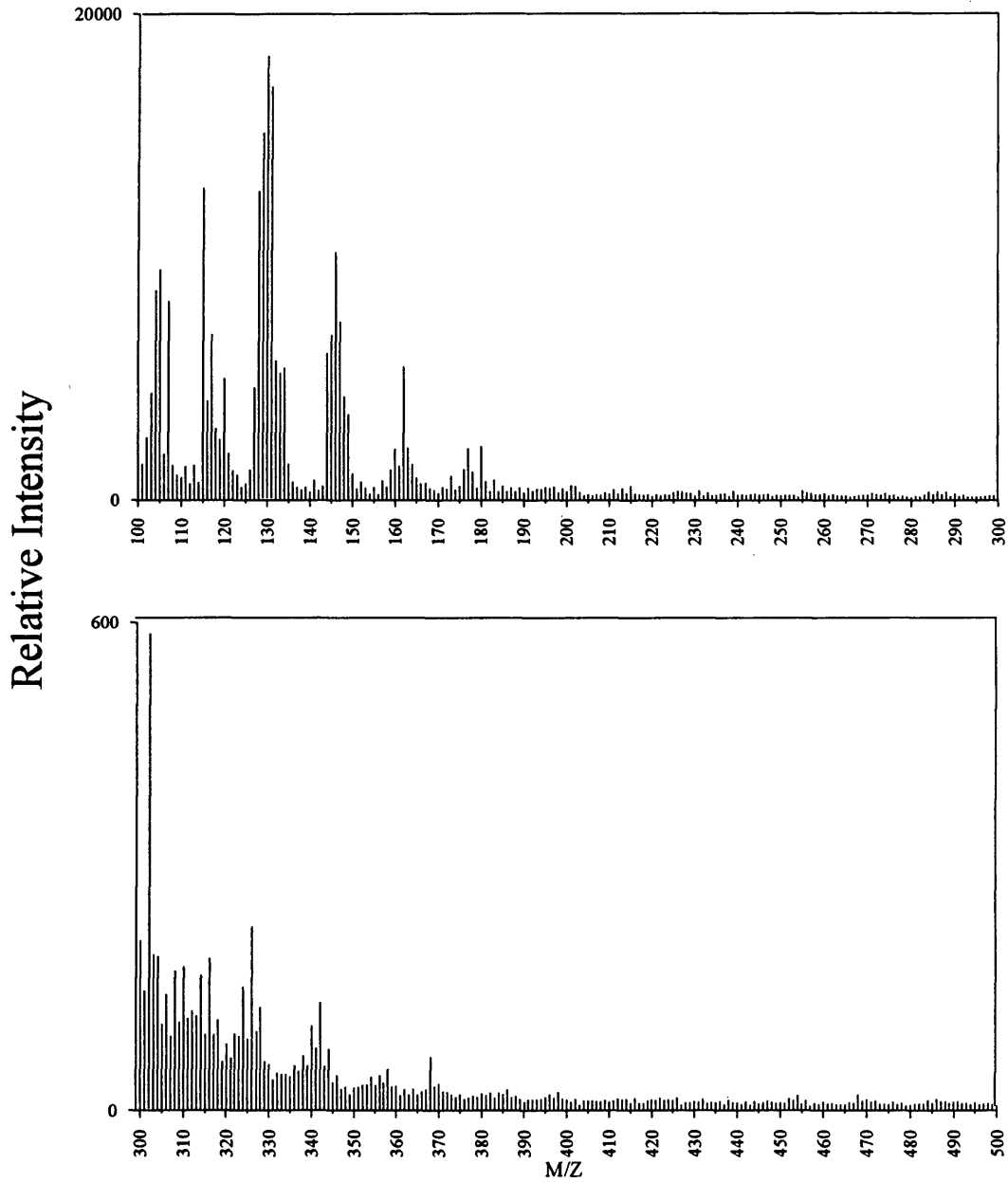


Figure 39: Py-MS spectrum of final deposit from model fuel.

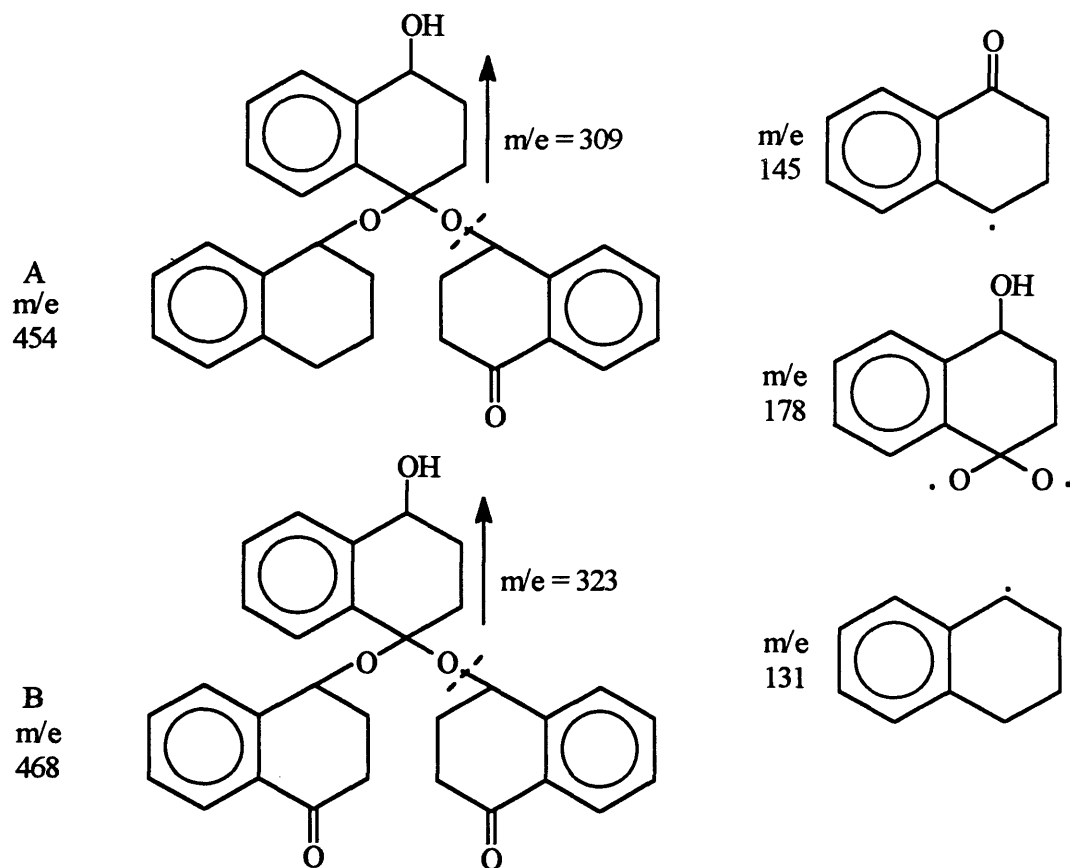


Figure 40: Possible structures for final deposit components.

From Py-MS, the 386 peak may represent a molecular ion of an initial deposit components (Figure 38). From the FT-IR, initial deposit was found to contain hydroxyl, and carbonyl functional groups. Proposed structures B and C have those features. From the ferrous thiocyanate colorimetric test for peroxide linkages, we conclude that the initial model fuel deposit contains many peroxide linkages (approximately 1.8 peroxide linkage per tetralin unit). Structure C (Figure 38) is more likely the molecular structure on this basis. Only small species were identified by GC-MS which helps little in interpreting the molecular structure of the initial deposit.

The Py-MS suggests two peaks (454 and 468) as possible molecular ions of final deposit components. FT-IR spectra indicate that final deposit contains less hydroxyl than initial deposit, and also contains carbonyl, and ether functional groups. Structures A and B correspond to these requirements. The ferrous thiocyanate colorimetric test for peroxide linkages indicates that there are no peroxide linkages in the final deposit in agreement with either proposed structure in Figure 40. Structures A and B contain less oxygen (14.1% O and 17.1% O, respectively) than that measured (see Table 2) in model deposits by Worstell (1980).

The effect of radical initiators on the model fuel and a real Jet A fuel are compared in Table 6. The amount of deposit formed is increased when either initiator is added to either fuel. The relative increases are more dramatic in the Jet A case.

Table 6: Effects of radical initiators upon the formation of final deposit for model and Jet A fuels.

Sample	Weight of model fuel deposit g x 10 ³	Weight of Jet A fuel deposit g x 10 ³
No additives	5.14	1.01
Benzoyl peroxides 1000 ppm	6.66	1.45
AIBN 1000 ppm	7.81	1.96

This result for Jet A and model fuel samples is different from that obtained by Worstell (1980) and Zarrabi (1987). The difference may be due to the following:

1. The Jet A fuel was stored in a refrigerator for several years. During this long period of time the Jet A may have autoxidized to produce high concentrations of intermediate products.

The same argument would not however apply to the model fuel and so cannot explain differences in the model fuel results.

2. In this study the experiment was carried out in sealed borosilicate glass vials to provide limited amounts of oxygen. Worstell and Zarrabi used screw-cap glass jars that were refilled with air every 24 hours. Christian (1958) concluded that various types of glass surfaces can affect the degradation rate of many fuels. He reported that soft glass has an inhibitory effect on the degradation of fuels, but borosilicate glass is essentially inert. Both type of glass and the amount of oxygen can effect the rate of deposition. In this experiment, the initiators concentration were 100, 1000, and 2000 ppm for both benzoyl peroxide and AIBN whereas Worstell used 1898 ppm for AIBN and 4908 ppm for benzoyl peroxide.

4. CONCLUSIONS

The main purpose of this study was to understand the role of radical initiators in deposit formation in fuels. The following are the main conclusions:

1. Radicals initiators do cause an increase in the amount of deposit formed during both initial and final stages of the process.

2. Radical initiators do cause an increase in the rates of tetralin autoxidation and of formation of the intermediate products.

3. Peroxide linkages were found in the initial model fuel deposit whereas ether bonds were not. Peroxide linkages disappeared from the final deposit and ether bonds formed. This result indicates that deposit changes during the stressing process. The amount of oxygen present in the reaction medium, temperature, and reaction time may influence the amount of peroxide linkages remaining in the deposit. Jet A deposit contains no peroxide linkages.

4. Initial deposit that forms from stressing the model fuel was found to consist of aromatic compounds containing hydroxyl, carbonyl and peroxide functional groups. Final deposit consists of aromatic compounds containing hydroxyl, carbonyl and ether , but not peroxide, functional groups.

5. Both initiators increase the amount of deposit formed in both model and Jet A fuels. Consequently, the fundamental hypothesis of this research, that acceleration of the earlier steps in the process could be used to diminish deposit formation, is disproved.

5. REFERENCES

Beaver, B., Fuel Sci. & Tech. Int., 9 No. 10, pp 1287 (1991).

Bolland, J. L., and G. Gee, Trans. Faraday Soc., 42, 236, 244 (1946 a).

Bolland, J., and G. Gee, Trans. Faraday Soc., 42, 234 (1946 b).

Bolland, J., and G. Gee, Trans. Faraday Soc., 42, 244 (1946 c).

Brinkman, D. W., M. L. Whisman and J. N. Bowden, U. S. Department of Energy, BETC/RI-78, 23 (1979).

Brooks, B., Ind. Eng. Chem., 18, 1198 (1926).

Bushueva, E. M., I. E. Bespolov, Chemistry and technol. of fuels and oils, 7, (9-10), 699-702, (1971).

Cernansky, N. P., R. S. Cohen and K. T. Reddy, Final report " Thermal Stability of Distillate Hydrocarbon Fuel" , NASA NAG-3-183 (1982).

Chen, W. C., and A Study of the Storage Deposit of a Model Fuel and Jet A Fuel, M. S. Thesis, Colorado School of Mines, T-2983 (1985).

Chertkov, Y. B., V. N. Zrelov, in *The Oxidation of Hydrocarbons in the Liquid Phase*; Emanuel, N. M., eds; Pergamon Press, Macmillan Co., 1965; pp 351-361.

Christian, J., A Chiantella, J. Johnson, and H. Carhart, *Ind. Eng. Chem.*, 50, 1153 (1958)

Clinkenbeard, W., *Symposium on Stability of Distillate Fuel Oils*, ASTM STP # 244, Philadelphia, Penn., P 32, 1959.

Dahlin K. E., S. R. Daniel, and J. H. Worstell, *Fuel*, 60, 477-480 (1981).

Daniel, S. R., "Studies of the Mechanisms of Turbine Fuel Instability" NASA, Contractor Report 167963 (1983).

Dryer, C., J. Morrell C. Lowry, and G. Egloff, *Ind. Eng. Chem.*, 26, 885 (1934).

Elmqvist, E., *Symposium on Stability of Distillate Fuel Oils*, ASTM STP # 244, Philadelphia, Penn., P 26, 1959.

Farmer, E., and A. Sundralingham, *J. Chem. Soc.*, 1942, 121.

Flood, D., J. Hladky, ., G. Edgar, *Ind. Eng. Chem.*, 26, 1234 (1933).

George, P., *Proc. Roy. Soc. (London)*, A186, 337 (1946 a)

George, P., *Trans. Faraday Soc.*, **42**, 217 (1946 b).

George, P., and A. Robertson, *Proc. Roy. Soc. (London)*, A185, 309 (1946 c).

Johnson, J., D. Fink, and A. Nixon, *Ind. Eng. Chem.*, **46**, 2166, (1954).

Mardles, T., and J. Eiseinger, *J. Inst. Pet. Tech.*, **15**, 657 (1926).

Martin, S., W. Gruse and A. Lowry, *Ind. Eng. Chem.*, **25**, 1234 (1933)

Morrell, J., C. Dryer, C. Lowry, and G. Egloff, *Ind. Eng. Chem.*, **26**, 655 (1934a).

Morrell, J., C. Dryer, C. Lowry, and G. Egloff, *Ind. Eng. Chem.*, **26**, 497 (1934b).

Mushrush, G. W., R. N. Hazlett and H. G. Eaton, *Ind. Eng. Chem. Rev.* **24**, 290 (1985).

Nixon, A., in *Autoxidation and Antioxidation of Petroleum*, in *Autoxidation and Antioxidations*, ed. W. Lundberg, Interscience Publishers, New York, P. 695 (1962).

Norris, M., and T. Thole, *J. Inst. Pet. Tech.*, **15**, 677 (1926).

Offenhauer, J. Brennan, and R. Miller, *Ind. Eng. Chem.* , 49, 1265 (1957).

Rahhal, S. and H. W. Richter, *J. Am. Chem. Soc.*, 110, 3126-3133 (1988).

Reddy, K. T., N. P. Cernansky, and R. S. Cohen, *Analytical Chemistry*, 64, pp.2273 (1992).

Robertson, A., *Nature*, 62, 153, (1948).

Robertson, A., and W. A. Waters, *Trans. Faraday Soc.*, 42, 201 (1946).

Robertson, A., and W. Waters, *J Chem. Soc.*, 1574 (1948a).

Robertson, A., and W. Waters, *J Chem. Soc.*, 1578 (1948b).

Robertson, A., and W. Waters, *J Chem. Soc.*, 1585 (1948c).

Schwartz, F., M. Whisman, C. Allbright, and C. Ward, *Bur. Mines Bull.* 626, 44 pp., 1964.

Schwartz, F., M. Whisman, C. Allbright, and C. Ward, *Bur. Mines Bull.* 660, 58 pp., 1972.

Taylor, W., Ind. Eng. Chem. , Prod. Res. Devel., 8, 375 (1969).

Taylor, W. F., J. Phys. Chem. **79** 2250 (1970).

Taylor, W., Ind. Eng. Chem. , Prod. Res. Devel., 15, 64 (1976).

Taylor, W., and J. Frankenfeld: Ind. Eng. Chem. , Prod. Res. Devel., 17, 86 (1978).

Taylor, W., and T. Wallace Ind. Eng. Chem. , Prod. Res. Devel., 7, 198 (1968).

Thompson, R., L. Drudge, and J. Chenicek, Ind. Eng. Chem., 41, 2715 (1949).

Wagner, C., and J. Hyman, Oil Gas J., May 12, 1929.

Walters, E., H. Minor, and D. Yubroff, Ind. Eng. Chem., 41, 1723 (1949).

Woodward, A., Mesrobian R, J. Chem. Soc..., 75, 6189 (1953).

Worstell, J. W., The Effects of Nitrogen Compounds on Jet A and Diesel Fuel, Ph.D. Thesis, Colorado School of Mines, T-2280 (1980)

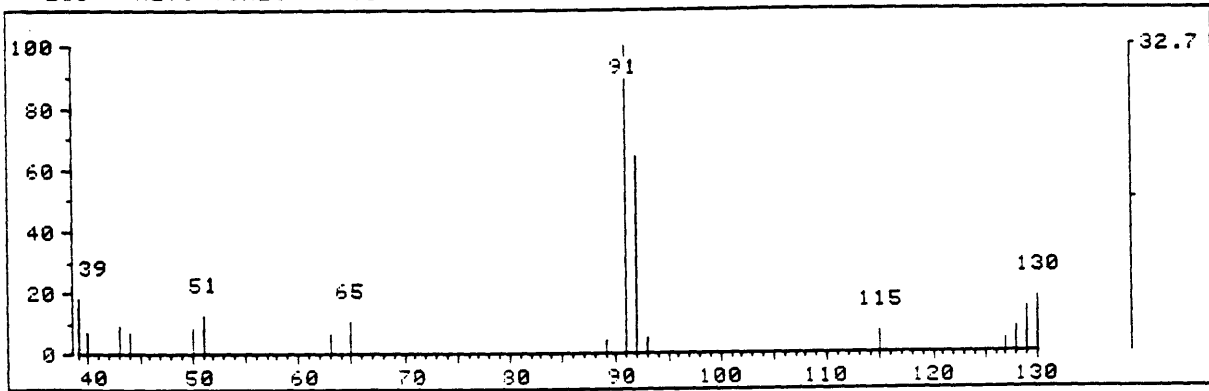
Yule, D., and T. Wilson, Ind. Eng. Chem., 23, 1254 (1931).

Zarrabi, K., Analysis and Characterization of 1-Tetralone Oxidation Products, Ph.D. Thesis, Colorado School of Mines, T-3171 (1987).

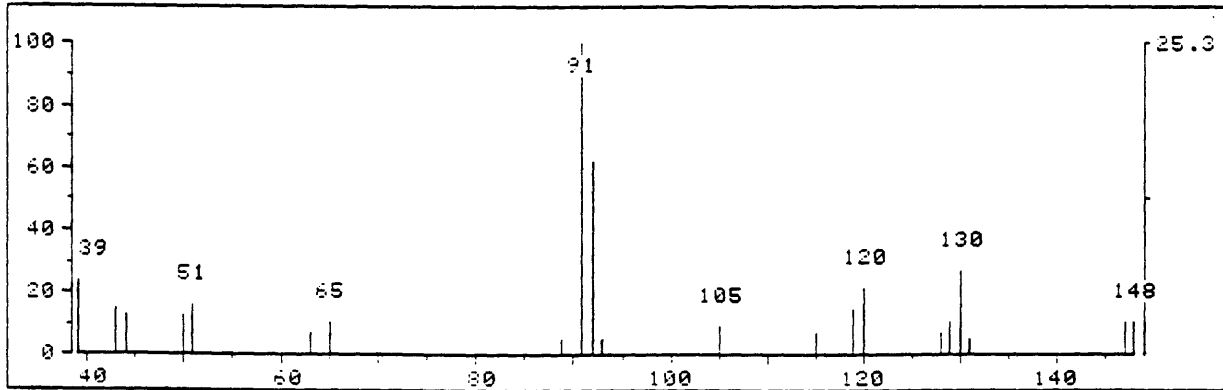
APPENDIX A

GC-MS Mass spectrum for initial deposit without additives

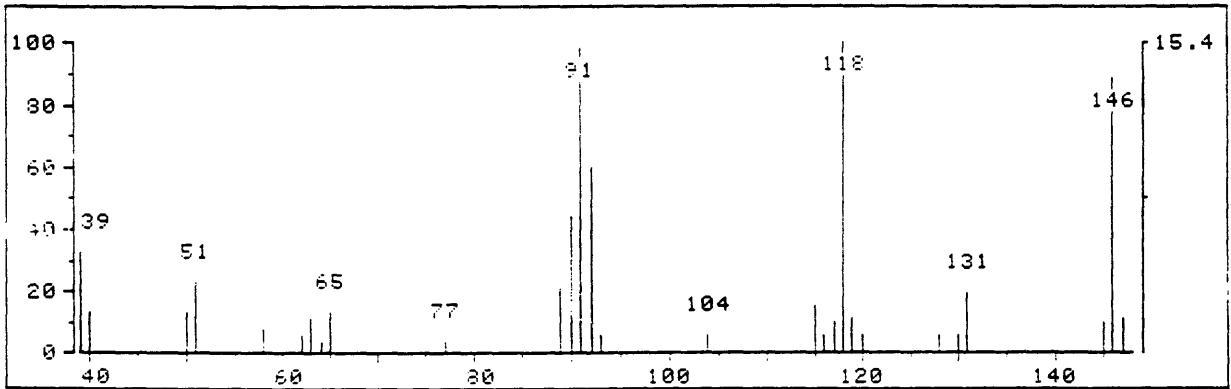
* 285 RET. TIME: 6.57 TOT ABUND= 291. BASE PK/ABUND: 91.1/ 95.



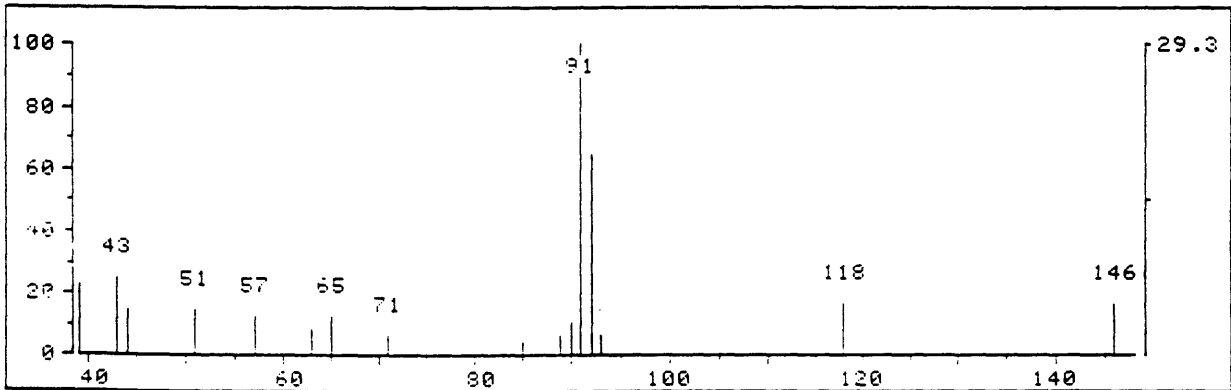
* 450 RET. TIME: 10.32 TOT ABUND= 218. BASE PK/ABUND: 91.1/ 55.



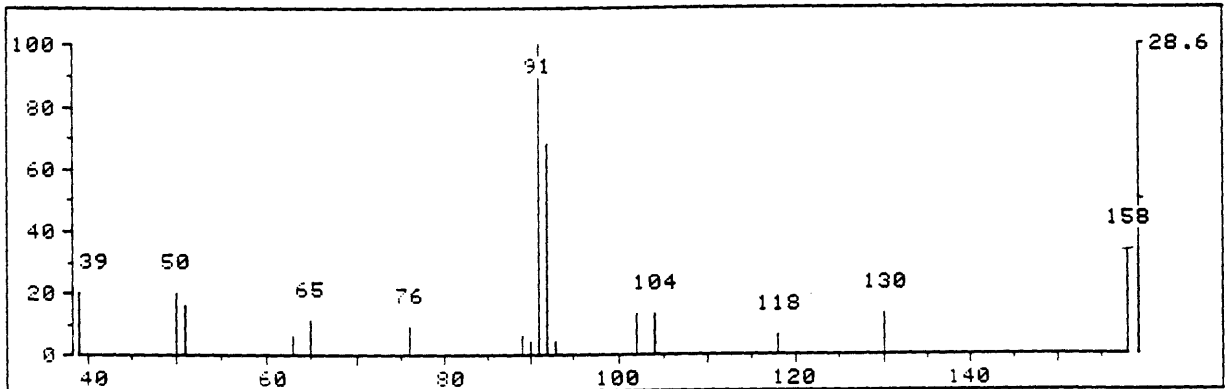
* 467 RET. TIME: 10.70 TOT ABUND= 338. BASE PK/ABUND: 118.1/ 52.



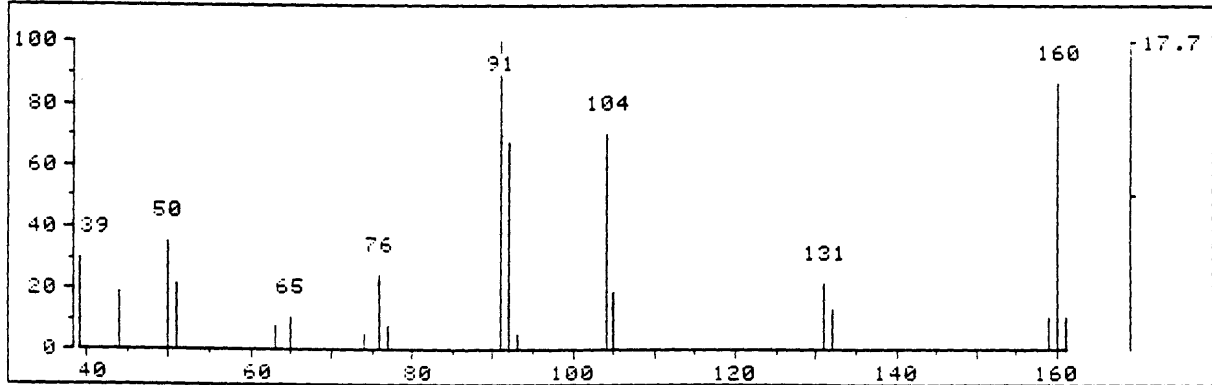
* 478 RET. TIME: 10.95 TOT ABUND= 164. BASE PK/ABUND: 91.1/ 48.

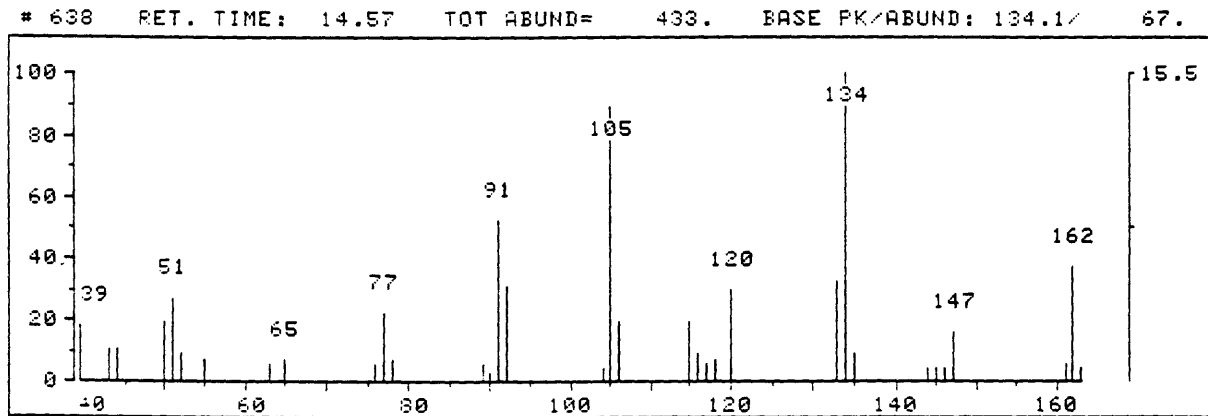
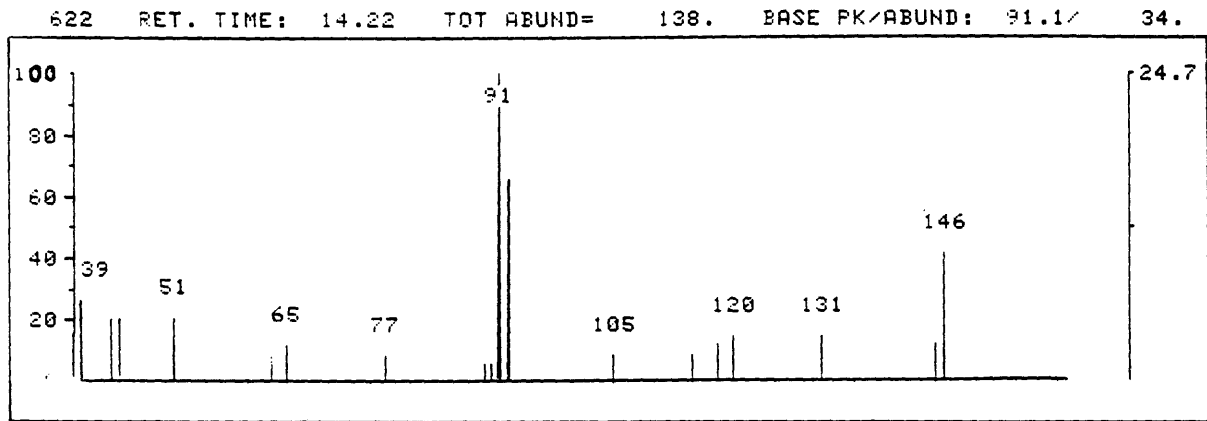


* 503 RET. TIME: 11.52 TOT ABUND= 154. BASE PK/ABUND: 91.1/ 44.

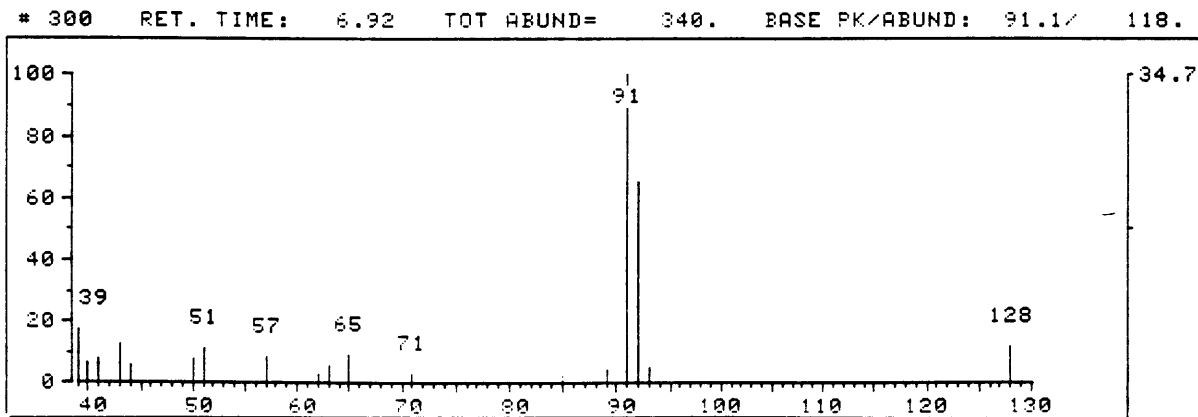
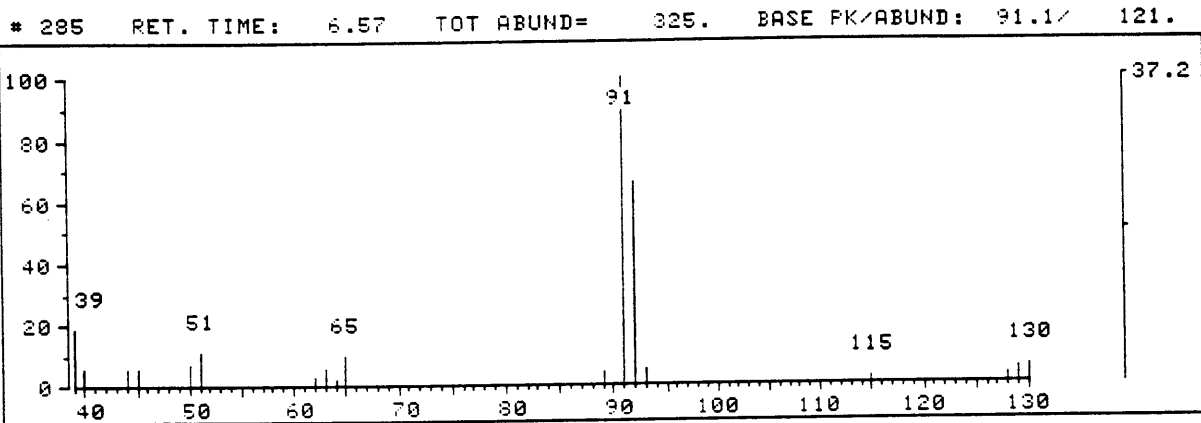


* 561 RET. TIME: 12.83 TOT ABUND= 210. BASE PK/ABUND: 91.1/ 37.

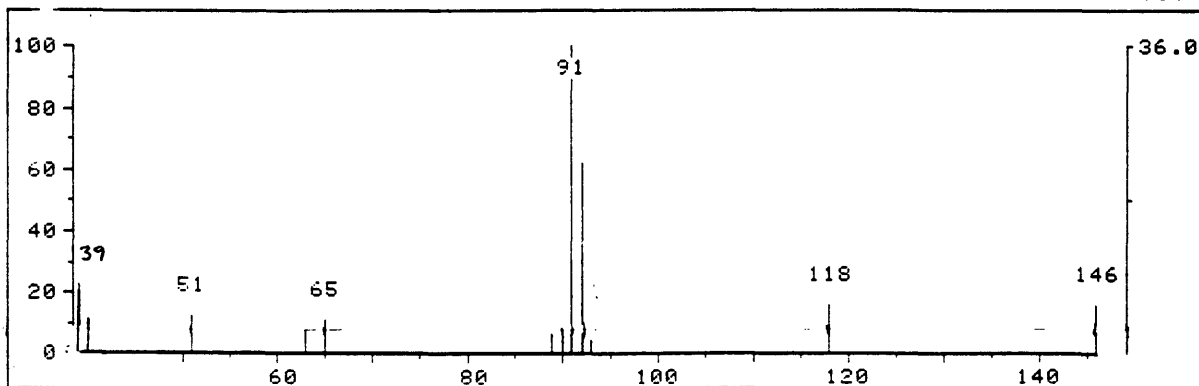




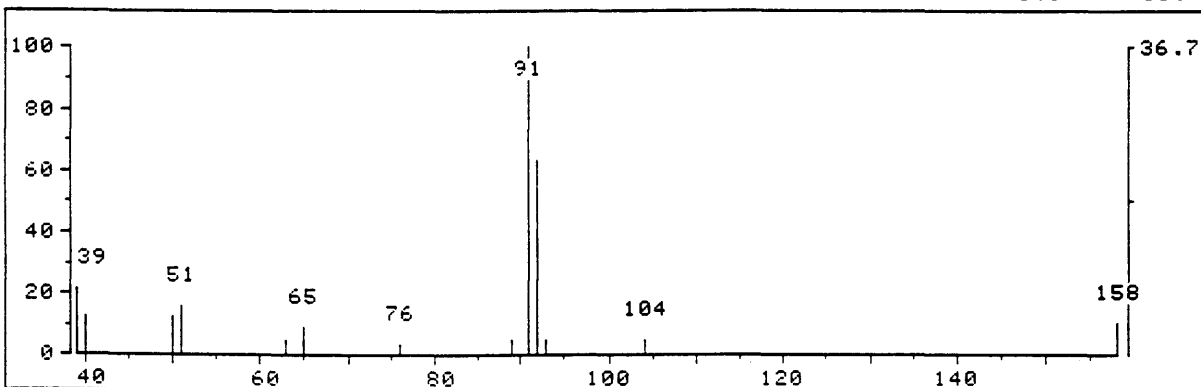
GC-MS Mass spectrum for initial deposit with 1000 ppm benzoyl peroxide.



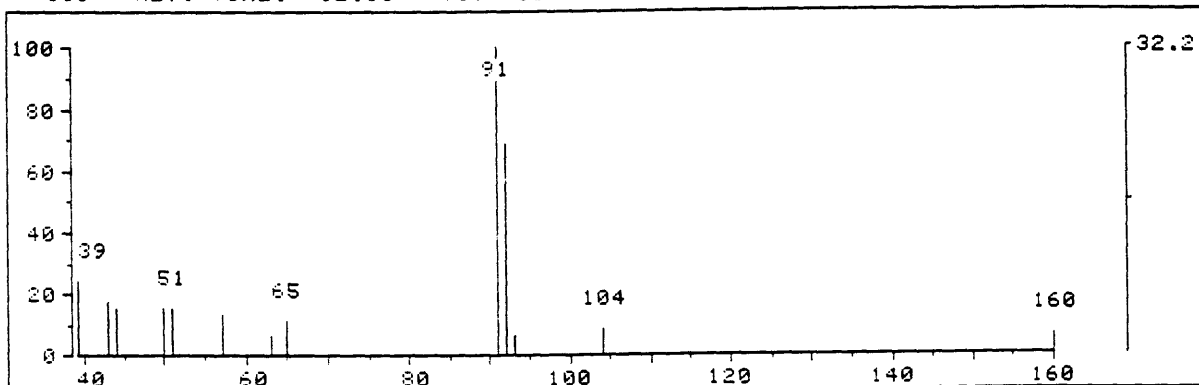
* 469 RET. TIME: 10.75 TOT ABUND= 175. BASE PK/ABUND: 91.1/ 63.



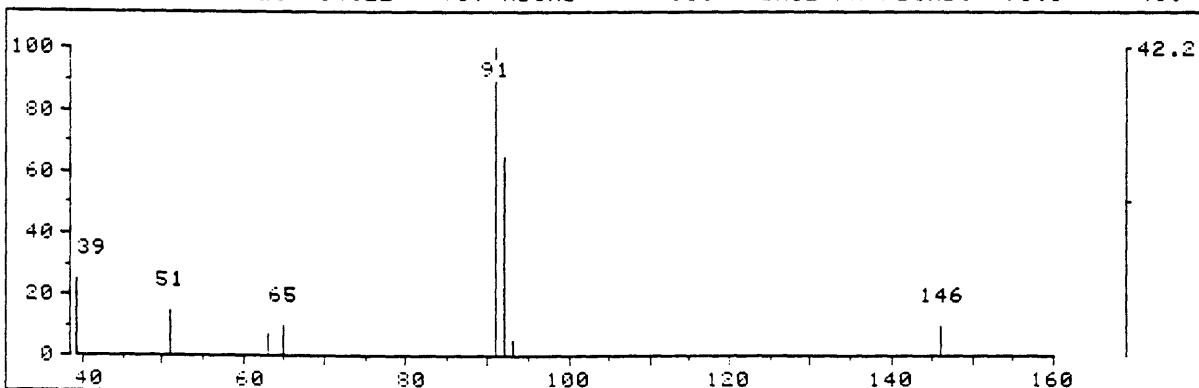
* 505 RET. TIME: 11.57 TOT ABUND= 150. BASE PK/ABUND: 91.1/ 55.



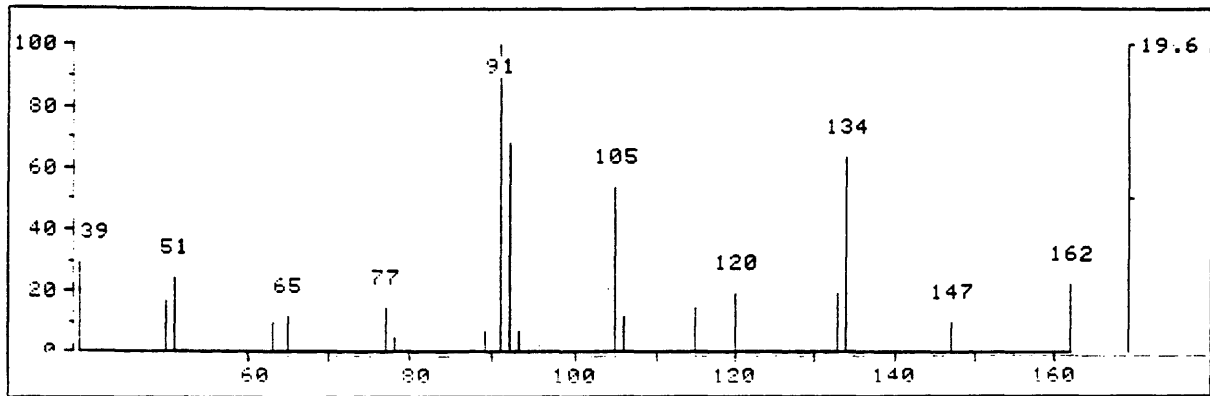
* 561 RET. TIME: 12.83 TOT ABUND= 140. BASE PK/ABUND: 91.1/ 45.



* 622 RET. TIME: 14.22 TOT ABUND= 95. BASE PK/ABUND: 91.1/ 40.

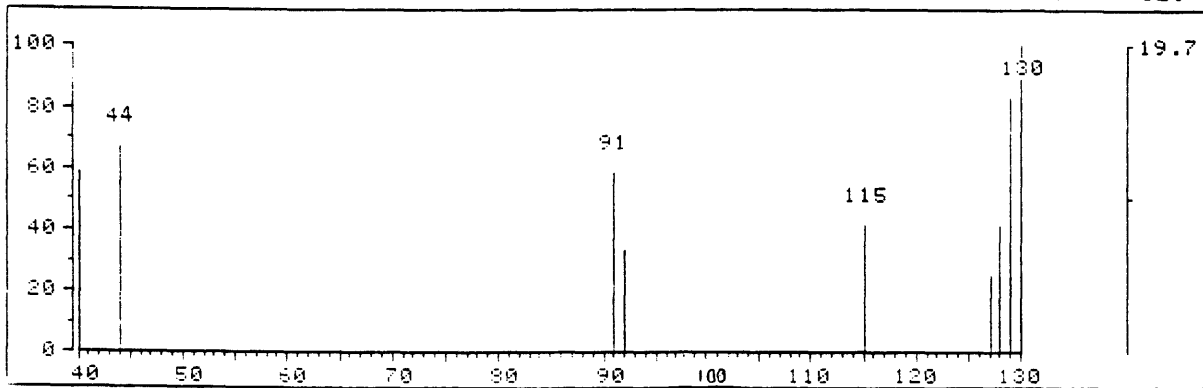


* 637 RET. TIME: 14.55 TOT ABUND= 209. BASE PK/ABUND: 91.1/ 41.

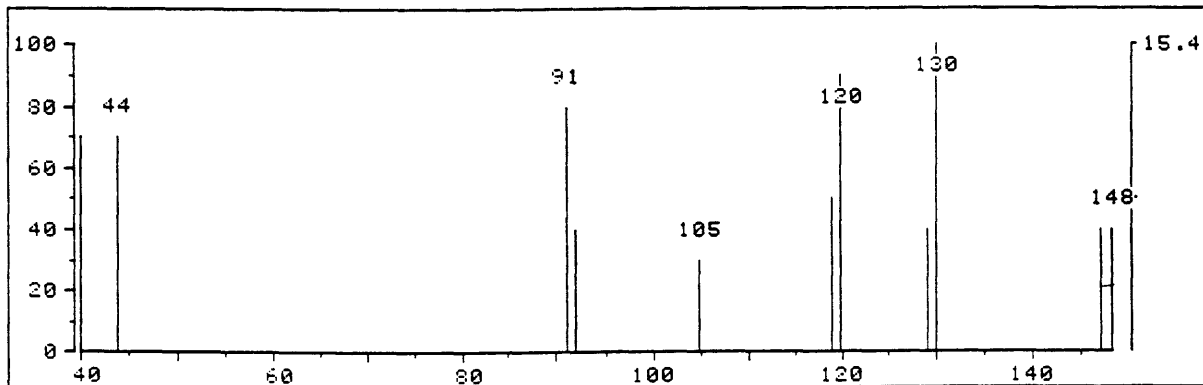


GC-MS Mass spectrum for initial deposit with 1000 ppm AIBN.

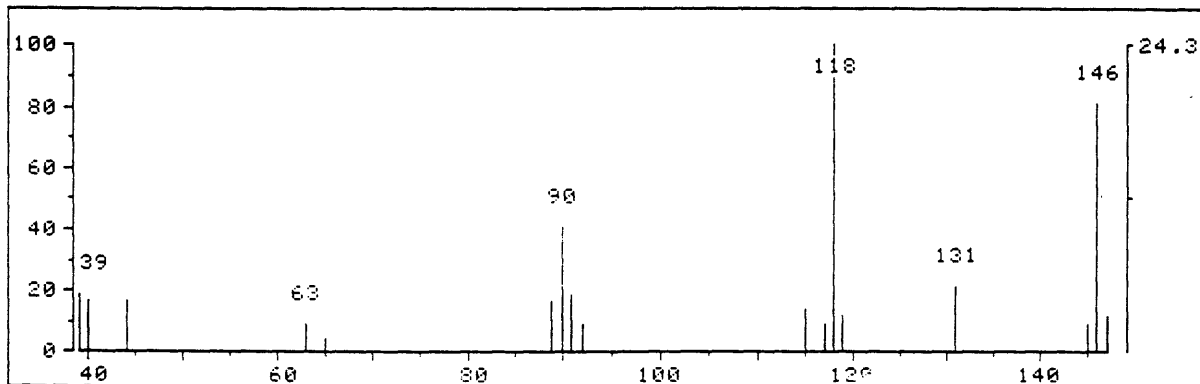
* 286 RET. TIME: 6.57 TOT ABUND= 61. BASE PK/ABUND: 130.1/ 12.



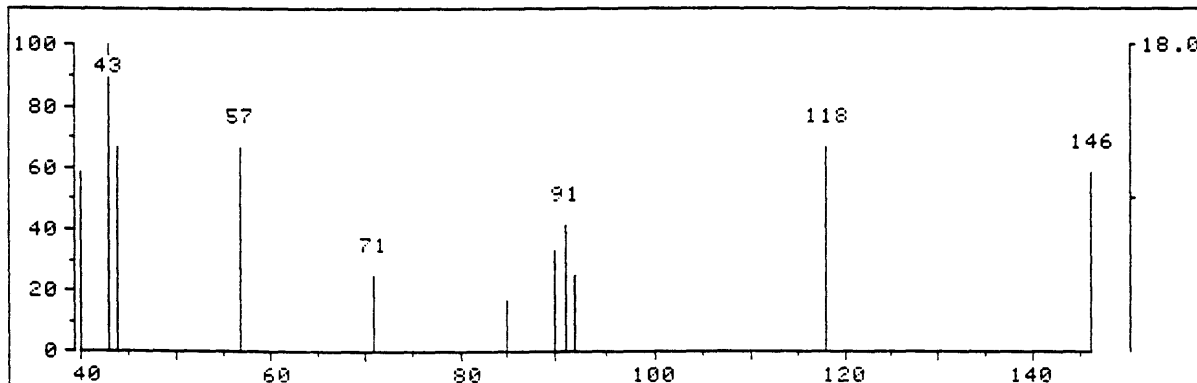
* 451 RET. TIME: 10.30 TOT ABUND= 65. BASE PK/ABUND: 130.1/ 10.



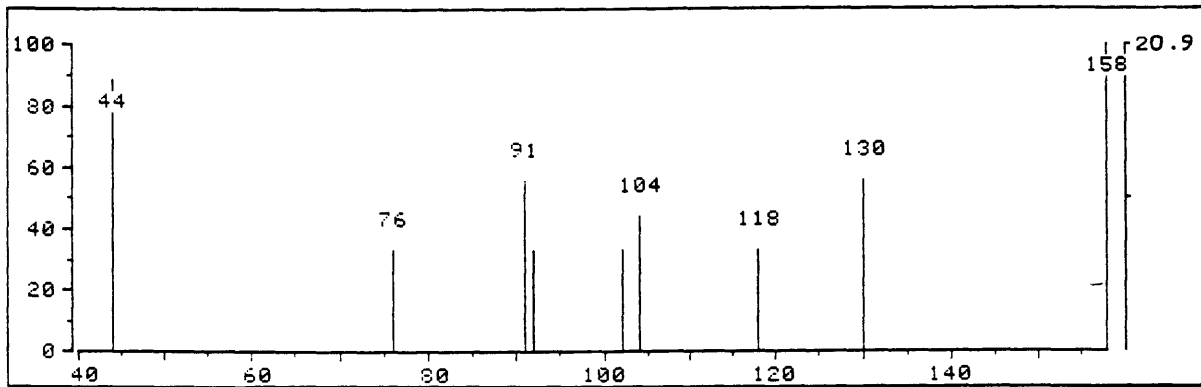
* 469 RET. TIME: 10.70 TOT ABUND= 173. BASE PK/ABUND: 118.1/ 42.



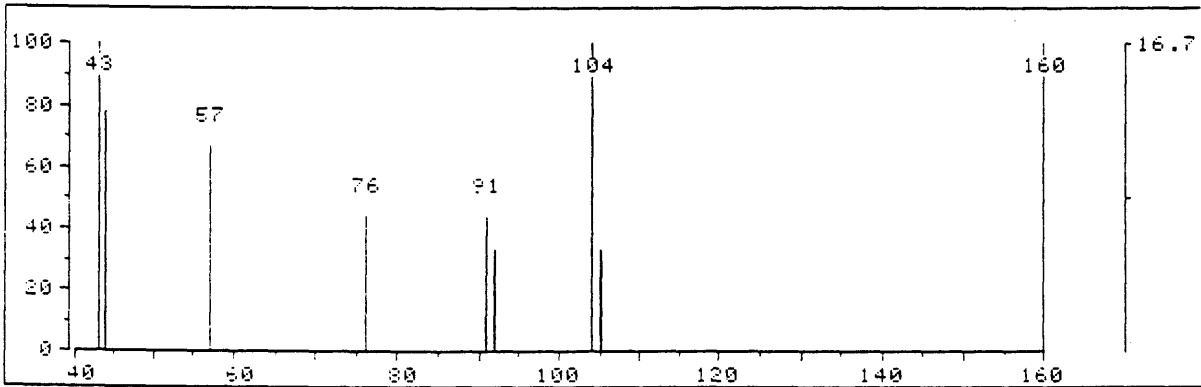
* 479 RET. TIME: 10.93 TOT ABUND= 67. BASE PK/ABUND: 43.1/ 12.



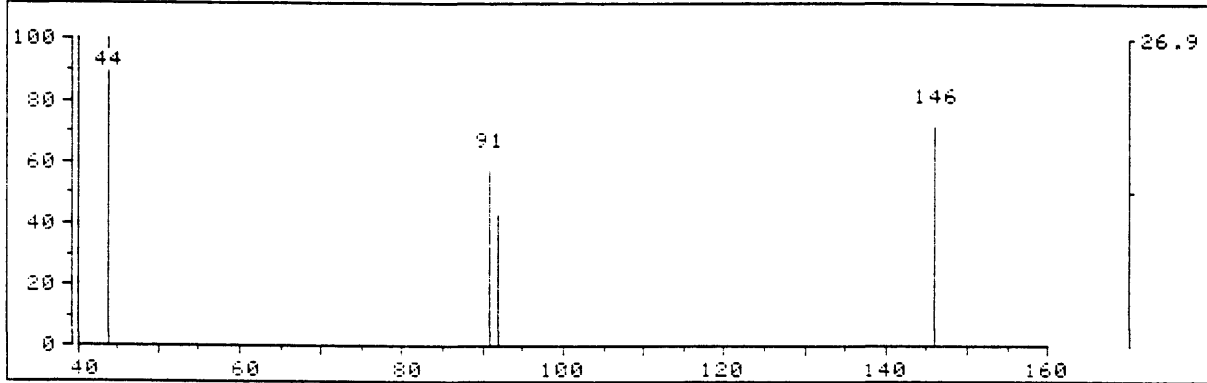
* 504 RET. TIME: 11.50 TOT ABUND= 43. BASE PK/ABUND: 158.1/ 9.



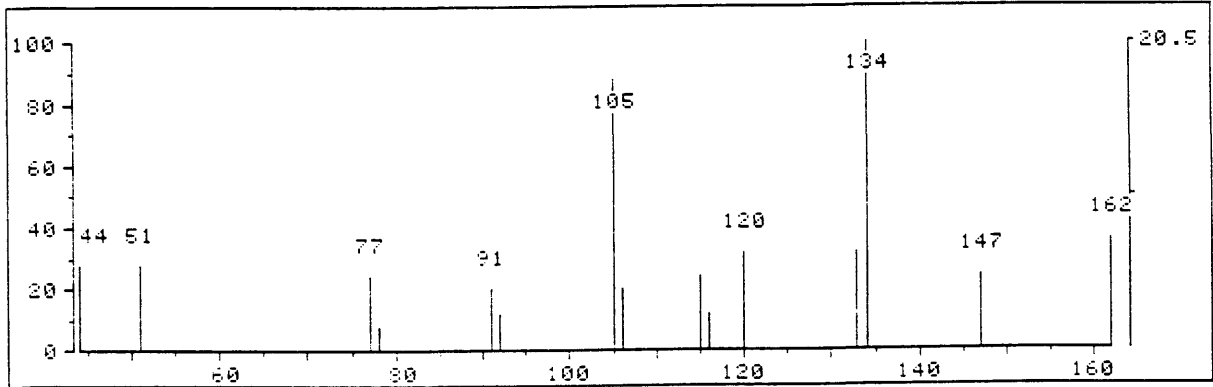
* 561 RET. TIME: 12.78 TOT ABUND= 54. BASE PK/ABUND: 43.1/ 9.



* 622 RET. TIME: 14.17 TOT ABUND= 26. BASE PK/ABUND: 40.0/ 7.

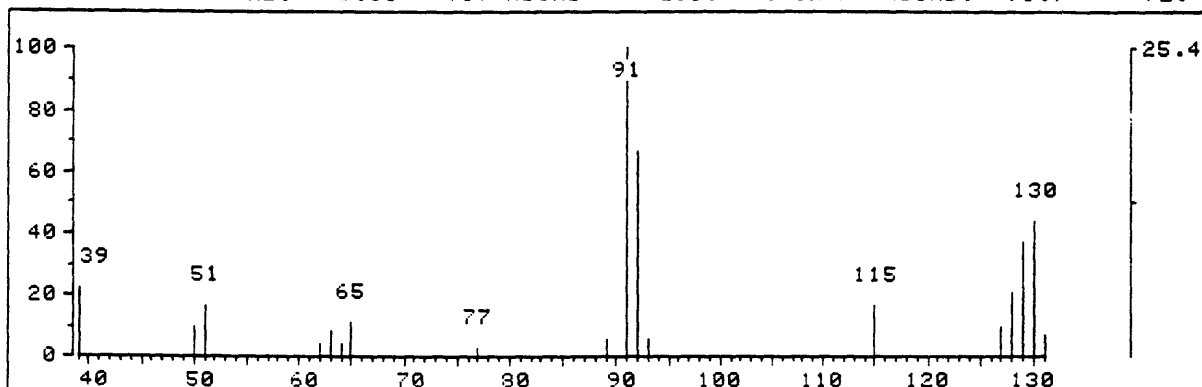


* 638 RET. TIME: 14.53 TOT ABUND= 122. BASE PK/ABUND: 134.1/ 25.

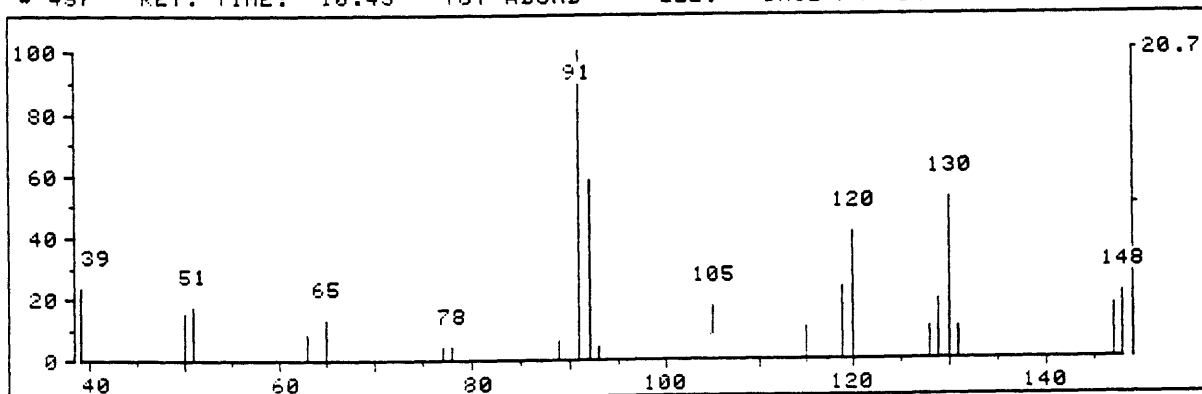


GC-MS Mass spectrum for final deposit without additives

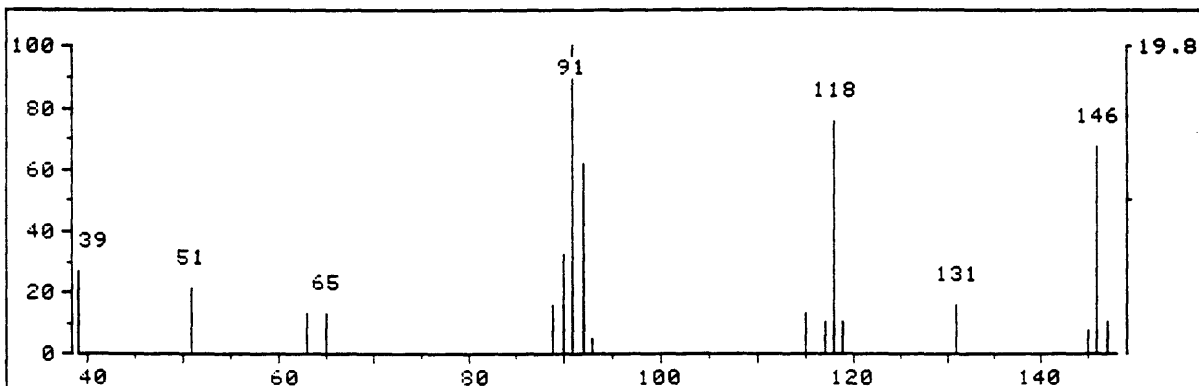
289 RET. TIME: 6.65 TOT ABUND= 283. BASE PK/ABUND: 91.1/ 72.



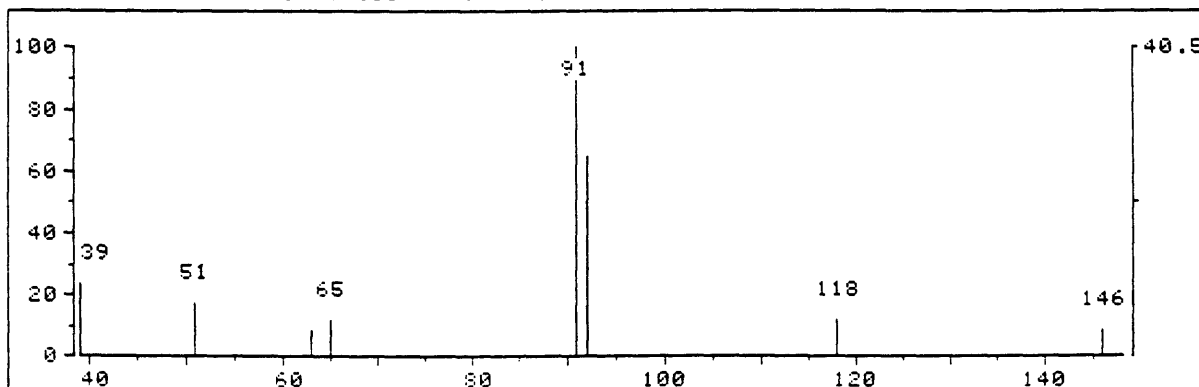
457 RET. TIME: 10.43 TOT ABUND= 222. BASE PK/ABUND: 91.1/ 46.



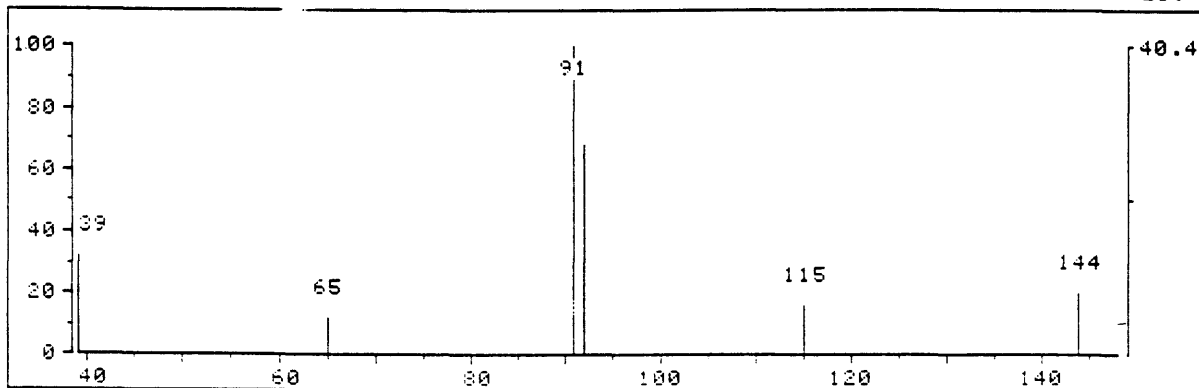
* 476 RET. TIME: 10.87 TOT ABUND= 187. BASE PK/ABUND: 91.1/ 37.



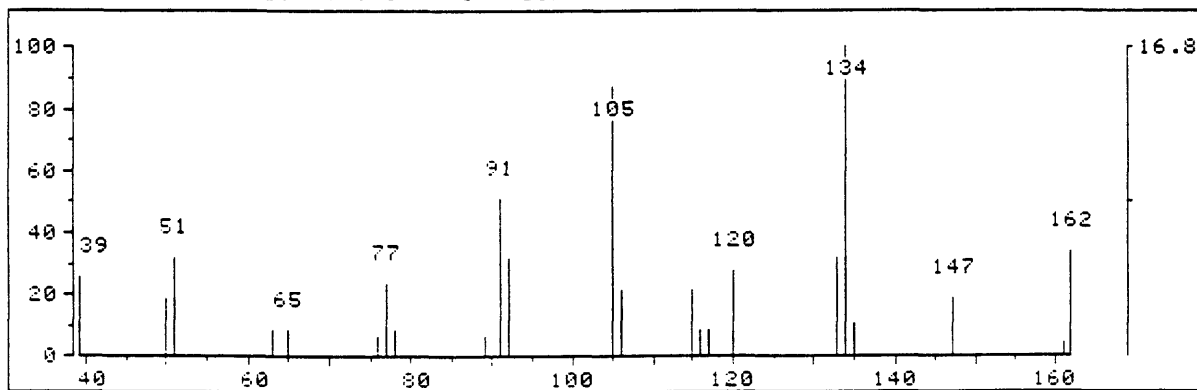
* 486 RET. TIME: 11.10 TOT ABUND= 84. BASE PK/ABUND: 91.1/ 34.



* 597 RET. TIME: 13.60 TOT ABUND= 62. BASE PK/ABUND: 91.1/ 25.

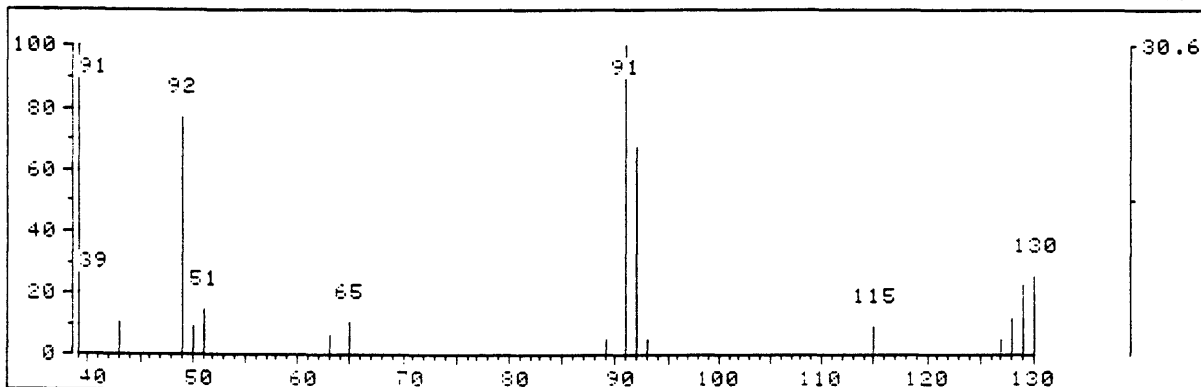


* 648 RET. TIME: 14.75 TOT ABUND= 280. BASE PK/ABUND: 134.1/ 47.

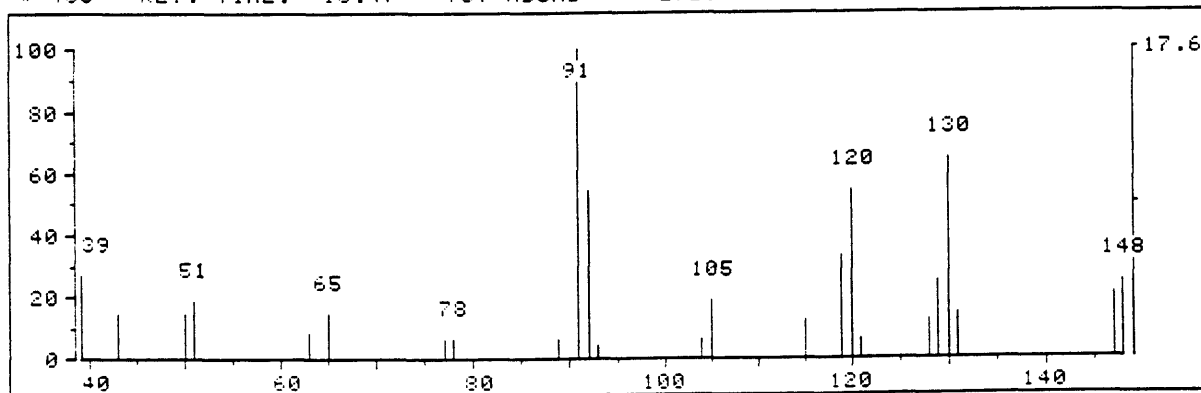


GC-MS Mass spectrum for final deposit with 1000 ppm benzoyl peroxide.

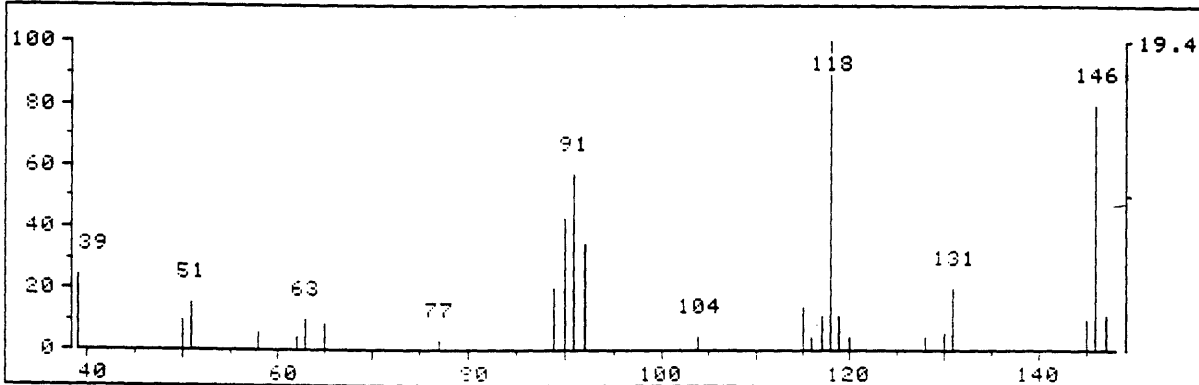
* 291 RET. TIME: 6.68 TOT ABUND= 242. BASE PK/ABUND: 91.1/ 74.



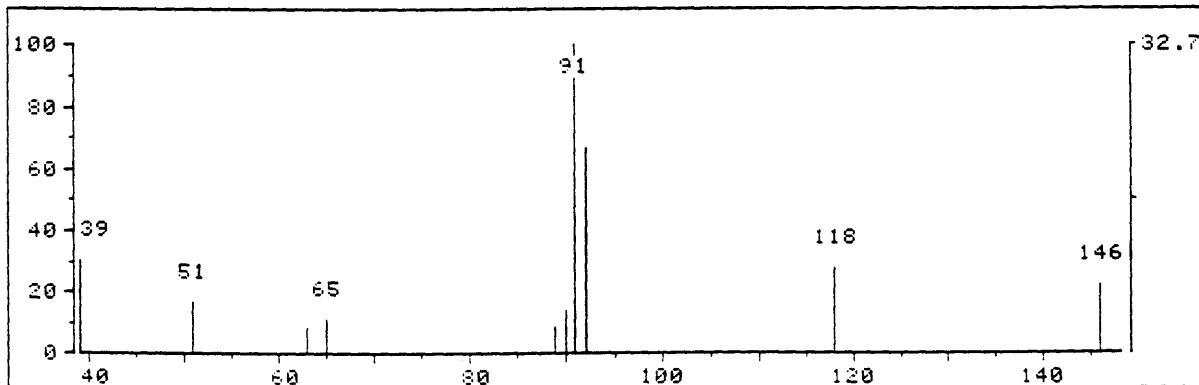
* 458 RET. TIME: 10.47 TOT ABUND= 272. BASE PK/ABUND: 91.1/ 48.



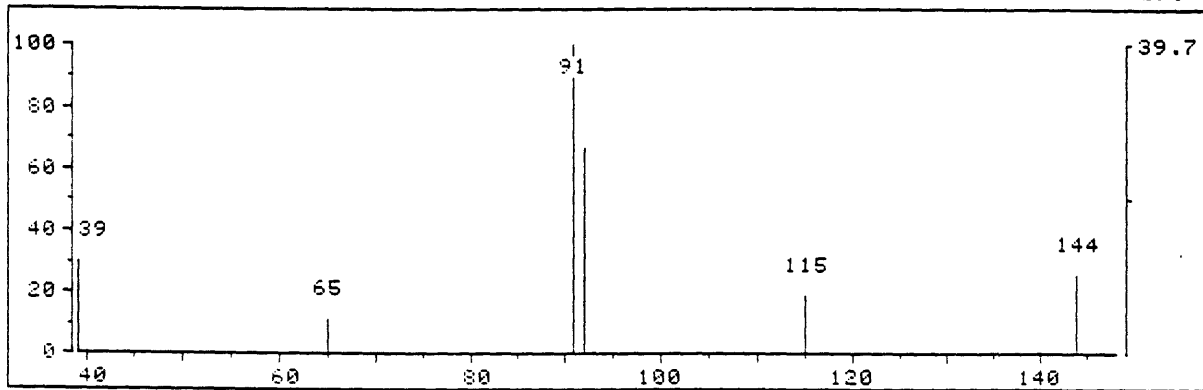
* 477 RET. TIME: 10.88 TOT ABUND= 361. BASE PK/ABUND: 118.1/ 70.



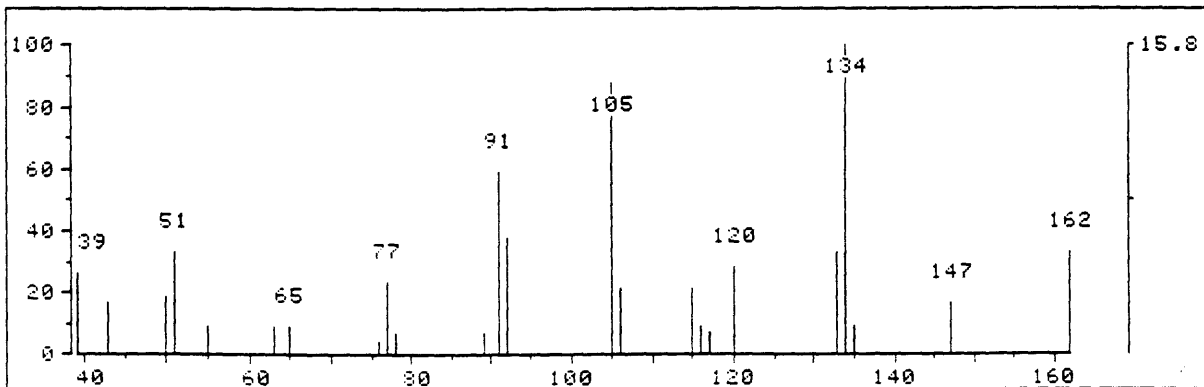
* 487 RET. TIME: 11.12 TOT ABUND= 110. BASE PK/ABUND: 91.1/ 36.



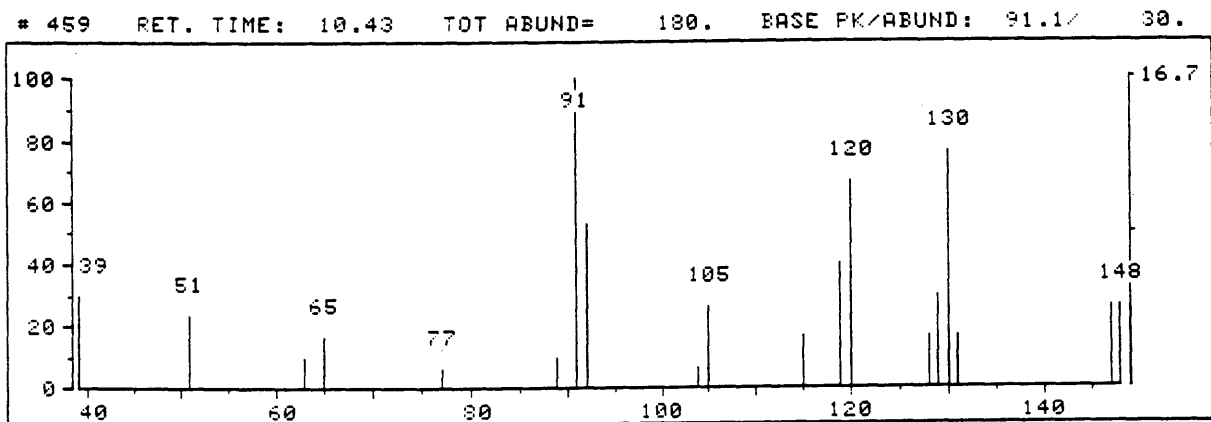
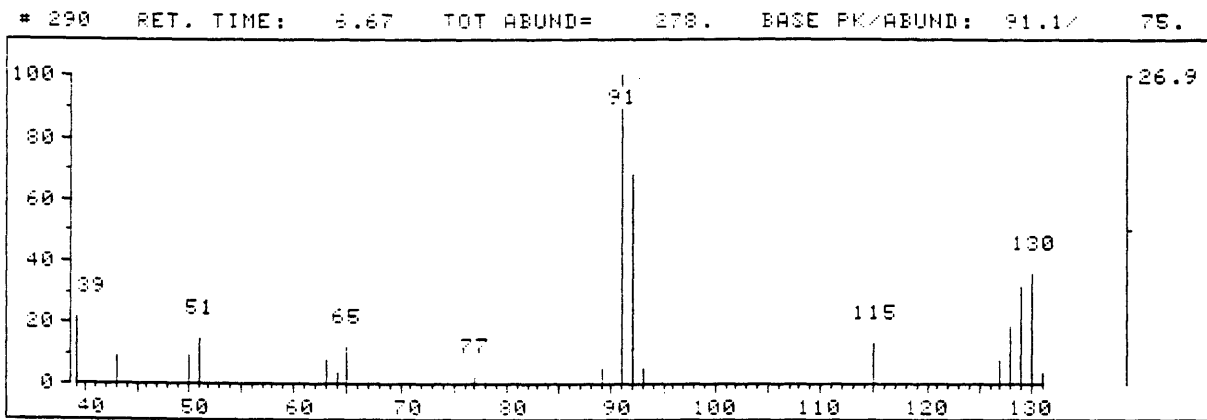
* 597 RET. TIME: 13.60 TOT ABUND= 68. BASE PK/ABUND: 91.1/ 27.



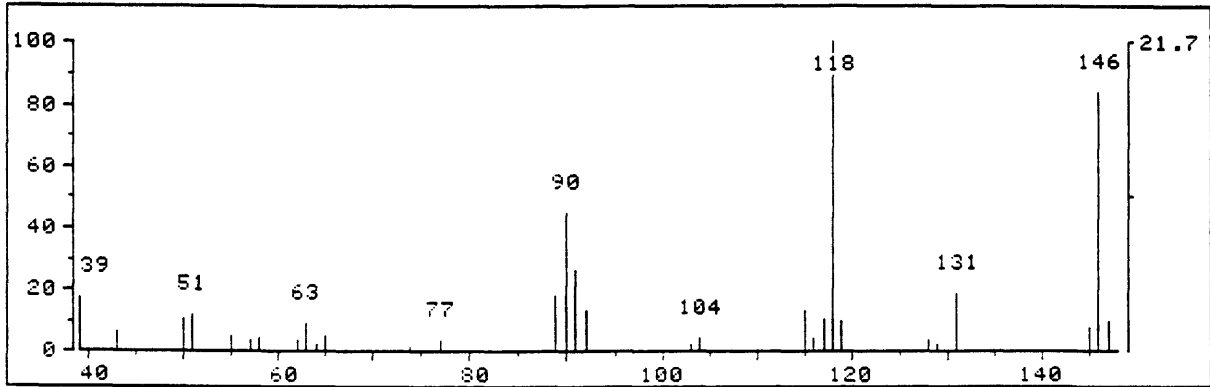
* 647 RET. TIME: 14.73 TOT ABUND= 266. BASE PK/ABUND: 134.1/ 42.



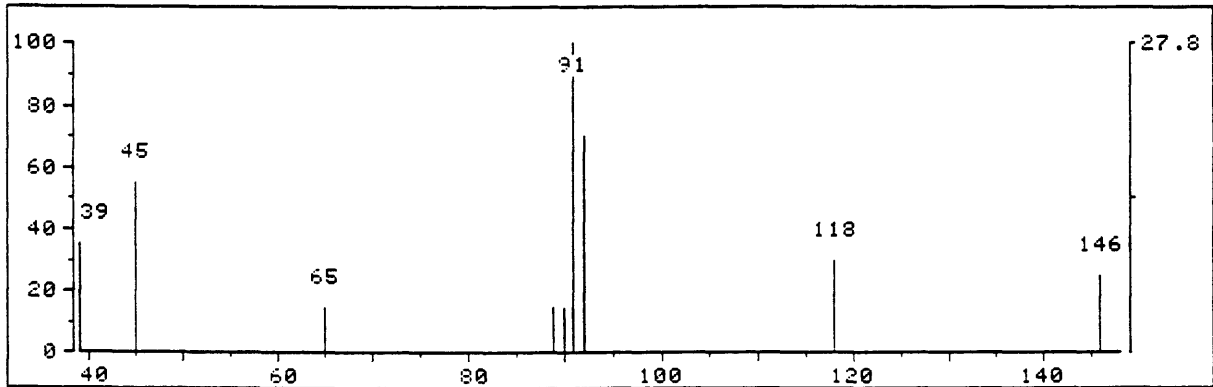
GC-MS Mass spectrum for final deposit with 1000 ppm AIBN.



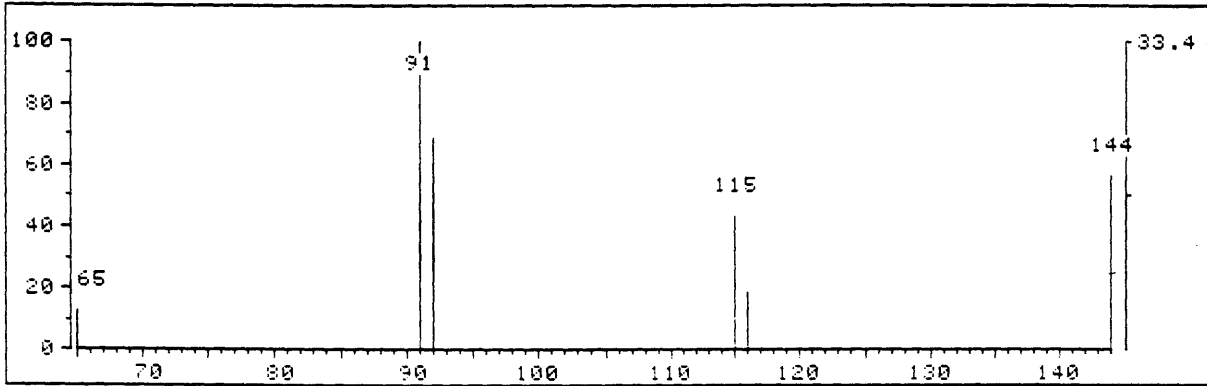
* 481 RET. TIME: 10.93 TOT ABUND= 508. BASE PK/ABUND: 118.1/ 110.



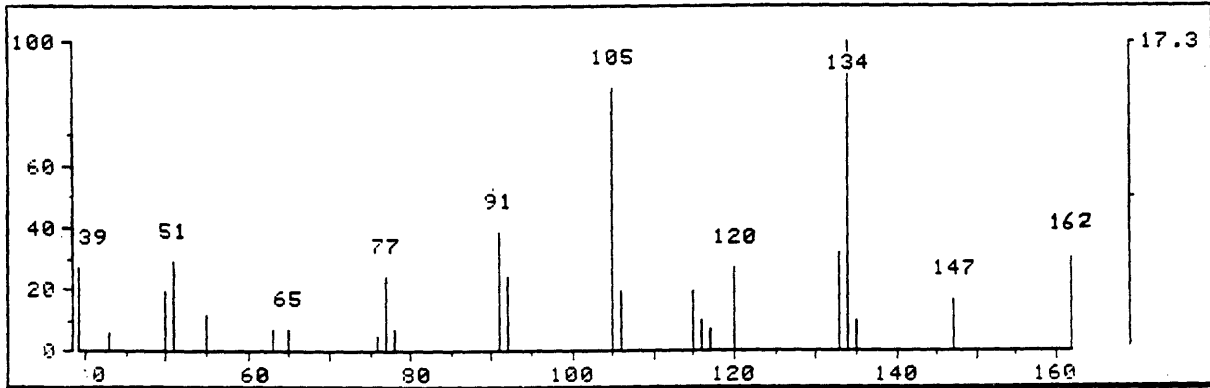
* 495 RET. TIME: 11.25 TOT ABUND= 72. BASE PK/ABUND: 91.1/ 20.



* 599 RET. TIME: 13.58 TOT ABUND= 48. BASE PK/ABUND: 91.1/ 16.



* 650 RET. TIME: 14.72 TOT ABUND= 237. BASE PK/ABUND: 134.1/ 41.



APPENDIX B

The following is an approximate calculation for the peroxide content in model fuel deposit:

The following equations were obtained from the calibration curve in Figure 9.

Absorbance of the initial deposit sample = 0.16 nm

Absorbance of the final deposit sample = 0.04 nm

Absorbance of blank = 0.041 nm

Absorbance of initial deposit - blank = 0.119 nm

$$x = \frac{y - 0.0007845}{781.32}$$

$$x = \frac{0.119 - 0.0007845}{781.32} = 1.51 \times 10^{-4} \text{ M}$$

Fe⁺³ conc. produced by the initial deposit =

$$1.51 \times 10^{-4} \text{ M} \times 25 = 3.78 \times 10^{-4} \text{ M}$$

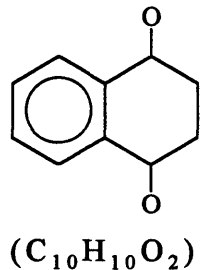
Moles of Fe⁺³ produced by the initial deposit =

$$3.78 \times 10^{-3} \times 0.025 = 9.456 \times 10^{-4} \text{ mol}$$

Moles of peroxide in the initial deposit =

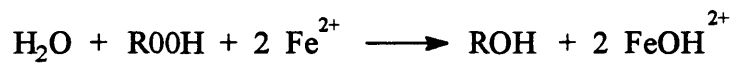
$$\frac{9.456 \times 10^{-5}}{2^*} = 4.73 \times 10^{-5} \text{ mol}$$

If we take as a reasonable structural model of the deposit a tetralin unit with two oxygens: (note that this unit has 19.8 % O)



Then

$$\left(\frac{4.73 \times 10^{-5} \text{ mole peroxide}}{0.00407 \text{ g deposit}} \right) \left(\frac{162 \text{ g deposit}}{\text{mole C}_{10}\text{H}_{10}\text{O}_2 \text{ unit}} \right) = 1.88 \frac{\text{mole peroxide}}{\text{mole C}_{10}\text{H}_{10}\text{O}_2 \text{ unit}}$$



* mole of peroxide is reacting with two mole of Fe⁺².

APPENDIX C

Concentration of tetralin hydroperoxide, tetralone, and tetralol in liquid phase stressed model (10 ml ampules) using HPLC.

